DEVELOPMENT OF A FISHERY INDEPENDENT INDEX OF ABUNDANCE FOR JUVENILE SOUTHERN BLUEFIN TUNA

Ann Cowling

Project 96/118

FRDC Large Milestone Report: Summary of Activities 1996-2000

January 2001

1. NON TECHNICAL SUMMARY

The parental stock of southern bluefin tuna (SBT) is at historically low levels, and there are concerns about the risk of poor recruitment and the possibility of recruitment collapse. To monitor the abundance of juvenile SBT and develop a fishery independent index of juvenile abundance, Australia and Japan established a large-scale collaborative research program in 1993. The aerial survey is one of the main projects in this program.

Annual aerial surveys with comparable protocols have been conducted over the Great Australian Bight for three months each summer since 1993. Estimates of surface abundance are derived from the data. The aims of this project are:

- ★ to conduct the 1997 to 1999 surveys and estimate various surface abundance indices
- ★ to conduct the necessary research to
  - ★ incorporate environmental variables into the estimates
  - ★ estimate the proportion of SBT at the surface under various environmental conditions and incorporate these estimates into the surface abundance estimates
  - ★ reduce uncertainty in the estimates arising from uncertainty in patch size and fish size estimates
- ★ to evaluate the usefulness of the indices of SBT abundance derived from this project.

Significant progress has been made in the areas of developing the indices of surface abundance from the aerial surveys, understanding how environmental variation affects the estimates of surface abundance and SBT surfacing behaviour, and understanding SBT surfacing behaviour. The extent of the data collected in this project is now greater than originally planned. New data include for example satellite sea surface temperature, data from CSIRO's Division of Atmospheric Research, and data collected in multiple plane experiments. These new data allow the development of a more detailed understanding of the processes governing the appearance and detection of surface schools of SBT in the GAB, and/or more understanding of the accuracy of the abundance estimates.

The results achieved to date in this project show that the majority of the goals of the project are achievable, but that to attain them at a level in which most of the information is extracted from the data will require further work after the completion of this project. This project has therefore been extended for a further two years by merging it with a closely related FRDC project, "Improved fishery independent estimates of Southern Bluefin Tuna recruitment through integration of environmental, archival tag and aerial survey data".

- Aerial surveys for juvenile southern bluefin tuna were conducted in the summers of 1997-2000 over the Great Australian Bight. The data collected in the surveys has allowed various surface abundance indices of SBT to be calculated. A time series of 8 years of consistent data is available covering the years 1993-2000.

- A first method of estimating surface abundance, which incorporates various environmental conditions was introduced in the 1998 aerial survey report. A second method was agreed to at the Aerial Survey Workshop held in Port Lincoln in 2000, and this analysis was introduced in the survey analysis in 2000.

- Surfacing rates are being determined from archival tags. The manufacturer of the 1993 to 1995 archival tags had major production problems in 1996 and 1997. No new tags were made. As a consequence, a new source of archival tags was located. These tags were first placed in the field in 1998. Data from these tags show that the location of SBT can be determined much more accurately. This advance in tag technology will be very beneficial to this project, as differences in surfacing behaviour at different locations (in different environmental conditions) will be more likely to be detectable.

- A total of 325 archival tags were released between June 1993 and March 1995. To date, 61 of these tags have been returned. However, only 7 contain reasonable amounts of data for the location and periods covered by the aerial survey. Data from 4 tags of these 7 tags was analysed in 1996, and from 5 tags of the 7 tags in 1997. Another 198 tags were released between January 1998 and February 2000. Of the 36 tags returned to date, 18 contain useful data. Of these 18 tags, 15 contain data for between 6 and 10 weeks in January to March in 1998 or 1999. To date, 9 of these 15 tags have been analysed, all with data from 1998.

- A LIDAR instrument was trialed in 1997, but it was not used again in the 1998 field season as the technology has not yet advanced sufficiently to allow school size and fish size to be routinely measured by the LIDAR and used to groundtruth the spotters estimates. As agreed in correspondence with FRDC, funds for the LIDAR work were used instead for groundtruthing experiments.

- Two groundtruthing procedures were implemented in the 1998 field season:
  - ★ Two plane experiments were conducted which enabled estimates of the errors associated with distance measurements and the spotters' school size and fish size estimates to be calculated. These error estimates will be particularly useful for assessing biases in the surface abundance indices due to probable measurement errors in distance and spotters' school size estimates.
  - ★ A separate research project was conducted from *MRV Southern Surveyor* in the GAB in February 1998. One of the aims of this project was to compare acoustic estimates of school size and composition with those given by aerial spotters. On the one day during the cruise period in which the weather was suitable for aerial spotting, a plane from the aerial survey directed the vessel to surface schools of SBT. While there is an observable (but weak) correlation between the aerial survey biomass estimates and sonar parameters, we cannot say without actual groundtruthing data which of the two sets of estimates are more accurate ([R13]).

- Further three plane groundtruthing experiments were conducted in the 1999 and 2000 field season using the two survey planes and a commercial spotting plane. The results showed that the spotters' estimates of patch size are consistent, but the spotters' estimates of fish size are not consistent.

- The surface abundance indices from the aerial surveys were used in the stock assessments presented at the 4th CCSBT Scientific Meeting, August 1998. The report of that meeting includes the following in the Advice and Recommendations section

  "The meeting also recognised that information on recent recruitment based on tagging studies, aerial surveys and possibly acoustic surveys was critical for providing timely advice on stock status and future management. Lack of future aerial survey information would seriously affect current and future assessments.

The meeting strongly recommends that the Commission note the priority research needs, and in particular, urge each member to support continuation of the aerial survey."

- In 1997/1998 an internal review of the aerial survey was conducted. The project collaborators, CSIRO and NRIFSF, held a full review of the project in September 1999, and a further workshop involving international experts was held in February 2000 in Port Lincoln.

- A number of new features have been identified in the data which make the analyses and incorporation of environmental conditions more complex than originally thought. These features improve our understanding of the data, the accuracy of the analyses, and SBT surfacing processes and will improve the final analyses of the survey data. However, the development of the survey has been delayed.

2. BACKGROUND

All recent assessments of southern bluefin tuna (SBT) indicate that the parental stock is at historically low levels. The current parental stock biomass has been judged to be below "commonly used scientific measures of biologically safe parental biomass" and there are concerns about the risk of poor recruitment and the possibility of recruitment collapse. There is also much uncertainty about whether the current catch level will allow for rebuilding of the SBT stock.

The current analytical assessment methods for SBT have a 4 to 5 year time lag in the estimates of the number of recruits, due to time lags in receiving catch data and the lack of a reliable index of juvenile abundance. In addition, there is much uncertainty about most recent estimates of recruitment as they are largely determined by the most recent juvenile catch rates. Therefore, current trends in recruitment remain one of the major unknowns in evaluating the status of this stock and its potential to rebuild under current catch rates. Moreover, there is no fishery independent information on stock or juvenile abundances. Lack of such information is a major limitation in evaluating the likelihood of stock rebuilding under current catch rates.

All recent scientific and management meetings, both under the previous informal trilateral arrangement and now under the Convention for the Conservation of Southern Bluefin Tuna, have considered the development of a fishery independent recruitment index of SBT to have a very high research priority. In response to this need, a developmental aerial survey program was started in 1990/91, and experimental surveys using line transect methods have been conducted annually during the fishing season in the Great Australian Bight since then.

In June 1993 a large scale five year collaborative program involving CSIRO and the Japanese National Research Institute of Far Seas Fisheries (NRIFSF) was established to monitor the abundance of juvenile SBT and develop a fishery independent index of juvenile abundance. The aerial survey project was established as one of the main projects in this program. Funding of the aerial survey part of this collaborative research program has come form a variety of Japanese and Australian sources; the Australian sources include CSIRO, SBTMAC, FRDC and FRRF. Each year a workshop is held to review and prioritise the collaborative research for the coming year. At the 1995 workshop, the aerial survey was reaffirmed as one of the highest priority projects.

During this project a great deal of data has been collected. The analysis of this data has increased our knowledge of SBT and their behaviour. We have revised some of our initial assumptions about the detection of SBT from planes and SBT distribution and behaviour. Our improved understanding of SBT distribution and surface abundance in the GAB will improve the final analysis of the data, but the greater complexity of the processes has slowed the development of the analysis. The development of this project has been delayed by a delay obtaining the archival tag data required by this project.

This report is an interim report, as the project has been extended for another two years, to allow more time for further analysis and integration of additional data from other sources. The project has been extended by combining it with FRDC Project Number 199/105, "Improved fishery independent estimates of Southern Bluefin Tuna recruitment through integration of environmental, archival tag and aerial survey data".

3. NEED

In the proposal for this project submitted in 1996, the following need was identified:

Analyses of the survey data collected to date indicate that the data can be used to provide estimates of the number of schools, total biomass and biomass by cohort for fish at the surface with reasonable coefficients of variation. The estimates have started to provide an initial useful comparison with VPA results, as estimates of some cohorts from the two methods began to overlap in 1995. However, there are still a number of research problems that need to be addressed in order to evaluate whether these estimates can provide a reliable index of juvenile abundance. The problems are associated with the unknown variability in the proportion of schools at the surface, the proportion of juveniles within the Bight, environmental effects on detectability of surface schools and tuna surfacing behaviour, and the reliability of estimates of fish and school sizes.

The biggest source of uncertainty and perhaps the biggest source of variation in the analyses of aerial surveys to date, is that no account is taken of the variability in the proportion of schools at the surface. If the proportion of schools at the surface varied little from year to year, this would not be a problem. However, surfacing behaviour of SBT appears to be strongly influenced by environmental conditions. Although the aerial survey is only conducted under weather conditions favorable to tuna surfacing, the aerial surveys to date have encountered substantial inter-annual differences, with sea-surface temperatures being perhaps the most important and variable. The variation in the proportion of surface schools must be accounted for to improve the interpretation of the aerial survey results. This issue will be a major focus of the research over the next four years.

This research will develop an integrated statistical model based on the recent and growing body of data on surfacing behaviour of SBT in the Great Australian Bight acquired from archival tags together with detailed environmental data collected in the aerial survey as well as from other sources. In addition, research using recently available laser technology (airborne LIDAR systems) that detects schools below the surface of the water will be conducted to try to estimate the proportion of surface schools.

Research is also needed to improve the reliability of the results including improvements in the estimates of school size, fish size, the effects and interactions of environmental factors on the detection and size of surface schools, and statistical methods for obtaining the variances of the estimates. These factors will all be addressed over the next 4 years.

Finally, the current developmental time series of aerial survey indices must be extended and improved. Without such an extension, it would not be possible to evaluate whether the aerial survey can provide a useful index of abundance. With the results from 1995/96 and the three additional years covered by this proposal, the aerial survey index will overlap the VPA estimates of recruitment for seven cohorts. This overlap will provide the basis for a statistical analysis of the aerial survey results as an index of recruitment, which is to be conducted as part of the current research proposal.

The results of this project have led to some reassessment of the needs.

A) the estimates of biomass by cohort are now assessed to be insufficiently reliable to compare with VPA results, and are no longer reported in the results of the analyses.

B) Incorporation of surfacing behaviour into the surface abundance estimates is not necessary under one of the models being investigated at present. Under this model, the results and interpretation of the surface abundance analysis is greatly strengthened by the model of surfacing behaviour as it provides independent verification of the surface abundance model. Under other methods of estimation of surface abundance, it is necessary to incorporate surfacing rates.

4. OBJECTIVES

[O1] To conduct an aerial survey for SBT over the Great Australian Bight each summer season from 1997 to 1999 and estimate various surface abundance indices.

[O2] To complete the statistical research required to:

(a) incorporate environmental variables into the estimates;

(b) incorporate estimates of the proportion of SBT at the surface under various environmental conditions;

(c) reduce the sampling error in the estimates due to uncertainty in school size and fish size estimates.

[O3] To complete an evaluation of the usefulness of the indices of SBT abundance derived from the aerial survey.

5. METHODS

[O1] To conduct an aerial survey for SBT over the Great Australian Bight each summer season from 1997 to 1999 and estimate various surface abundance indices.

The area of the GAB searched during the surveys lies between 128°E and 135°E, running from the coast to about the 700-800m depth contour of the continental shelf. Fifteen equally spaced North-South transect lines are searched during the surveys; Figure 1. Two planes fly in the surveys, with two spotters in each plane. During each flight, information is collected about detected schools of SBT. Environmental data (windspeed and direction, airtemperature, swell, haze, glare) are also collected.

The survey takes place over the 3 months from January to March each year, on days when the weather conditions are suitable for survey operations (windspeed less than 10 knots). Each plane is able to search 2 or 3 lines per day. Thus one survey replicate takes anywhere between 3 days and 1 month to complete, depending on the weather conditions. The survey is replicated 4 to 8 times per season. Further details of the survey design, implementation and methodology are given in [R4], [R6], [R8], [R10] and [R11].

The main index of abundance estimated from the surveys is mean surface biomass density during the survey period in the survey area.

The statistical methodology used in the analysis each year is described in [R4], [R6], [R8], [R10] and [R11]. A number of methods of constructing indices have been used in the analyses to date.

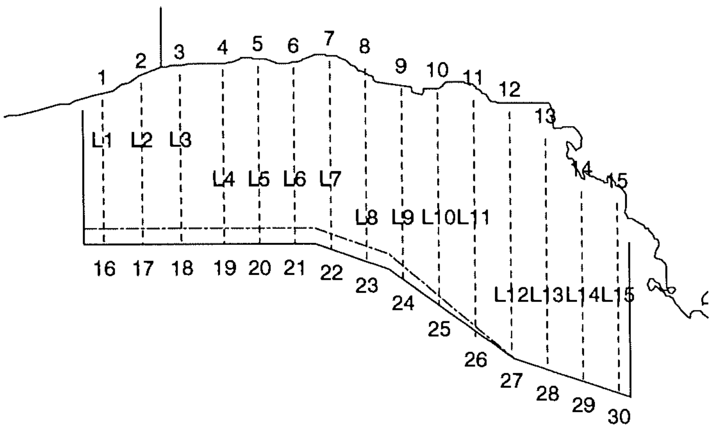

Figure 1: Transect lines of 1999 and 2000 aerial surveys

[O2(a)] Incorporation of environmental variables into the estimates

Larger quantities of SBT are detected during the surveys during warm calm conditions. Therefore, there is a need to adjust the survey estimates for the between year and within year differences in the weather conditions.

A first method of estimating surface abundance, which incorporates various environmental conditions in a statistical modelling approach was introduced in the 1998 aerial survey report [R6].

The 2000 Port Lincoln workshop ([R2]) agreed to a statistical modelling approach using the line as the unit of analysis. Many transect lines are searched during the surveys without detecting any SBT. In a model-based approach, the large number of zero observations must be allowed for appropriately. This is done using a two stage model with environmental, spatial and temporal covariates: first we model the probability of presence or absence, and second, model the biomass provided SBT were detected. This is a well known statistical method. It is more fully described and developed in [R4], using the half line as the unit.

[O2(b)] Incorporation of estimates of the proportion of SBT at the surface under various environmental conditions

In this project, we aim to analyse data from archival tagged SBT in the GAB to determine surfacing rates in different spatial, temporal and environmental conditions. Archival tag development and deployment is not funded from this project, although the development of the tag technology has been proceding during this project. There has been a delay in receiving data from archival tagged SBT in the GAB, which has delayed the development of this project.

The manufacturer of the 1993 to 1995 archival tags had major production problems in 1996 and 1997. No new tags were made. As a consequence, a new source of archival tags was located. These tags were first placed in the field in 1998. Data from these tags show that the location of SBT can be determined much more accurately.

A total of 325 archival tags were released between June 1993 and March 1995. To date, 61 of these tags have been returned. However, only 7 contain reasonable amounts of data for the location and periods covered by the aerial survey.

Five of these 7 tags were analysed in [R14] using weather observations from the Ceduna weather station as explanatory variables, together with SST from the tags, and moon phase.

Another 198 tags were released between January 1998 and February 2000. Of the 36 tags returned to date, 18 contain useable data. Of these 18 tags, 15 contain data for between 6 and 10 weeks of the aerial survey period.

In 1999, a new study of surfacing behaviour was begun using a more detailed classification of surfacing behaviours than the previous analyses. The classification scheme is reported in [R5], and the data from 9 tags in the GAB in 1998 are analysed in [R7].

[O2(c)] Reduction of the sampling error in the estimates due to uncertainty in school size and fish size estimates.

LIDAR is a remote sensing technology developed by the US military. A beam of light of a single frequency is emitted, is reflected by an object in its path, and the returned light can be analysed to provide an image of the reflecting object. In 1997 experiments using a LIDAR carried in the plane were conducted with the aim of determining whether LIDAR technology can be used to

A) Estimate the size of schools of SBT
B) Estimate the size of fish within schools
C) Detect sub-surface schools of SBT that are not detectable to the spotters.

Two experts from Arete Associates brought their LIDAR to Port Lincoln to work on this project. The actual LIDAR experiments are described in detail in [R3] and [R12].

In 1998, 1999 and 2000, validation experiments were designed and conducted to collect independent patch size and fish size estimates to assess whether these could be used to calibrate the spotters' patch size and fish size estimates.

In these experiments, the spotters in several planes simultaneously estimated the patch size and fish size of the same patch. This was repeated for a number of different patches. One plane led and identified suitable fairly isolated patches for the study. When a suitable patch was identified, the lead plane called the other planes to that patch on the radio. The lead plane maintains the lowest altitude and is easily followed by the higher planes. The following planes keep a safe distance from the lead plane but close enough to quickly get to the same patch. The plane at the highest altitude confirms that all planes are looking at the same patch. Further details are given in [R4], [R6] and [R8].

[O3] To complete an evaluation of the usefulness of the indices of SBT abundance derived from the aerial survey.

In 1997/1998 an internal review of the aerial survey was conducted. The project collaborators, CSIRO and NRIFSF, held a full review of the project in September 1999; [R1] and [R9]. A further workshop involving international experts was held in February 2000 in Port Lincoln, [R2].

6. RESULTS

[O1] To conduct an aerial survey for SBT over the Great Australian Bight each summer season from 1997 to 1999 and estimate various surface abundance indices.

Annual reports summarising the results of each year's fieldwork, description of the development in the analytical methods and updated indices of abundance have been produced every year since this project commenced; [R4], [R6], [R8], [R10], [R11].

The search effort and sighting rates are summarised in Table 1 below.

	1993	1994	1995	1996	1997	1998	1999	2000
No of replicates completed	4	8	8	7	5	5	4	4
Total flying time	213	405	438	332	287	297	238	177
Total time in effort	112	215	206	173	129	124	77	51
Total nm searched in effort	10174	20261	20793	18243	12799	11937	7499	5960
# SBT sightings (0-5 yr olds)	267	289	295	186	189	146	56	82
# SBT sightings/100 nm	2.62	1.43	1.42	1.02	1.48	1.22	0.75	1.38

Table 1: Search effort and sighting rates; entire Bight; 1993-2000.

The survey data have been analysed in different ways since the project started, and different analyses lead to different conclusions about possible trends in surface abundance. Several reviews of the project have been held to discuss the survey data, its analysis and interpretation. A workshop involving international experts was held in Port Lincoln in February 2000. The workshop agreed on a number of new approaches to the analysis of the survey data. These analyses are included in the 2000 Aerial Survey Report ([R4]). During the extended project we intend to investigate the reasons for the different trends given by different approaches, with the aim of deciding the most appropriate method of analysis.

The strip transect method of analysis is relatively simple, but does not adjust for differences in weather conditions between years. The second method of analysis, using a statistical modelling approach allows us to understand the relative importance of the different environmental variables with affect presence/absence and biomass of SBT.

To date, we have assumed that the apparent increase in surface abundance of SBT in higher air temperatures is related to the association between airtemperature and sea surface temperature (SST). Therefore we have only included either air temperature or SST in any model. In analyses including air temperature, there is a significant decline in presence/absence of SBT between 1993 and 2000. However, when SST is substituted for air temperature in these models, there is no significant decrease. It is necessary to study the SST/airtemperature relationship further to determine whether airtemperature, SST or both should be included in the model.

In 1999 and 2000, changes within the South Australian SBT industry meant that only one trained spotter was available to spot in each survey plane. As a result, we started to train young spotters to work in future aerial surveys. The effect of using trainee spotters is not clear – we are sure that they detected less than a trained spotter, but it is not clear exactly how much less. Consequently there is some uncertainty in the survey results for these two years.

The results of the strip transect analysis are shown in Figure 2. The 1999 and 2000 estimates lie between the two lines on the graph for those years. The use of trainee spotters has lead to additional uncertainty in the estimates and hence upper and lower limits for the estimates in those years are given in Figure 2. The method of calculating the limits is explained in more detail in [R4].

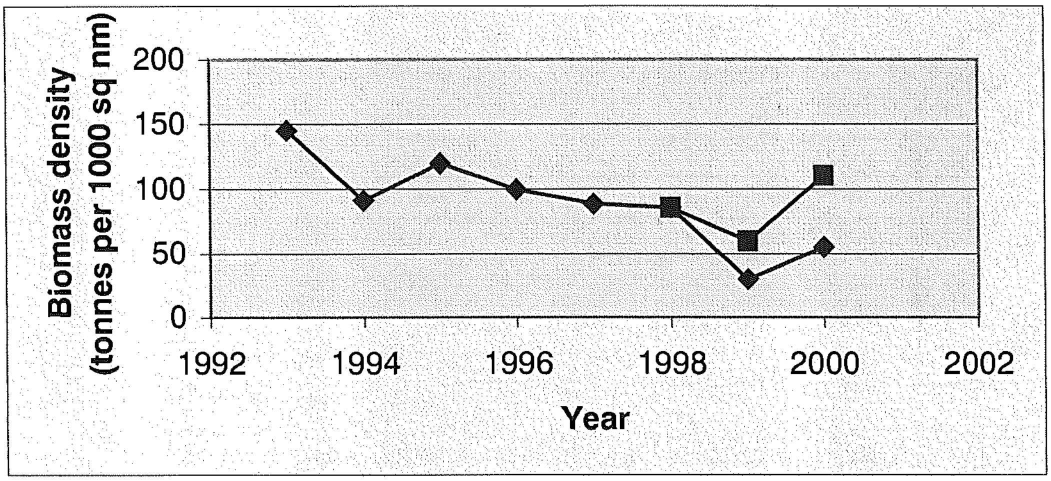

Figure 2: Annual estimates of surface biomass density of juvenile SBT in the GAB, 1993-2000, strip transect method.

The results of the strip transect analysis indicate that there has been no major increase or decrease in the surface biomass density of SBT between 1993 and 2000.

[O2(a)] Incorporation of environmental variables into the estimates

A method of estimating surface abundance which incorporated the varying environmental conditions during the surveys was introduced in the 1998 aerial survey report [R6].

Another method of incorporating environmental conditions into the survey was agreed to at the 2000 aerial survey workshop in Port Lincoln, and is included in the 2000 aerial survey report [R4]. This method allows us to give the annual surface abundance estimates at standardised environmental conditions, allowing direct year to year comparison of the estimates. However, as mentioned above, further work is needed to understand certain environmental associations before we can be confident of the results of these analyses.

[O2(b)] Incorporation of estimates of the proportion of SBT at the surface under various environmental conditions

In the 1997 analysis of five archival tags presented in [R14], the most effective explanatory variable was found to be time of day allowing for 4 different 24-hourly patterns during a lunar cycle, each pattern lasting for a week. During the week of the full moon, SBT tended to spend little time on the surface, whereas during the other weeks they spent more time on the surface. They also spend more time on the surface when the SST is high.

The fitted models had little explanatory power. This may be because the weather at sea may have little correlation with that at Ceduna weather station. Therefore for the 2000 analysis of this data, weather data was obtained from CSIRO's Division of Atmospheric Research.

In 1999, a more detailed classification of surfacing behaviours was introduced than that used in the previous analyses. This classification scheme (presented in [R5]) was used in analysis in [R7] in 2000. Using this classification scheme, the variables most strongly associated with surfacing rates were SST, depth, moon phase, month and air temperature. The tag-to-tag differences were also significant.

[O2(c)] Reduction of the sampling error in the estimates due to uncertainty in school size and fish size estimates.

The results of the LIDAR trial are given in [R3] and [R12]. They show that while LIDAR has the potential to measure fish size and patch size, the technology has not yet advanced sufficiently to allow school size and fish size to be routinely measured under field conditions. Further work is required on increasing the resolution and developing real time processing of the data. SBT are not highly reflective fish, especially when seen from above, which makes them difficult to see with a laser unless the resolution is improved sufficiently to considerably increase the contrast. Further technological development of the LIDAR instrument was not in the scope of this project. To date this research/development has not been completed as it requires funding by interested parties.

[R9, p38-39] gives a preliminary analysis of the age composition of SBT caught within individual patches in conventional tagging experiments carried out in the GAB between 1991 and 1997. The analysis shows that patches of fish do not comprise a single age of fish as had previously been assumed. Therefore the method used in the survey analyses to estimate abundance by ageclass in [R10] and [R11] will contain a large measure of error, as it involves attributing a single age to each sighting of SBT based on the estimated dominant ageclass. As such, in the 1999 and later reports, estimates by ageclass are not given.

A comparison of the fish size estimates given by the spotters in 2 planes in 1998 and 3 planes in 1999 and 2000 are shown in Figures 3-6. In each of these 3 years it is clear that there is little consistency in fish size estimates between spotters. This may be because of the large range of fish sizes within a patch and the short glimpse of fish obtained while circling the patches. This is further evidence that an alternative method of estimating abundance by age class should be developed if possible.

A comparison of the patch size estimates given by the spotters in 2 planes in 1998 and 3 planes in 1999 and 2000 are shown in Figures 7-10. There is remarkable consistency in patch size estimates between spotters. The correlation between the 1998 estimates is 0.78, and the correlation between the 1999 estimates is between 0.83 and 0.93 for the different pairs of spotters. Although one spotter's estimates are generally higher than those of the other spotters, because they are so highly correlated, they can be adjusted to a common level each year.

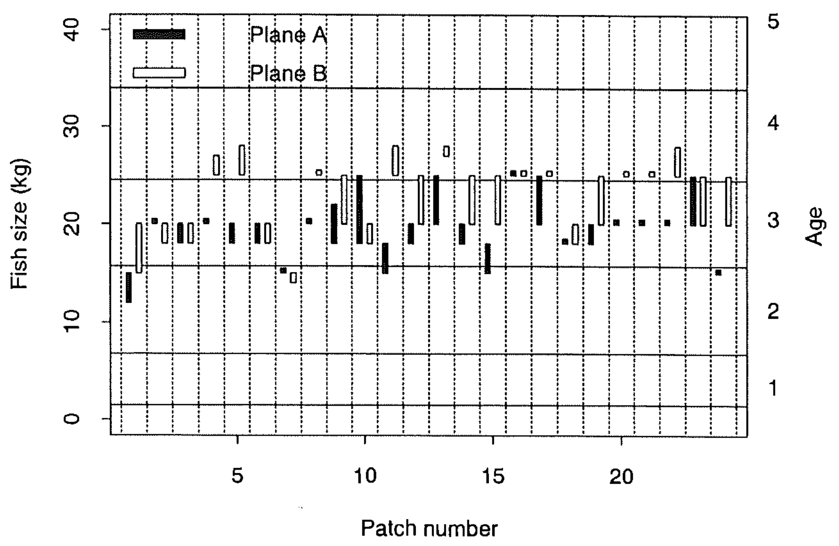

Figure 3: Spotters' fish size estimates, 2 plane experiment, 1998

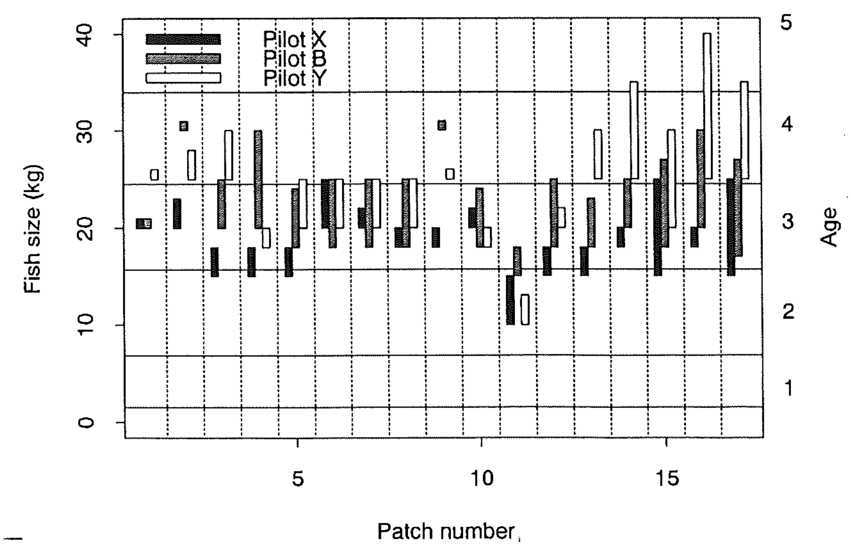

Figure 4: Spotters' fish size estimates, 3 plane experiment, 1999

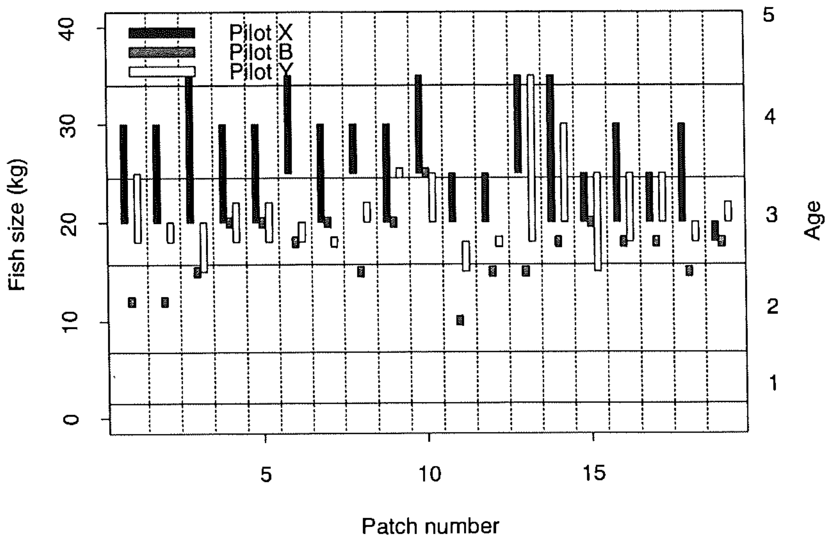

Figure 5: Spotters' fish size estimates, 3 plane experiment, 9 March 2000

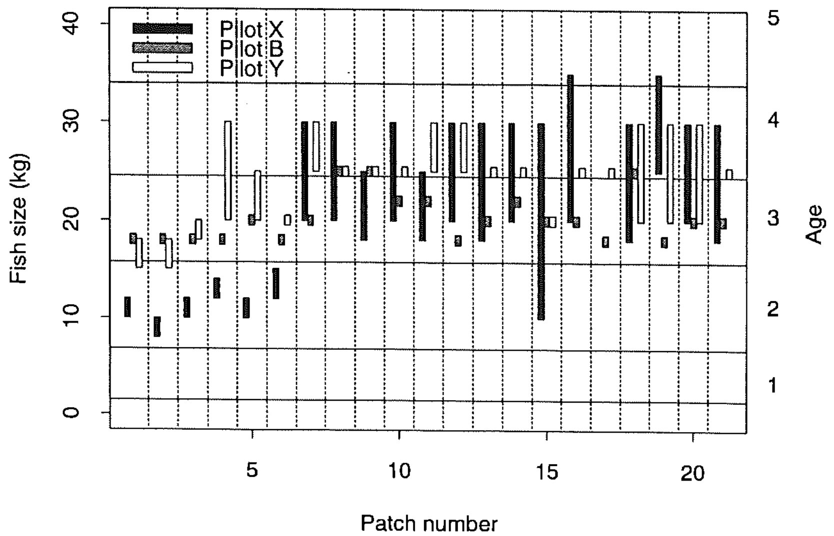

Figure 6: Spotters' fish size estimates, 3plane experiment, 10March 2000

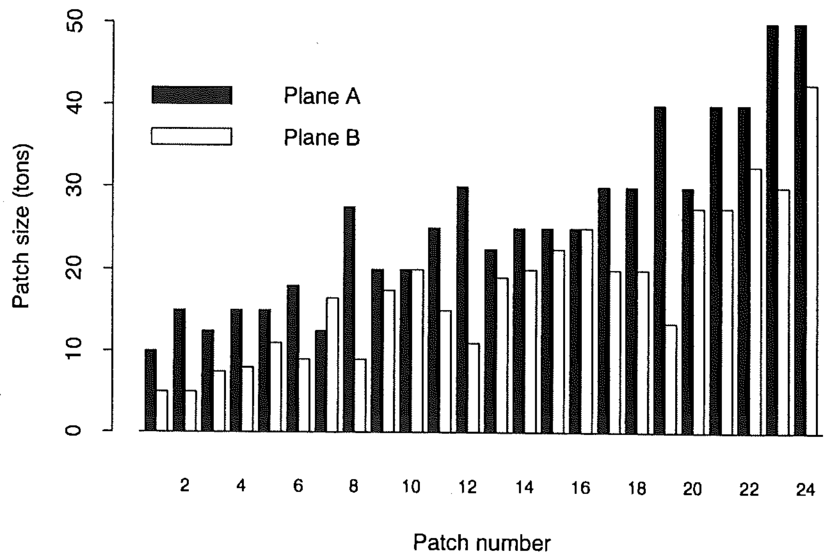

Figure 7: Spotters' patch size estimates, 2 plane experiment, 1998

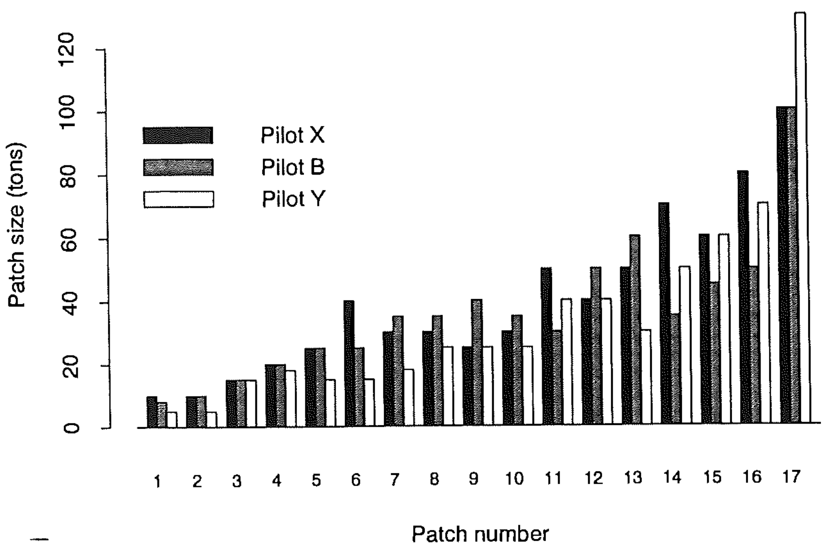

Figure 8: Spotters' patch size estimates, 3 plane experiment, 1999

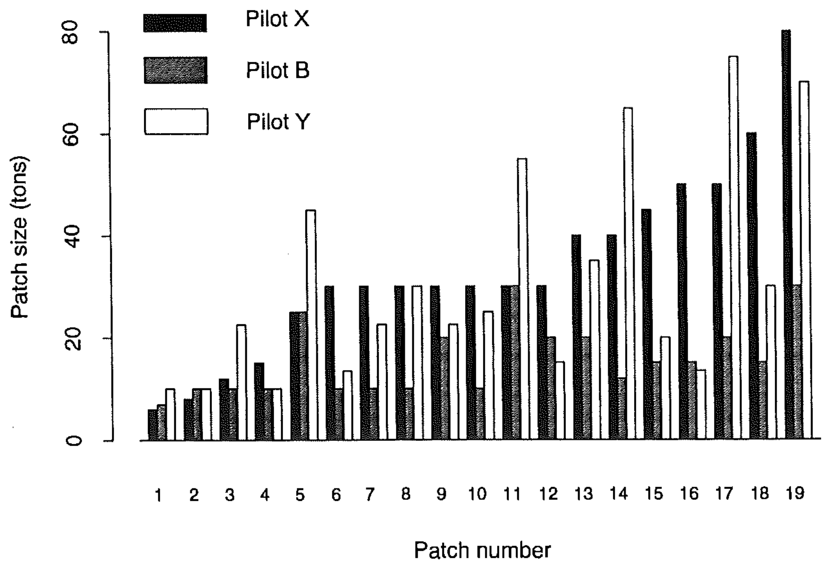

Figure 9: Spotters' patch size estimates, 3 plane experiment, 9 March 2000

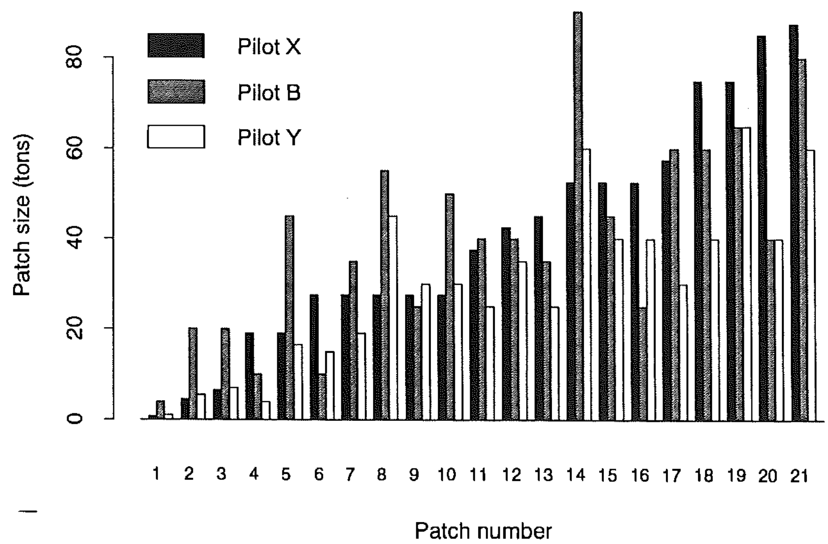

Figure 10: Spotters' patch size estimates, 3 plane experiment, 10 March 2000

[O3] To complete an evaluation of the usefulness of the indices of SBT abundance derived from the aerial survey.

The results from this project to date have shown that there are problems in the estimation of biomass by ageclass. The unreliability of these estimates means that only the estimates for pooled ageclasses are given in the later years of this project. The pooled estimates will have more limited use. The indices derived from the surveys to date provide a quantitative measure of surface abundance in the GAB. The results suggest that there may have been some increase or decrease in abundance since 1993, but the results since 1993 do not show any major change in abundance. A recruitment collapse has not occurred.

The surface abundance indices from the aerial surveys were presented at the 4th CCSBT Scientific Meeting, August 1998. The report of that meeting includes the following in the Advice and Recommendations section:

> "The meeting also recognised that information on recent recruitment based on tagging studies, aerial surveys and possibly acoustic surveys was critical for providing timely advice on stock status and future management. Lack of future aerial survey information would seriously affect current and future assessments.
>
> The meeting strongly recommends that the Commission note the priority research needs, and in particular, urge each member to support continuation of the aerial survey."

In 1997/1998 an internal review of the aerial survey was conducted. The project collaborators, CSIRO and NRIFSF, held a full review of the project in September 1999 ([R1], [R9]), and a further workshop attended by international experts was held in February 2000 in Port Lincoln ([R2]). These reviews have focussed on survey methodology and survey analysis.

At the STBMAC Research Sub-Committee Workshop on Future Directions for Recruitment Monitoring held in Port Lincoln in August 2000, a set of criteria against which to evaluate this project was proposed and the participants agreed with the criteria.

7. BENEFITS

The Australian SBT industry will benefit from the research, as improved and more timely assessment of the SBT resource will provide a better basis for setting catch limits.

8. FURTHER DEVELOPMENT

Considerable and significant progress has been made in the areas of developing the indices of surface abundance derived from the aerial surveys, understanding how environmental variation affects SBT surfacing behaviour, and analysing SBT surfacing behaviour. The extent of the data collected in this project is now greater than originally planned. New data include for example satellite sea surface temperature, data from the Bureau of Meteorology, and data collected in multiple plane experiments. These new data allow the development of a more detailed understanding of the processes governing the appearance and detection of surface schools of SBT in the GAB, and/or more understanding of the accuracy of the abundance estimates.

9. CONCLUSION

The results achieved to date in this project show that the majority of the goals of the project are likely to be achievable, but that to attain them at a level in which most of the information is extracted from the data will require further work after the completion of this project. This project has therefore been extended for a further two years.

10. ACKNOWLEDGMENTS

This research is part of a collaborative research project to monitor the abundance of Southern Bluefin Tuna that is being conducted between Australia (through the CSIRO) and Japan (through the National Research Institute of Far Seas Fisheries of the Japan Fisheries Agency). The research was funded by the Australian government and tuna industry through AFMA and FRDC, and the Japanese government through JAMARC.

We thank Song Chen, the scientist in charge of the aerial surveys in 1993--94; Barry Brady, Derek Hayman, Neville Harding, Lyall Jaensch, Andrew Jakobs, Milo Mislov, Kevin Warren, Tony Warren, Simon Bey, Chris McGown, Lana Schultz, Bob Stanley, Diane Stanton, Paul Waide and Mardi van der Weilen for their dedicated survey spotting and recording work in the 1993--2000 surveys; James Forbes, Helen Galea, Colin Millar and Jeremy O'Reilly of CSIRO Marine Laboratories for providing programming support to the project from 1993-2000; Jeff Cordell, Erik Madsen, Alex Papij and Matt Sherlock of CSIRO Marine Laboratories for providing electronic assistance; and Kevin Williams and Deidre Waddington for their support to the survey.

REFERENCES

[R1] Anon (1999). Aerial Survey Design Workshop. Caloundra, 1999.

[R2] Anon (2000). Report of the Aerial Survey Workshop. Port Lincoln, 2000.

[R3] Cowling, A (1997) Report on the LIDAR trials for 1997. RMWS/97/17. 1997 Recruitment Monitoring Workshop. Hobart.

[R4] Cowling, A (2000) Data analysis of the aerial surveys (1993-2000) for juvenile southern bluefin tuna in the Great Australian Bight. RMWS/00/3. 2000 Recruitment Monitoring Workshop. Hobart.

[R5] Cowling, A, Gunn, J and O'Reilly, J (1999). Integrated Analysis Project: a basis for improved annual estimates of SBT recruitment to the GAB. RMWS/99/10. 1999 Recruitment Monitoring Workshop. Caloundra.

[R6] Cowling, A and Millar, C (1998). Data analysis of the aerial surveys (1991-1998) for juvenile southern bluefin tuna in the Great Australian Bight. RMWS/98/3. 1998 Recruitment Monitoring Workshop. Hobart. Report for the CCSBT Scientific Meeting. CCSBT/SC/9807/8.

[R7] Cowling, A, Hobday, A, O'Reilly, J and Gunn, J (2000). 1999-2000 Integrated Analysis Project Report. RMWS/00/6. 2000 Recruitment Monitoring Workshop. Hobart.

[R8] Cowling, A and O'Reilly, J (1999). Data analysis of the aerial surveys (1993-1999) for juvenile southern bluefin tuna in the Great Australian Bight. RMWS/99/3. 1999 Recruitment Monitoring Workshop. Caloundra.

[R9] Cowling, A and O'Reilly, C (1999). Background to review of aerial survey. Caloundra, 1999.

[R10] Cowling, A, Polacheck, T and Millar, C (1996). Data analysis of the aerial surveys (1991-1996) for juvenile southern bluefin tuna in the Great Australian Bight. RMWS/96/4. 1996 Recruitment Monitoring Workshop. Hobart. Report for the CCSBT Scientific Meeting. CCSBT/SC/96/21.

[R11] Cowling, A, Polacheck, T and Millar, C (1997). Data analysis of the aerial surveys (1991-1997) for juvenile southern bluefin tuna in the Great Australian Bight. RMWS/97/4. 1997 Recruitment Monitoring Workshop. Hobart. Report for the CCSBT Scientific Meeting. CCSBT/SC/9707/21.

[R12] Griffis, A (1997) Report on the 1997 LIDAR trial. RMWS/97/5. 1997 Recruitment Monitoring Workshop. Hobart.

[R13] Kloser, R (1998). Assessment of acoustics as a research tool to determine the distribution, biomass and behaviour of southern bluefin tuna schools and their prey in the Great Australian Bight. RMWS/98/6. 1998 Recruitment Monitoring Workshop. Hobart.

[R14] Millar, C and Cowling, A (1997) SBT Surfacing Behaviour. RMWS/97/26. 1997 Recruitment Monitoring Workshop. Hobart.

APPENDIX 1: INTELLECTUAL PROPERTY

APPENDIX 2: STAFF

Staff engaged on the project:
Dr Ann Cowling
Mr Colin Millar
Mr Jeremy O'Reilly

RMWS/97/ 4

Data Analysis of the Aerial Survey (1991-1997) for Juvenile Southern Bluefin Tuna in the Great Australian Bight

Ann Cowling, Colin Millar, Tom Polacheck
CSIRO Division of Marine Research
PO Box 1538
Hobart, Tasmania, 7001

Data Analysis of the Aerial Surveys (1991–1997) for Juvenile Southern Bluefin Tuna in the Great Australian Bight

Ann Cowling　　Colin Millar　　Tom Polacheck

June 1997

Abstract

The 1997 aerial survey was conducted over the Great Australian Bight between 2 January 1997 and 20 March 1997. Annual aerial surveys have been conducted since 1991 based on line transect methodology. The data from the surveys have been used to provide annual surface abundance indices of juvenile SBT. A major advantage of an aerial survey is that a high proportion of the survey area can be searched in each replicate. The same level of coverage and number of replicates would be prohibitively costly for any ship based survey.

The 1991 survey was conducted in much higher average windspeeds than the later surveys, so the 1991 results are not strictly comparable to those of the later surveys. The surface biomass estimates for any year range between 48.6 and 163.5 tonnes/1000 sq nm and the surface sighting density estimates range between 1.05 and 2.21 sightings/1000 sq nm. There are no statistically significant trends in the biomass estimates, either increasing or decreasing. However, there is some slight but not statistically significant evidence of a decrease in abundance between 1993 and 1997.

Surface abundance indices by age-class are also calculated from the surveys. Three year old fish are estimated to be the most abundant, followed by 2 then 4 year olds. Very few sightings of 0, 1 or 5 year-olds are made. The year to year variation in the abundance estimates for 3 year olds is very similar to that in the indices for juvenile SBT.

There is considerable variation in the surface abundance estimates between replicates in any year. This variation is thought to be in part due to changes in environmental conditions between replicates, affecting the proportion of SBT at the surface. Environmental conditions also affect the ability of the spotters to detect surface schools but the estimation procedure adjusts for differences in detectability in different replicates, removing this source of variation from the estimates.

The extent to which variation in the surface abundance estimates follows variation in the true abundance is unknown. If the proportion of SBT of any age-class in the Bight during the survey period is relatively constant from year to year, and if the proportion of schools on the surface during the survey can be relatively well modelled, the surface abundance estimates will provide a good index of juvenile abundance. It is only when there is sufficient overlap with VPA recruitment estimates that it will be possible to evaluate the extent to which the aerial survey provides a reliable estimate of recruitment (assuming that the VPA estimates are extremely reliable).

Contents

List of Tables

List of Figures

1 Introduction

All recent assessments of the southern bluefin tuna (SBT) population agree that the parental biomass is at very low levels. However, substantial uncertainty and disagreement exists about the probability of the stock recovering while catches remain at their current levels. A significant source of uncertainty is the lack of reliable estimates of recruitment or the number of young fish that have entered the population in the past few years. It is these young fish that will form the parental stock in the future and provide the potential for rebuilding of the stock.

The current analytical assessment methods for SBT have a 4 to 5 year time lag in the estimates of the number of recruits due to time lags in receiving catch data and the lack of any index of juvenile abundance. Current trends in recruitment remain one of the major unknowns in evaluating the status of this stock and its potential to rebuild under current catch levels. Moreover, little fishery independent information on stock or juvenile abundance exists. Lack of such information is a major limitation to improving the precision of the more recent abundance estimates from the VPA assessments.

There are major difficulties in obtaining fishery-based indices of abundance for 1–5 year olds. The surface fishery does not provide interpretable CPUE indices of 1–3 year olds (in part because the use of aerial spotting means that there is no simple relationship between sighting effort and fishing mortality rates) and these ages are not well represented in the longline catches. In addition, the longline CPUE-based indices, particularly for younger ages (4–5 year olds), may not be reliable because of contractions in the fishery, changes in targeting practices and technological improvements.

Recent scientific and management meetings on SBT have considered the development of a fishery independent index of SBT recruitment to have a very high research priority. In response to this need, a developmental aerial survey project was initiated in 1990/91, and annual surveys have been conducted during the summer fishing season over the Great Australian Bight (GAB) since then. The main objectives of the survey are:

1. to estimate the surface abundance of SBT in the Bight region during the summer season of each survey year,

2. to establish a relative abundance index of SBT recruitment over a medium to long term time span.

The aerial survey is based on line transect methodology (Burnham et al (1980), Buckland et al (1993)). Line transect methodology accounts for the decreasing probability of detecting objects located further from the trackline, and also for the higher probability of detecting larger objects (schools) than small ones at greater distances from the trackline. Line transect methods have been used for many years to estimate the abundance of terrestrial animal and marine mammal populations. However, most aerial surveys for pelagic fish species have not used them. We are not aware of any other line-transect-based aerial surveys to construct a consistent time series of relative abundance indices for a wide-ranging and highly mobile pelagic fish.

The ability of the aerial survey indices to detect temporal trends in the actual population will depend upon the variability associated with the index and the length of the time series. It is unlikely that temporal trends can be detected until we have accumulated comparable survey data for another 2–4 years.

In Section 2 of this report, we review the three different survey designs used in 1990/91, 1992 and 1993–1997. In Section 3, we describe the field methods used in the survey. In Section 4, we outline the statistical methods used in the data collection and analysis, and in Section 5, we give the results of the data analysis. In Section 6, we describe the environmental conditions experienced during each survey season. Finally, in Section 7, we discuss the results, and their implications. Appendices 1–5 contain more detailed results of the data analysis.

2 Survey design

The 1990/91 and 1992 surveys were designed and conducted by David Morgan (Morgan 1991, 1992). The 1993–1997 surveys have used a design developed from the results of the previous surveys at a workshop attended by Japanese and Australian scientists in 1992. Spatial stratification is used to control spatial heterogeneity; restrictions on survey operations are used to minimise changes in surfacing probability; block structure, synopticity and replication are used to minimise temporal variability.

The 1993–1997 design has been used for 5 years now, and sufficient data has been collected for a preliminary review of its effectiveness, and some suggestions for changes. The design was discussed in the light of the accumulated sighting data in Cowling et al (1996). It is clear that there is considerable scope for increasing the efficiency of the design. However, design changes should be made only infrequently in order to maintain the continuity of the series, and therefore if changes are made, they should be based on a considered review of sufficient data, and should be such that the continuity of the series is maintained.

Meaningful comparisons of the survey results between years can only be made if the data is consistent from year to year. Therefore, before presenting the survey results, we examine the differences in the three survey designs. The most important differences between the 1993–1997 surveys and the two previous surveys are in the area surveyed, and the different weather conditions for survey operation in 1991. There are also differences in the amount of survey effort, the stratification used, and the shape of the trackline.

2.1 1990/91 survey

The 1990/91 survey (Morgan 1991) was a feasibility study. The survey area comprised four fixed 1° bands of longitude (128–129°W, 130–131°W, 132–133°W, and 134–135°W) across the Bight. The formal survey was run from November 1990 to April 1991, with some SBT surfacing trials conducted after April.

Four zones were defined within each band: coastal, mid-shelf, shelf-edge and off-shelf zones. These zones did not constitute a statistical stratification as each zone was given the same search effort/unit area. The survey data showed that relatively few sightings were made in the off-shelf zone, and so in the following surveys the off-shelf zone was deleted.

The transect lines of the 1990/91 survey comprised fixed north/south and random east/west lines: Figure 2.1 on page 6 shows the transect lines of the fifth replicate.

The 1990/91 survey flew when the wind speed at the sea surface was below 12 knots. However, the survey data showed that few sightings were made when the wind speed was over 10 knots. Thus in the following years, the survey only started in sea surface winds of 8 knots or less and remained operating if the wind speed was less than 10 knots.

2.2 1992 survey

Because of funding constraints, the 1992 survey (Morgan 1992) was restricted to two months and a limited area. It operated only in January and February, and covered just the two eastern 1° bands (132–133°W, 134–135°W). Its aims were to focus on specific methodological and design aspects of the survey. As mentioned above, it excluded the off-shelf stratum and flew only in winds of 10 knots or less. The survey used the same transect line design as the 1990/91 survey.

2.3 1993–1997 surveys

The 1993–1997 surveys were conducted between 1 January and 31 March each year over the GAB between 128°W and 135°W, from the coast to the 700–800 meter depth contour of the continental shelf; see Figure 2.2.

At the 1992 Survey Design Workshop (Anon (1992)), experienced commercial SBT spotters reported that abundance is higher in the inshore and shelf-edge regions of the survey area, and extremely high in three small areas ("hot spots") in the easternmost block. The survey area was therefore divided into inshore, middle, shelf-edge and hot-spot strata within which the spotters believed the SBT abundance to be relatively homogeneous. More survey effort was placed in these three high abundance strata to improve the precision of the estimates (Buckland et al (1993)). The trackline consisted of randomly positioned north/south lines, connected in the inshore and shelf-edge strata with zig-zag lines. This trackline placement ensured that, within each stratum, all areas had an equal probability of being searched.

For SBT schools to be detected, the environmental conditions must be suitable for them to surface, and weather conditions must be suitable for aerial spotting. To maximise the probability of detecting any schools of SBT present on the surface, the aerial survey operates only between 11 am (true local time) and dusk, and only if

- there is less than 1/3 coverage of low cloud
- visibility at 1500 ft is greater than 5 n.mile

- the wind speed at the sea surface is 8 knots or less (and up to 10 knots if the survey has started.

The 1994–97 surveys used two planes in January and February in order to increase the survey effort and reduce sampling error. The 1994, 1995 and 1997 surveys continued until late March, but there was insufficient funding available for this in 1996.

Weather fronts move from west to east across the Bight. In Anon (1992) it was suggested based on commercial spotting experience that windows of acceptable weather for the survey often occur in north/south bands of about 1.5° of longitude. The survey area was therefore divided into 5 parallel blocks, each less than 1.5 degrees wide, running from the coast to the shelf-edge. A replicate of the survey can sometimes be completed in a single window of good weather as it crosses the Bight from west to east, surveying the blocks from west to east but it may take up to 3 weeks to complete a replicate. Two planes operating in different (but often adjacent) blocks have been used since 1994, showing that the band of acceptable weather is usually greater than 3 degrees wide.

Each replicate is treated as giving a snapshot view of the spatial distribution of surface schools in the Bight at a particular time. The survey is replicated as many times as funding, weather and time permit.

The remaining source of variability in the surface abundance estimates is changes in the proportion of the SBT population of any age in the survey area. This variation cannot be removed by the survey design. For more detail on the previous and current aerial survey designs, see Morgan (1991), Morgan (1992), Anon (1992).

In Section A.7.3 of Cowling et al (1996), the southernmost limit of the survey area was discussed, and it was recommended that in a redesigned survey, the southern boundary should be extended. An experimental 5th stratum was therefore added to the 1997 survey including deeper water (up to 1500m) than that surveyed in 1993–1996 (up to 800m); see Figure 2.3. This area was surveyed in 1991 and a reasonably high abundance of SBT was found in some parts. The additional area lies to the south of Blocks 1 to 4. Block 5 already includes this depth of water. Low survey effort was placed in this stratum. The additional trackline was surveyed, leaving from the southernmost point of the middle NS transect. The positions of the new design points are shown in Table 2.1.

2.4 Comparability of data sets

The 1990/91 survey had 9 replicates of data collected between November 1990 and April 1991, with the first 3 replicates in 1990, Replicates 4 to 8 from January to March 1991 (apart from one block in Replicate 4 surveyed in December 1990), and Replicate 9 in April 1991. The 1992 to 1996 surveys were all conducted between 1 January and 31 March. There were 5 replicates of the survey in 1992, 4 replicates in 1993, 8 replicates in 1994 and 1995, 7 replicates in 1996 and 5 replicates in 1997.

Based on the differences in survey timing, location and conditions, the following data selection plan was used to allow valid comparisons between years.

1. To make the 1990/91 survey comparable with the 1993–1997 surveys, only the survey effort and sightings made between January and March 1991, in the survey area enclosed by the boundaries shown in Figure 2.2, and in wind speeds less than 10 knots were included. This makes the survey period, area and wind condition comparable to the 1993–1997 surveys. From now on, we shall call this subset of the 1990/91 dataset the 1991 survey.

2. To compare the 1992 survey with the other surveys, we give estimates for the eastern Bight. We use only those parts of the 1991 and 1992 data inside the boundaries of Blocks 4 and 5 (the easternmost blocks; see Figures 2.1 and 2.2).

The basic unit for the statistical analysis is a sighting and abundance estimates based on line transect theory require the assumption that sightings are made independently (see for example Ripley (1981, p140)). The definition of an independent sighting in the aerial survey presents some difficulties because surface patches (single tightly packed groups) tend to occur in clusters. The distance between patches varies from less than one nm to several nm. We need a rule specifying the maximum distance between patches in the same sighting. Such a rule has been developed over the seven years of the survey. However, there is a difference in the rule used in 1991 and 1992 and the rule used after that. What we would now define as one sighting with two patches was previously called two sightings, each with one patch. Therefore in the 1991 and 1992 surveys we expect to find a higher encounter rate (n/L) and smaller mean sighting size than in the later surveys.

The variable scale and amount of spatial clustering of the sightings is shown in Figures 2.4 to 2.6. Some areas have no sightings and other areas have a number of sightings. The figure also shows that there is temporal variation in the location of the sightings from one replicate to another. There is also temporal variation within a replicate — it takes between 3 days adn 3 weeks to complete surveying the 5 blocks in one replicate.

There is another difference between the 1991 and 1992 surveys and the later surveys. In the earlier surveys the spotters estimated the average size of the patches (in tonnes) and the average size of the fish within each patch (in kg) in each sighting whereas in the later surveys they estimated the size of each patch and the size of fish in each patch in each sighting.

Tables 2.2 and 2.3 give the amount of survey effort and number of sightings each year for the entire Bight and the eastern Bight. Table 2.2 shows that the encounter rates for the entire Bight were very similar in 1991, 1994, 1995 and 1997, lower in 1996, and almost double in 1993. In the eastern Bight, the 1996 sighting rate was well below the rates for all previous years of the survey. However, encounter rate is a raw measure of abundance—it is confounded by detectability, and so these figures should be interpreted with great caution and formal interpretation should only be made in combination with estimates adjusted for detectability.

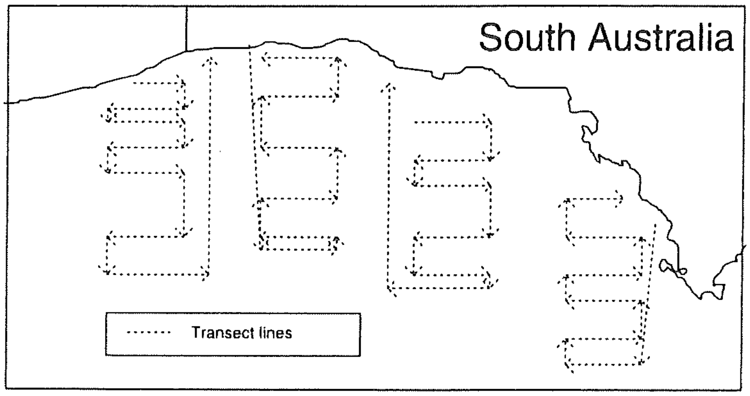

Figure 2.1: Design of 1991 survey showing the area covered, and the transect lines of the 5th replicate

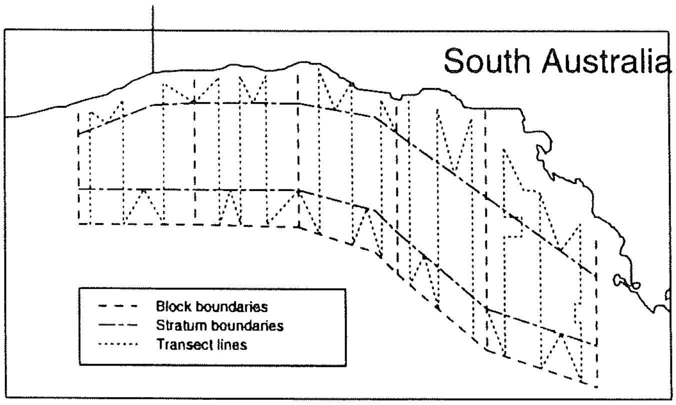

Figure 2.2: Design of 1993–1996 surveys showing the area covered, the block and stratum boundaries, and the transect lines of the 5th replicate of the 1995 aerial survey

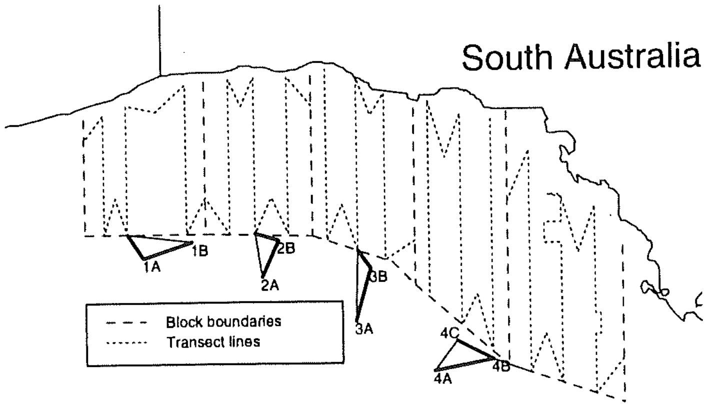

Figure 2.3: The additional way points for the 1997 aerial survey

1A	-33.933	128.75	-33°56'	128°45'
1B	-33.733	129.383	-33°44'	129°23'
2A	-34.183	130.3	-34°11'	130°18'
2B	-33.717	130.517	-33°43'	130°31'
3A	-34.75	131.517	-34°45'	131°31'
3B	-34.083	131.717	-34°05'	131°43'
4A	-35.4	132.533	-35°24'	132°32'
4B	-35.25	133.3	-35°15'	133°18'
4C	-35.017	132.833	-35°01'	132°53'

Table 2.1: Positions of the new design points

1997, Replicate 1

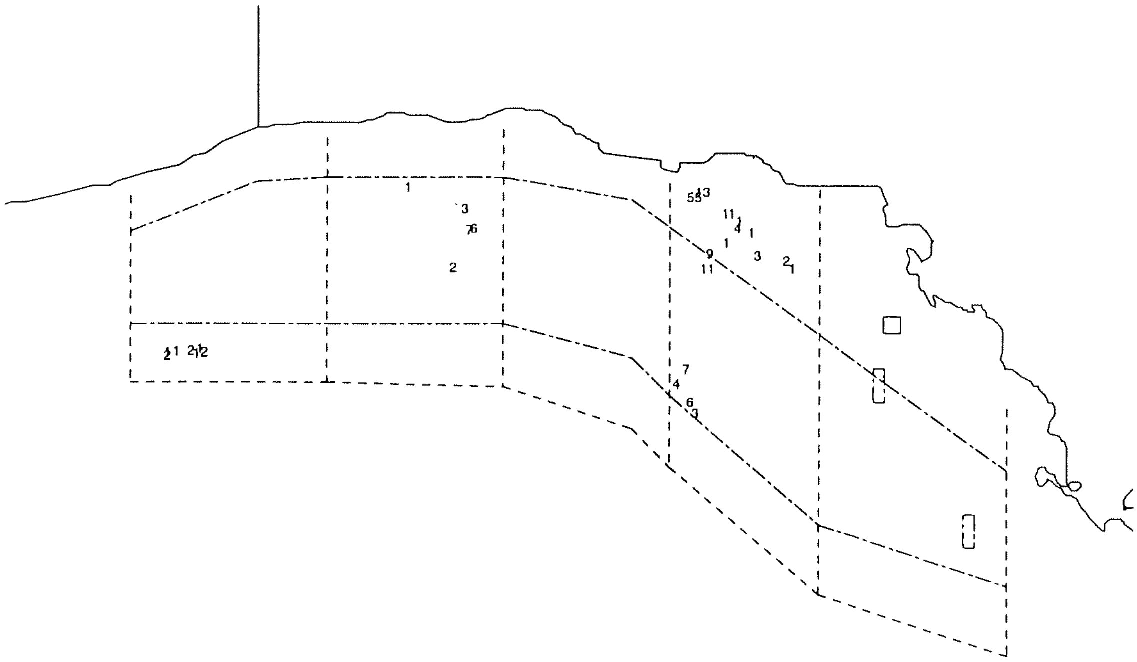

1997, Replicate 2

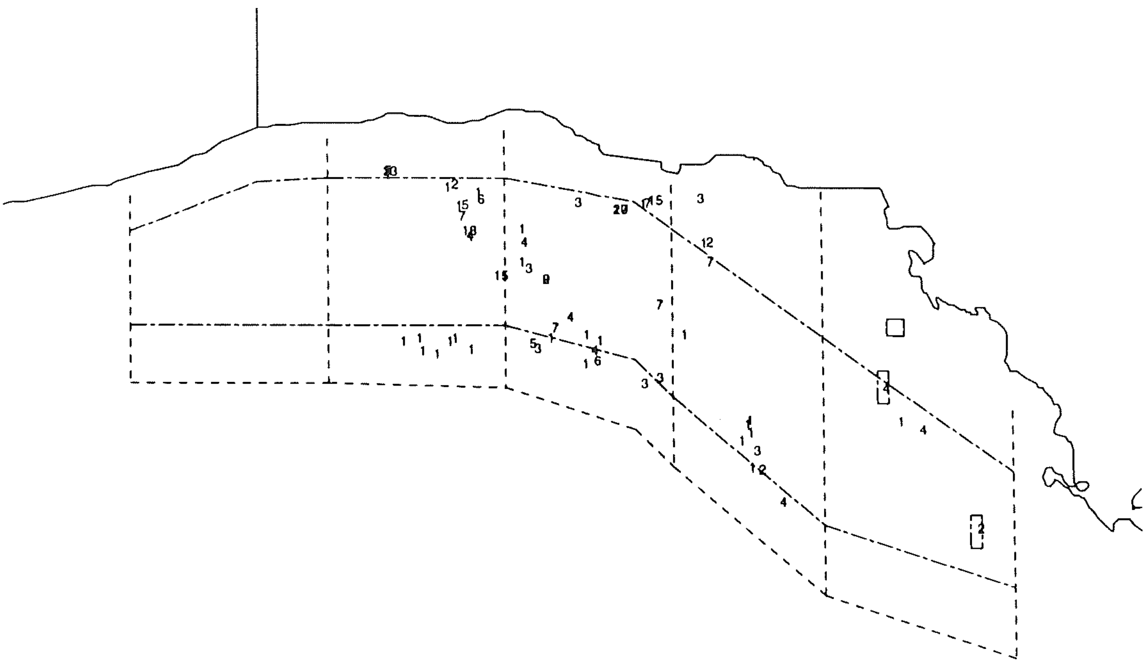

Figure 2.4: Location of SBT sightings in 1997 survey; Replicates 1 and 2. The numbers show the number of patches in each sighting.

1997, Replicate 3

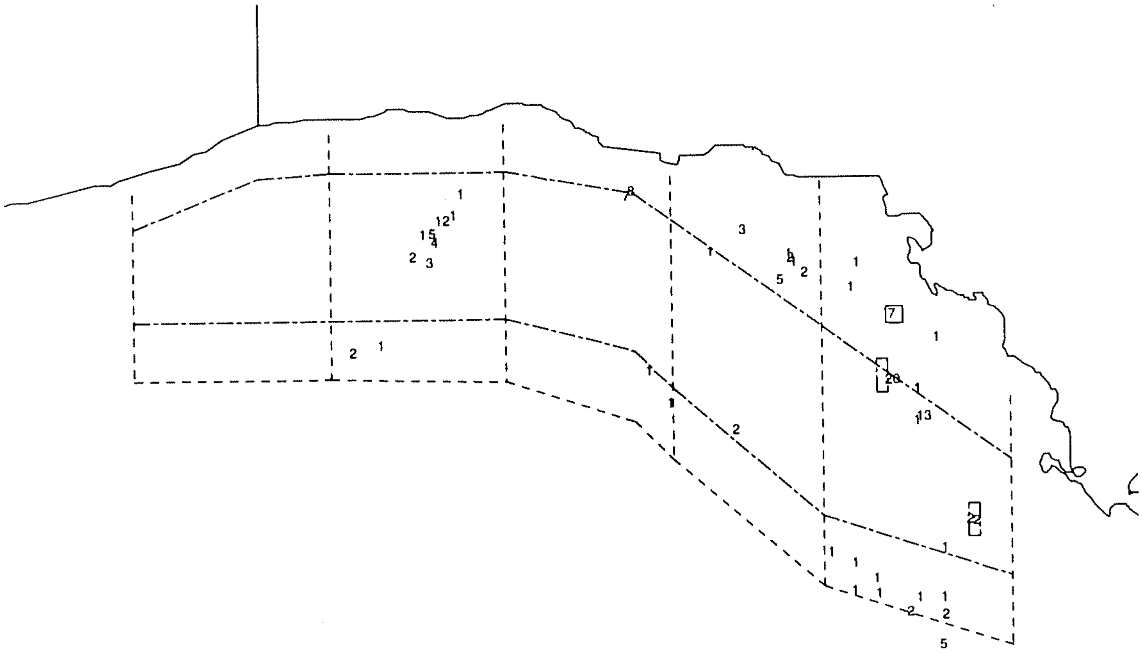

1997, Replicate 4

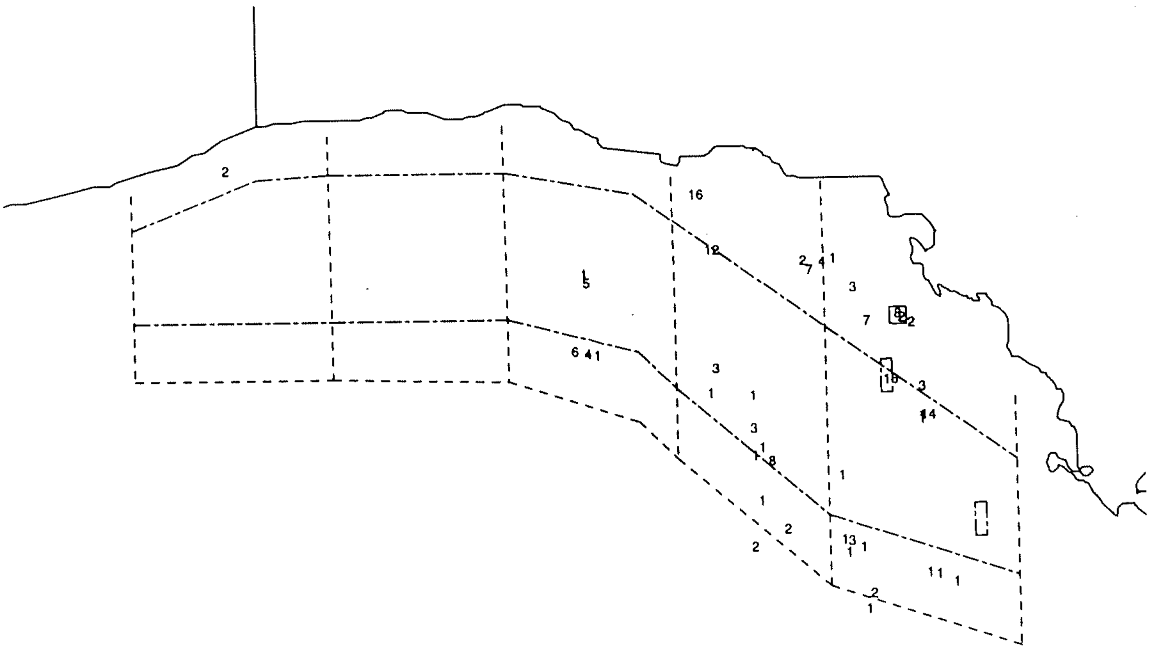

Figure 2.5: Location of SBT sightings in 1997 survey; Replicates 3 and 4. The numbers show the number of patches in each sighting.

1997, Replicate 5

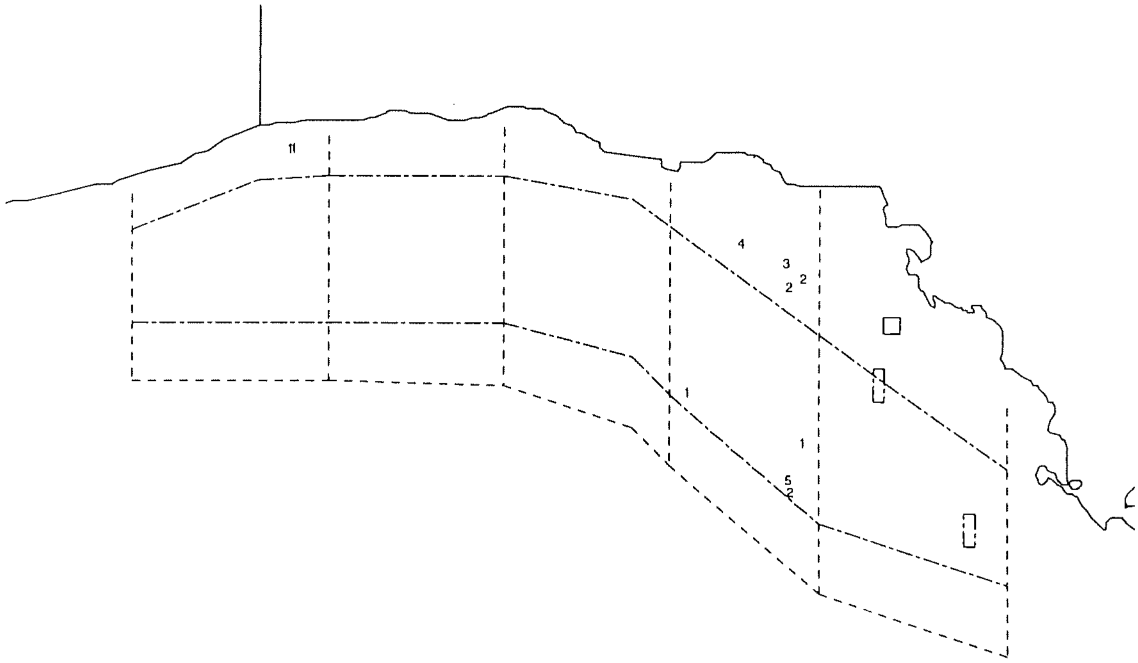

Figure 2.6: Location of SBT sightings in 1997 survey; Replicate 5. The numbers show the number of patches in each sighting.

	1991	1993	1994	1995	1996	1997
No of replicates completed	5	4	8	8	7	5
Total flying time	NA	213	405	438	332	287
Total time in effort	75	112	214	206	171	129
Total Nm searched in effort	7,587	10,174	20,191	20,793	18,265	12,845
No of SBT sightings (0–5 yr olds)	106	267	289	295	186	189
No of SBT sightings per 100 Nm	1.40	2.62	1.43	1.42	1.02	1.47

Table 2.2: Search effort and sighting rates; entire Bight; 1990/91 and 1993–1997; excluding additional 5th stratum surveyed in 1997.

	1991	1992	1993	1994	1995	1996	1997
No of replicates completed	5	4	4	8	8	7	5
Total flying time	NA	87	NA	NA	NA	NA	NA
Total time in effort	43	45	52	93	92	75	58
Total Nm searched in effort	3,442	3,741	4,562	8,896	9,245	8,577	5,796
No of SBT sightings (0–5 yr olds)	68	90	133	152	147	57	109
No of SBT sightings per 100 Nm	1.98	2.41	2.92	1.71	1.59	0.66	1.88

Table 2.3: Search effort and sighting rates; eastern Bight; 1991–1997. Note that from the 1991 and 1992 surveys, only the sightings and transect lines lying in Blocks 4 and 5 of the 1993–1997 surveys (ie west of 132° 18') have been included.

3 Field methods

The survey plane is a Rockwell Aerocommander 500S fitted with an automatic pilot so the pilot can work as a spotter, an infra-red radiation thermometer for estimating sea-surface temperature, and a global positioning system (GPS). Two experienced tuna spotters, one of whom is also the pilot, sit in the front seats of the plane. Flying along a transect line at 120 knots and an altitude of 1500 ft, the spotters scan the sea surface through 90° from dead ahead to abeam of the plane, searching for surface schools of SBT. A data recorder behind them records environmental and sighting information and monitors the electronic equipment recording sea-surface temperature and position.

There is good visibility through the front and side windows of an Aerocommander. At 1500 ft, the area from directly below the plane to about 400 m in front of the plane and to about 100 m to the side of the plane is not visible.

When a sighting of SBT is made, the GPS position is recorded (P_1). The plane continues along the transect line until the pilot judges that the school is at 90° to the plane, when another waypoint is recorded (P_2). At this point, the plane leaves the transect and flies directly to the school and circles it. The two spotters independently estimate a range for the size of individual fish in each patch (in kg) and the size of each patch (in tonnes). Another waypoint is recorded (P_3) directly over the centre of the school, and the plane flies back to P_2 to resume searching the transect at the point of departure.

Environmental observations are recorded at the start and end of each transect and at 30 minute intervals during the transect. The observations include wind speed and direction, air temperature, bearing of sun relative to transect line, amount of high and low cloud, glare, haze and swell. For each sighting of SBT, in addition to the waypoints and estimates, the time at which each waypoint is reached, and the behaviour of the fish are recorded. Behaviour is described as "deep" or "shallow", and "feeding", "rippling" or "flattening".

The perpendicular distance from the school to the transect line is calculated as the perpendicular distance between the point P_3 and the line joining P_1 and P_2. Point estimates of fish and school size are obtained as the midpoint of the corresponding range. The biomass estimates are produced based on the spotters' size estimates.

To ensure that the two planes implement the survey procedures consistently and to allow for cross comparison of fish and school size estimates, each pilot flies the same plane throughout the survey but the spotters change planes after each replicate and the data recorders after every second replicate.

The spotters' size estimates are based on many years of commercial spotting experience, and calibration of the estimates with the subsequent catches by fishing boats. Chen and Polacheck (1993) give more detailed information on the school size and fish size estimates, and the calculation of sighting distances. The continuity in spotters has contributed consistency to the size estimates: only six spotters have been used since 1991, although the same four have been employed in each of the last three surveys.

4 Statistical methodology

The main objective of the statistical analysis of the aerial survey data is to develop an annual index of relative abundance for juvenile SBT, which provides a reliable measure (in terms of bias and variance) of the annual trends in the global abundance of juvenile SBT, preferably by age. The current analysis gives two indices of abundance: D_0, the mean density of SBT sightings during the survey period in the survey area, and D_1, the mean surface biomass density during the survey period in the survey area. Other indices could be developed based on alternative statistical estimators. These could include estimators which incorporate factors for temporal variation in abundance or surfacing rates during any year's survey.

4.1 Estimation of abundance from a replicated survey

The surface abundance of SBT in the GAB varies through the survey period, with highest abundance often occurring between mid-January and late-February. This variation may be due to changes in the true abundance in the survey area during the 3 months of the survey (due to movement in or out of the area, removals or natural mortality), or due to changes in surfacing behaviour during the survey.

The survey is replicated, and both the surface abundance and its variance can be estimated for each replicate. We give two statistical models for the surface abundance estimate in any replicate of the survey in a particular season, and for each model, give the mean surface abundance estimate and its variance.

Model 1

Let $\hat{D}_i$ be the estimate of surface abundance (D_0 or D_1) in the i-th replicate. In this model, $\hat{D}_i$ estimates the surface abundance of SBT in the survey area at the time of replicate i. This potentially varies through the survey period, and so the expected value of $\hat{D}_i$ varies through the survey.

$$\hat{D}_i = D_i + \epsilon_i, \qquad i = 1, \ldots, r$$

where $E(\epsilon_i) = 0$, $\mathrm{var}(\epsilon_i) = \sigma_i^2$, r is the number of replicates, and the ϵ_i are independent. ϵ_i is the estimation error measuring the variation in the estimated abundance about the true abundance.

In this model, $E(\hat{D}_i) = D_i$, and $\mathrm{var}(\hat{D}_i) = \sigma_i^2$. The mean abundance D over the survey period and its variance are estimated by

$$\hat{D} = \frac{1}{r}\sum_{i=1}^{r} \hat{D}_i, \tag{4.1}$$

and

$$\widehat{\mathrm{var}}(\hat{D}) = \frac{1}{r(r-1)}\sum_{i=1}^{r}(\hat{D}_i - \hat{D})^2. \tag{4.2}$$

Then,

$$E\{\widehat{\text{var}}(\hat{D}_i)\} = \frac{1}{r}\left[\frac{1}{r-1}\left\{\sum_{i=1}^{r} D_i^2 - \frac{1}{r}\left(\sum_{i=1}^{r} D_i\right)^2\right\} + \frac{1}{r}\sum_{i=1}^{r}\sigma_i^2\right].$$

Clearly, there are two components to $\widehat{\text{var}}(\hat{D})$. The first is variation in abundance between replicates and the second is estimation error.

Model 2

In this model, $\hat{D}_i$ estimates the surface abundance of the SBT population which has a random component which varies around an annual mean. Thus the expected value of $\hat{D}_i$ is constant, and variation in abundance between replicates is a random effect. For this model to be appropriate, the replicates should be surveyed at random times through the survey period.

$$\hat{D}_i = D_i + \epsilon_i, \qquad i = 1, \ldots, r$$

We assume that the ϵ_i are independent, $E(\epsilon_i) = 0$, $\text{var}(\epsilon_i) = \sigma_i^2$, $\text{var}(D_i) = \rho^2$, and that ρ^2 and ϵ_i are independent for all i. Thus ρ^2 is the between replicates variance. Then

$$E(\hat{D}_i) = D,$$

and again, we estimate D and its variance by (4.1) and (4.2). Again,

$$E\{\widehat{\text{var}}(\hat{D}_i)\} = \frac{1}{r}\left(\rho^2 + \frac{1}{r}\sum_{i=1}^{r}\sigma_i^2\right),$$

with two components, between replicates variance and estimation error.

These two models are analogous to fixed and random effect models in ANOVA. Note that the two models yield exactly the same estimate for mean density and its variance. However, model structure is important when developing a model accounting for variation in abundance between replicates, and also for survey design.

For either model, the variance of the mean abundance estimate in (4.2) should be can be decreased by increasing the number of replicates of the survey. The estimation error component of the variance can be reduced by good survey design and estimation techniques (see also Section 4.2). It is estimated by

$$\widehat{\text{var}}_e(\hat{D}_i) = \frac{1}{r^2}\sum_{i=1}^{r}\widehat{\text{var}}(\hat{D}_i).$$

4.2 Estimation of abundance from a line transect survey using the kernel method

Juvenile SBT are found in surface schools of widely varying sizes throughout the survey area. The number of sightings decreases with distance from the trackline, and large schools are detectable at greater distances than small schools (Figure 4.1).

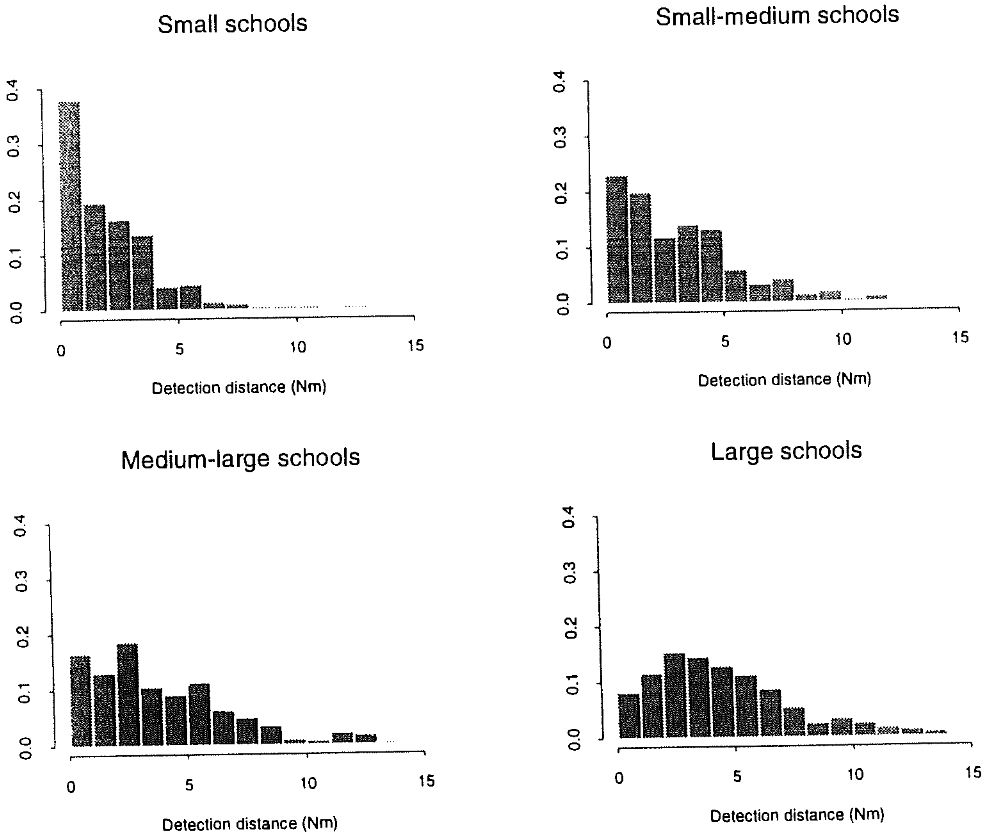

Figure 4.1: Histograms of the marginal *pdf* of the detection distance x for different sizes of schools; pooled 1993–1996 data.

To remove possible bias due to the differential detectability of small and large schools, both the detection distance, x, and the size of the school, y, have been incorporated in the probability density function (*pdf*) of detected schools, $f(x, y)$ in several ways; see for example Drummer and McDonald (1987), Quang (1991), Buckland et al. (1993), Chen (1996b). All of these approaches use the fundamental relationships

$$D_0 = E(n)\, f(0)/2L \quad \text{and} \quad D_1 = E(n)\, \beta(0)/2L$$

derived, for example, in Buckland et al. (1993) and Quang (1991) respectively. Here, n is the total number of sightings, L is the total length of the transect lines, f is the marginal *pdf* of the perpendicular sighting distance x, and $\beta(0) = \int_0^\infty y f(0, y)\, dy$.

It is assumed in these approaches that all surface schools on the trackline are detected. However, even if this is not the case, provided the probability of detecting schools on the trackline is relatively constant from year to year, we will still obtain a valid relative index of abundance.

The estimates of D_0 and D_1 are given by

$$\widehat{D}_0 = n\, \hat{f}(0)/2L \quad \text{and} \quad \widehat{D}_1 = n\, \hat{\beta}(0)/2L, \tag{4.3}$$

where $\hat{f}(0)$ and $\hat{\beta}(0)$ are estimates of $f(0)$ and $\beta(0)$ respectively. The variances of $\widehat{D}_0$ and $\widehat{D}_1$ (estimation error component) and are estimated by

$$\widehat{\mathrm{var}}_e(\hat{D}_0) = \frac{1}{4}\Big[\{\hat{f}(0)\}^2 \widehat{\mathrm{var}}\left(\frac{n}{L}\right) + \left(\frac{n}{L}\right)^2 \widehat{\mathrm{var}}\{\hat{f}(0)\}\Big], \tag{4.4}$$

and

$$\widehat{\mathrm{var}}_e(\hat{D}_1) = \frac{1}{4}\Big[\{\hat{\beta}(0)\}^2 \widehat{\mathrm{var}}\left(\frac{n}{L}\right) + \left(\frac{n}{L}\right)^2 \widehat{\mathrm{var}}\{\hat{\beta}(0)\}\Big], \tag{4.5}$$

where, writing k for the number of transect lines surveyed, n_i for the number of sightings in transect line i, and l_i for the length of transect line i,

$$\widehat{\mathrm{var}}\left(\frac{n}{L}\right) = \frac{1}{k-1}\sum_{i=1}^{k} \frac{l_i}{L}\left(\frac{n_i}{l_i} - \frac{n}{L}\right)^2.$$

The estimation error component of the variance of the abundance estimates can be minimised by good survey design to minimise $\widehat{\mathrm{var}}(n/L)$, and choosing an efficient technique for estimating $f(0)$ and $\beta(0)$ which gives a low value for $\widehat{\mathrm{var}}\{\hat{f}(0)\}$ and $\widehat{\mathrm{var}}\{\hat{\beta}(0)\}$. In a well designed survey, the transect lines are placed so that the observed values of n_i/l_i are as even as possible for all transect lines, while still ensuring representative coverage. Therefore, the transect lines should be placed parallel to any density gradient; Buckland et al. (1993).

To analyse the SBT aerial survey data, we use the non-parametric kernel estimator of $f(x, y)$ (Chen 1996a, 1996b). Kernel estimates have the three important properties that Burnham et al (1980) recommended for robust estimation of abundance from line transect survey data: they are model robust, pooling robust, and fit the shape criterion $\frac{\partial}{\partial x} f(x, y)\Big|_{x=0} = 0, \forall y$. In an empirical study of common abundance estimators, Chen (1996b) shows that the kernel estimator also has the fourth property: it is more efficient than other common estimators. In addition, they implicitly take account of the distance r between the observer and the detected object, which is explicitly allowed for in hazard rate models. These estimates are asymptotically unbiased.

The kernel estimates of $f(0)$ and $\beta(0)$ are given by (see Chen 1996b, page 1288 and equation (4.4) on page 1287)

$$\hat{f}(0) = \frac{1}{n}\sum_{i=1}^{n}\frac{2}{h_{xi}}K(x_i/h_{xi})$$

and

$$\hat{\beta}(0) = \frac{1}{n}\sum_{i=1}^{n}\frac{4}{h_{xi}}\phi(x_i/h_{xi})[y_i\{\Phi(y_i/h_{yi}) - 1/2\} + h_{yi}\phi(y_i/h_{yi})]$$

where K is the Gaussian kernel, ϕ and Φ are the density and distribution function of a $N(0,1)$ random variable, h_{xi} and h_{yi} are the appropriate adaptive bandwidths for each equation as described in Chen 1996b, and n is the number of sightings.

To estimate $\text{var}\{\hat{f}(0)\}$, write $Z_i = \frac{2}{h_{xi}}K(x_i/h_{xi})$ and note that the Z_i are independent (approximately) and identically distributed random variables and that $\hat{f}(0) = \bar{Z}$. Therefore

$$\widehat{\text{var}}\{\hat{f}(0)\} = \frac{1}{n(n-1)}\Big\{\sum_{i=1}^{n(n-1)} Z_i^2/n - \hat{f}(0)^2\Big\}.$$

Then to estimate $\text{var}\{\hat{\beta}(0)\}$, write $Z_i = \frac{4}{h_{xi}}\phi(x_i/h_{xi})[y_i\{\Phi(y_i/h_{yi}) - 1/2\} + h_{yi}\phi(y_i/h_{yi})]$, so that

$$\widehat{\text{var}}\{\hat{\beta}(0)\} = \frac{1}{n(n-1)}\Big\{\sum_{i=1}^{n} Z_i^2/n - \hat{\beta}(0)^2\Big\}.$$

In each case, the Z_i are only approximately independent as the adaptive bandwidths used in each Z_i are calculated using all the sightings. These estimates of variance and bootstrap estimates of $\text{var}\{\hat{f}(0)\}$ and $\text{var}\{\hat{\beta}(0)\}$ will be performed before the 1998 analysis.

4.3 Estimation of abundance in the aerial survey

In previous analyses of the aerial survey data we gave two sets of abundance estimates, pooled estimates and replicate estimates. In the pooled estimates, $f(0)$ and $\beta(0)$ were estimated separately in each of the four survey strata using the combined data from all replicates. In the replicate estimates, $f(0)$ and $\beta(0)$ were estimated separately in each stratum within each replicate. Abundances were then estimated for each replicate of the survey. The pooled estimates of abundance for each replicate were not independent because of the common $f(0)$ and $\beta(0)$ used in all replicates. In the replicate estimates, there were insufficient data in each stratum within replicate for reliable estimation of $f(0)$ and $\beta(0)$, although abundances were estimated independently in each replicate.

In the 1997 analysis we estimate $f(0)$ and $\beta(0)$ separately in each replicate. This gives independent estimates of abundance in each replicate and corrects for differences in detectability due to changing conditions between replicates (eg weather conditions, school sizes, etc). In the 1997 analysis, the tabulated standard errors for mean abundance estimate are the total variance given in (4.2). Tabulated standard errors for any replicate are the estimation error component of variance. In previous analyses, the tabulated standard errors for mean abundance estimates were only the estimation error component of the variance given in (4.4) and (4.5). The calculation of the estimation error component has been revised (corrected) in the 1997 analysis (see below).

In the 1997 analysis, we give two sets of estimates. In the first set (ee estimates), only sightings and effort from the north/south transects are used (ie the zig-zag transect lines are omitted). Thus there is equal survey effort in all spatial strata; in the second set (ue estimates), all the data is used. The unequal survey effort in the survey strata is reflected in the analysis.

In calculating the total variance using (4.2), abundance must be independently estimated in each replicate of the survey. This means that $f(0)$ and $\beta(0)$ must be independently estimated in each replicate using only the sightings from that replicate. An analysis using all the sightings made during the surveys would be preferred. This would require a stratified analysis recognising the unequal survey effort in the various survey strata and estimating $f(0)$ and $\beta(0)$ in each stratum. The replicate estimates in the previous analyses of the data did this. However, there were insufficient sightings in each stratum within each replicate to reliably estimate $f(0)$ and $\beta(0)$.

The advantage of the ue estimates is that they do use all the sightings from all the surveys, but they pool the data from all strata within each replicate to estimate $f(0)$ and $\beta(0)$. Thus they are only partially stratified and may therefore be biased if $f(0)$ and $\beta(0)$ vary between the survey strata. The advantage of the ee estimates is that by using only the sightings from the north/south transects there is equal survey effort in all strata. They are unbiased and the pooling robustness property of the estimators provides robustness against spatial variation in abundance within any replicate. Their disadvantages are that they do no use all the sightings (effectively "wasting" data) and may have a higher variance due to lower survey effort (total transect length surveyed). The two estimators are further discussed with reference to the actual estimates obtained in Section 4.4.

The method of estimating the age of SBT in each sighting is described and discussed in Section 5.4.

ee estimates

The school density and biomass estimates for age-class a in replicate r ($\hat{D}_{0ar}$ and $\hat{D}_{1ar}$) are given by

$$\hat{D}_{0ar} = \frac{n_{ar}\hat{f}_{ar}(0)}{2L_r} \quad \text{and} \quad \hat{D}_{1ar} = \frac{n_{ar}\hat{\beta}_{ar}(0)}{2L_r},$$

where n_{ar} is the number of sightings of age-class a SBT in replicate r and L_r is the total transect length in replicate r (omitting the zig-zag transect lines).

Estimates of mean school density and biomass for age-class a ($\hat{D}_{0a}$ and $\hat{D}_{1a}$) during the survey period are given by

$$\hat{D}_{0a} = \frac{1}{r}\sum_r \hat{D}_{0ar} \quad \text{and} \quad \hat{D}_{1a} = \frac{1}{r}\sum_r \hat{D}_{1ar},$$

with estimated variances of

$$\widehat{\text{var}}(\hat{D}_{0a}) = \frac{1}{r(r-1)} \sum_{i=1}^{r} (\hat{D}_{0ar} - \hat{D}_{0a})^2 \quad \text{and} \quad \widehat{\text{var}}(\hat{D}_{1a}) = \frac{1}{r(r-1)} \sum_{i=1}^{r} (\hat{D}_{1ar} - \hat{D}_{1a})^2,$$

comprising both between replicate variance and estimation error. It should be noted that there is a component of variance due to estimating the age of the fish which has not been taken into account in these variance estimates.

Estimates of total (all ages) school density and biomass in replicate r ($\hat{D}_{0r}$ and $\hat{D}_{1r}$) are given by

$$\hat{D}_{0r} = \frac{n_r \hat{f}_r(0)}{2L_r} \quad \text{and} \quad \hat{D}_{1r} = \frac{n_r \hat{\beta}_r(0)}{2L_r},$$

where n_r is the number of sighting in replicate r (ommiting the zig-zag transect lines).

Estimates of total (all ages) mean (over replicates) school density and biomass ($\hat{D}_0$ and $\hat{D}_1$) are given by

$$\hat{D}_0 = \frac{1}{r} \sum_r \hat{D}_{0r} \quad \text{and} \quad \hat{D}_1 = \frac{1}{r} \sum_r \hat{D}_{1r}.$$

The estimation error components of these variances are estimated by

$$\begin{aligned}
\widehat{\text{var}}_e(\hat{D}_{0far}) &= \frac{1}{4}\left[\{\hat{f}_r(0)\}^2 \widehat{\text{var}}\left(\frac{n_{ar}}{L_r}\right) + \left(\frac{n_{ar}}{L_r}\right)^2 \widehat{\text{var}}\{\hat{f}_r(0)\}\right], \\
\widehat{\text{var}}_e(\hat{D}_{1ar}) &= \frac{1}{4}\left[\{\hat{\beta}_r(0)\}^2 \widehat{\text{var}}\left(\frac{n_{ar}}{L_r}\right) + \left(\frac{n_{ar}}{L_r}\right)^2 \widehat{\text{var}}\{\hat{\beta}_r(0)\}\right], \\
\widehat{\text{var}}_e(\hat{D}_{0r}) &= \frac{1}{4}\left[\{\hat{f}_r(0)\}^2 \widehat{\text{var}}\left(\frac{n_r}{L_r}\right) + \left(\frac{n_r}{L_r}\right)^2 \widehat{\text{var}}\{\hat{f}_r(0)\}\right], \\
\widehat{\text{var}}_e(\hat{D}_{1r}) &= \frac{1}{4}\left[\{\hat{\beta}_r(0)\}^2 \widehat{\text{var}}\left(\frac{n_r}{L_r}\right) + \left(\frac{n_r}{L_r}\right)^2 \widehat{\text{var}}\{\hat{\beta}_r(0)\}\right], \\
\widehat{\text{var}}_e(\hat{D}_{0a}) &= \frac{1}{r^2} \sum_r \widehat{\text{var}}(\hat{D}_{0ar}), \\
\widehat{\text{var}}_e(\hat{D}_{1a}) &= \frac{1}{r^2} \sum_r \widehat{\text{var}}(\hat{D}_{1ar}), \\
\widehat{\text{var}}_e(\hat{D}_0) &= \frac{1}{r^2} \sum_r \widehat{\text{var}}(\hat{D}_{0r}), \quad \text{and} \\
\widehat{\text{var}}_e(\hat{D}_1) &= \frac{1}{r^2} \sum_r \widehat{\text{var}}(\hat{D}_{1r}).
\end{aligned}$$

ue estimates

In this analysis we recognise the survey strata. Let w_s be the weight of stratum s (proportional to the area of stratum s). The school density and biomass estimates for age-class a in stratum s in replicate r ($\hat{D}_{0asr}$ and $\hat{D}_{1asr}$) are given by

$$\hat{D}_{0asr} = \frac{n_{asr} \hat{f}_{ar}(0)}{2L_{sr}} \quad \text{and} \quad \hat{D}_{1asr} = \frac{n_{asr} \hat{\beta}_{ar}(0)}{2L_{sr}},$$

where n_{asr} is the number of sightings of age-class a SBT in stratum s of replicate r and L_{sr} is the total transect length in stratum s of replicate r (now including the zig-zag transect lines).

Estimates of mean school density and biomass for age-class a during the survey period are given by

$$\hat{D}_{0a} = \frac{1}{r}\sum_r\sum_s w_s\hat{D}_{0asr} \quad \text{and} \quad \hat{D}_{1a} = \frac{1}{r}\sum_r\sum_s w_s\hat{D}_{1asr}.$$

Estimates of total (all ages) school density and biomass in stratum s in replicate r ($\hat{D}_{0sr}$ and $\hat{D}_{1rs}$) are given by

$$\hat{D}_{0sr} = \frac{n_{sr}\hat{f}_r(0)}{2L_{sr}} \quad \text{and} \quad \hat{D}_{1sr} = \frac{n_{sr}\hat{\beta}_r(0)}{2L_{sr}}. \tag{4.6}$$

Combining over strata, estimates for replicate r are

$$\hat{D}_{0r} = \sum_s w_s\hat{D}_{0sr} \quad \text{and} \quad \hat{D}_{1r} = \sum_s w_s\hat{D}_{1sr}.$$

Thus the estimate of mean total (all ages) school density and biomass are given by

$$\hat{D}_{0} = \frac{1}{r}\sum_r\sum_s w_s\hat{D}_{0sr} \quad \text{and} \quad \hat{D}_{1} = \frac{1}{r}\sum_r\sum_s w_s\hat{D}_{1sr}.$$

The estimation error components of these variances are estimated by

$$\begin{aligned}
\widehat{\text{var}}_e(\hat{D}_{0a}) &= \frac{1}{4r^2}\sum_r\left[\{\hat{f}_{ar}(0)\}^2\sum_s w_s^2\widehat{\text{var}}\left(\frac{n_{asr}}{L_{sr}}\right) + \left(\sum_s w_s\frac{n_{asr}}{L_{sr}}\right)^2\widehat{\text{var}}\{\hat{f}_{ar}(0)\}\right],\\
\widehat{\text{var}}_e(\hat{D}_{1a}) &= \frac{1}{4r^2}\sum_r\left[\{\hat{\beta}_{ar}(0)\}^2\sum_s w_s^2\widehat{\text{var}}\left(\frac{n_{asr}}{L_{sr}}\right) + \left(\sum_s w_s\frac{n_{asr}}{L_{sr}}\right)^2\widehat{\text{var}}\{\hat{\beta}_{ar}(0)\}\right],\\
\widehat{\text{var}}_e(\hat{D}_{0r}) &= \frac{1}{4}\left[\{\hat{f}_{r}(0)\}^2\sum_s w_s^2\widehat{\text{var}}\left(\frac{n_{sr}}{L_{sr}}\right) + \left(\sum_s w_s\frac{n_{sr}}{L_{sr}}\right)^2\widehat{\text{var}}\{\hat{f}_{r}(0)\}\right],\\
\widehat{\text{var}}_e(\hat{D}_{1r}) &= \frac{1}{4}\left[\{\hat{\beta}_{r}(0)\}^2\sum_s w_s^2\widehat{\text{var}}\left(\frac{n_{sr}}{L_{sr}}\right) + \left(\sum_s w_s\frac{n_{sr}}{L_{sr}}\right)^2\widehat{\text{var}}\{\hat{\beta}_{r}(0)\}\right],\\
\widehat{\text{var}}_e(\hat{D}_{0}) &= \frac{1}{r^2}\sum_r\widehat{\text{var}}(\hat{D}_{0r}), \quad \text{and}\\
\widehat{\text{var}}_e(\hat{D}_{1}) &= \frac{1}{r^2}\sum_r\widehat{\text{var}}(\hat{D}_{1r}).
\end{aligned}$$

Tabulated standard errors

In this report, when tabulating standard errors, we give the total error calculated using (4.2) for all mean (over replicates) abundance estimates (ie the total abundance estimates and the age-class estimates), and the estimation error component of variance for estimates are given for abundance estimates for each replicate..

In the age-class abundance estimates, there is an additional component of variance due to the estimation of the age of the fish in each patch, which has not been taken into account in estimating the total error. At present we do not have any data with which to assess this component of variance. SBT patches commonly consist of a range of sizes of fish but the size range has not been taken into account in estimating the variance of age-class abundance estimates. Neither has growth of SBT over the 3 months of the survey been taken into account in estimating the age of schools, although 2 year-olds may grow by 40% and 3 year olds by 20% over this time.

4.4 Comparison of ee and ue abundance estimates

The ee estimates are systematically higher than the ue estimates (compare Tables A.1 and A.2, and A.3 and A.4, and note that as the survey effort was not stratified in 1991 and 1992, ue estimates are not given for these years). This suggests that one set may be biased.

1. The ee estimates could be biased because of the low numbers of detections per replicate used in the kernel estimator, which is only asymptotically unbiased.
2. The ue estimates could be biased as the estimate within any stratum is only partially stratified. There are insufficient sightings within some strata and replicates to separately estimate $f(0)$ and $\beta(0)$ within these strata and replicates and so pooled (over strata) estimates of $f(0)$ and $\beta(0)$ are used. If $f(0)$ and $\beta(0)$ vary between the survey strata the ue estimates will be biased.

Comparing estimates of $f(0)$ and $\beta(0)$ in each replicate for ee and ue analyses (Tables A.5 and A.6, and A.7 and A.8), the estimates are not systematically higher for either analysis. Thus the lower number of detections used in estimating $f(0)$ and $\beta(0)$ in the ee estimates would not appear to be the source of the bias.

We consider now whether $f(0)$ and $\beta(0)$ vary between strata within a replicate. Previous analyses have shown (for example Cowling et al (1996, p41)) that schools are largest in the inshore region and smallest in the shelf-edge stratum, and it is known that large schools are detectable to a greater distance from the transect line than small schools. This indicates that $f(0)$ and $\beta(0)$ do vary between inshore and shelf-edge strata in any replicate. We therefore believe that it is the ue estimates that are biased. They are lower than the ee estimates because $\sum_s w_s \frac{n_{sr}}{L_{sr}}$ is lower than $\frac{n_r}{L_r}$.

In view of the bias in the ue estimates the ee estimates are preferred, and are tabulated in all summary tables. There is a tendency for the ee estimates to have a higher estimate of total error than the ue estimates, but the difference is not usually large. The tendency of the variance of the ue estimates to be lower than that of the ee estimates is likely to be a result of the considerably higher survey effort rather than a result of survey stratification.

Survey stratification results in a gain in the precision of survey estimates if the density of sightings within any stratum is relatively homogeneous and if the allocation of survey effort to each stratum has been made to minimise the variance of the final density estimate for fixed total line length (this is known as optimal allocation). In the aerial survey, the density of sightings within strata is not homogeneous (see Figure 2.4 to 2.6) and the allocation of survey effort to each stratum is not close to optimal allocation.

4.5 Estimation of mean school size

A size-bias corrected estimator of the mean school size, $\widehat{SS}$, is given by

$$\widehat{SS} = \widehat{D}_1/\widehat{D}_0,$$

where $\widehat{D}_1$ and $\widehat{D}_0$ are given in (4.3). The bootstrap is used to calculate the variance of the size estimates in each replicate, and is also used to bias-correct the estimates $\widehat{SS}$. These estimates are given in Table A.9 in Appendix A.2 for 1991 and 1993–1997, using the N/S transects (ee data). The table also gives the mean school sizes unadjusted for size-bias, $\bar{y}$. The difference between the size-bias corrected mean school size ($\widehat{SS}$) and the unadjusted mean school size ($\bar{y}$) demonstrates again that there is size bias present in the sightings (see also Figure 4.1).

5 Surface abundance estimates; 1991–1997

In this section we give summaries of the ee estimates of SBT abundance for 2–4 year olds in the entire Bight, the eastern Bight and by age-class. The effect of the environmental conditions is discussed in Section 6. More detailed tables showing the ee and ue estimates by replicate are found in Appendix A.1 on page 42, where tables giving the specific components of the density estimates are also given (eg $\hat{f}(0)$ and $\hat{\beta}(0)$).

5.1 Surface abundance estimates; entire Bight; 1991 and 1993–1997

The annual mean surface abundance estimates are given in Table 5.1 and Figure 5.1.

In general $\hat{D}_1$ has a higher *cv* then $\hat{D}_0$. This is because of the additional variation in $\hat{D}_1$ due to including estimates of the mean school size. However the information on school biomass in $\hat{D}_1$ makes it the more useful index for stock assessment purposes.

Both series indicate that there has been no abrupt change in recruitment over the survey period. Further, the biomass estimates in Figure 5.1 can be interpreted as indicating that there has been a slight increase, slight decrease or no change in biomass abundance over the 7 year period.

In the 1991 and 1992 surveys a different definition of sighting was used than in later years and the spotters estimated the average size of patches and average size of SBT within each patch in each sighting whereas in later years they gave separate estimates for each patch. (See Section 2.4). The difference in definition of sighting would be expected to show in the average number of patches per sighting (Tables A.10 and A.11). These tables suggest a slight increase in the number of patches per sighting over the period of the survey suggesting the need to further refine the definition of a sighting to ensure consistency between years. The varying definitions of sighting would lead to a slight decrease in $\widehat{D}_0$ over the survey if abundance was constant. However it would not affect $\widehat{D}_1$, as this would be self-correcting.

The different methods of estimating the biomass of a sighting should not affect the average size of sighting, but Table A.12 shows that in 1991 the average size of a sighting was somewhat lower than in later years. However the 1991 survey was conducted in generally higher wind-speeds than the later surveys (Figure 6.1) and in higher wind-speeds school size estimates tend to be lower than in low wind-speeds (Figure A.8), possibly explaining this difference. The different wind condition in the 1991 survey suggest that in spite of the efforts made to make the data sets comparable, the 1991 biomass estimates should be regarded as possibly different.

However, the issue of how much of the variability in patch size is true year to year variation and how much is estimation error remains to be answered. The use of LIDAR or sonar in conjunction with the aerial survey may help resolve this question.

Ignoring the 1991 biomass estimate, the 1993–1997 biomass estimates suggest a slightly declining trend in surface biomass over the 5 year period, although it is not statistically significant. It is not clear why the surface biomass estimate was lower in 1994 than in other years, but it is not significantly lower than 1993 or 1995 at the 95% level.

5.2 Surface abundance estimates; eastern Bight; 1991–1997

The annual mean surface abundance estimates are given in Table 5.2 and Figure 5.2.

The surface biomass and sighting density estimates for the eastern Bight both indicate no abrupt change in recruitment. Ignoring the 1991 biomass estimates, the 1992–1997 biomass estimates are consistent with a slight increase or a slight decrease in biomass. However, any change is not statistically significant.

Year	No of sightings n	Transect length L	Biomass estimate ($\widehat{D}_1$)	Sighting density estimate ($\widehat{D}_0$)	School size E(y)
1991	96	7,587	48.6 (25.4)	1.28 (0.69)	45.7 (20.0)
1993	169	7,495	163.5 (57.6)	2.21 (0.29)	72.0 (21.1)
1994	213	15,112	89.8 (12.8)	1.33 (0.38)	87.4 (19.2)
1995	211	14,503	159.5 (37.8)	2.09 (0.27)	74.2 (13.2)
1996	146	13,204	112.6 (32.4)	1.05 (0.24)	86.9 (22.8)
1997	142	9,091	110.0 (29.3)	1.41 (0.34)	68.9 (11.9)

Table 5.1: Estimated surface abundance of 2–4 year-old SBT; entire Bight; 1991 and 1993–1997; equal effort (ee) estimates

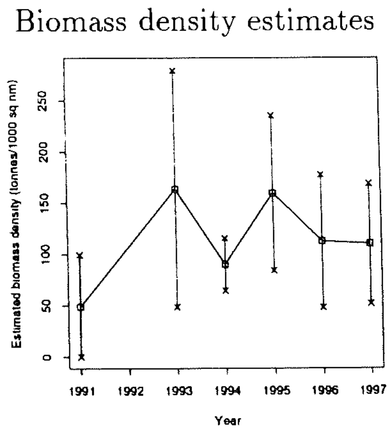

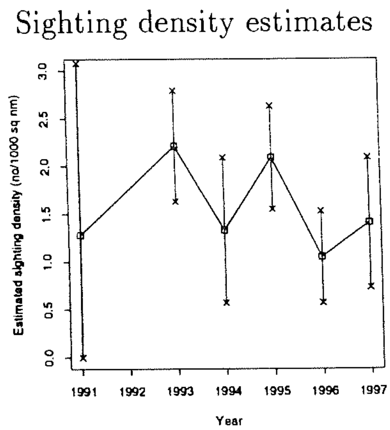

Figure 5.1: Abundance estimates; entire Bight; 1991 and 1993–1996. Estimate shown by □. Vertical bars show 2 standard errors above and below the estimate. Plot on left is $\widehat{D}_1$, and on the right is $\widehat{D}_0$.

Year	No of sightings n	Transect length L	Biomass estimate $(\widehat{D}_1)$	Sighting density estimate $(\widehat{D}_0)$	School size E(y)
1991	62	3,442	56.4 (25.1)	1.43 (0.64)	25.0 (12.6)
1992	64	2,833	162.9 (94.1)	2.02 (0.38)	68.2 (24.5)
1993	94	3,494	177.2 (89.2)	2.55 (0.97)	87.3 (42.5)
1994	118	6,817	113.7 (21.9)	1.67 (0.54)	188.2 (114.3)
1995	90	6,343	173.5 (50.9)	2.26 (0.49)	82.0 (22.6)
1996	41	6,337	53.0 (29.1)	0.55 (0.28)	68.2 (35.8)
1997	84	4,117	157.9 (46.9)	1.68 (0.37)	85.3 (25.1)

Table 5.2: Estimated surface abundance of 2–4 year-old SBT; eastern Bight; 1991–1997; equal effort (ee) estimates

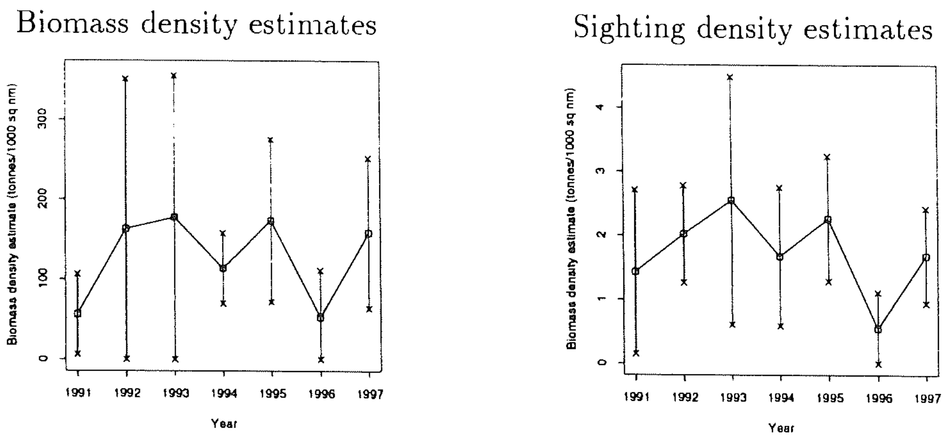

Figure 5.2: Abundance estimates; eastern Bight; 1991–1997. Estimate shown by □. Vertical bars show 2 standard errors above and below the estimate. Plot on left is $\widehat{D}_1$, and on the right is $\widehat{D}_0$.

	1991	1993	1994	1995	1996	1997
ee estimates	1.20	1.08	1.27	1.09	0.47	1.44
ue estimates	1.21	0.93	1.03	0.95	0.39	1.38

Table 5.3: Ratio of surface biomass estimates ($\hat{D}_1$); eastern Bight to entire Bight; 1991 and 1993–1997; ee and ue estimates.

5.3 Comparison of surface abundance estimates; entire Bight and eastern Bight

The eastern Bight estimates of abundance are generally higher than those for the entire Bight, the ratio of the surface biomass estimates for the two being relatively stable in 1991 and 1993–1995 (Table 5.3). However, in 1996 the abundance in the eastern Bight was less than half that in the entire Bight, and in 1997 it was higher than in previous years. The spotters suggest that the low abundance in the eastern Bight in 1996 was due to low sea surface temperatures in that region, (especially Block 5) that year. When SST's are low they detect few surface schools of SBT.

The changing proportions in the eastern and entire Bight illustrates a point of survey design discussed further in Appendix 6 of Cowling et al (1996): a survey boundary should not cut a high abundance area as the proportion on either side of the boundary may change from year to year.

5.4 Surface abundance estimates by fish age-class

The age of SBT in a sighting is estimated using the mean of the spotters' estimates of fish size (in kg) for the sighting, the SBT weight-length relationship (Robins (1963)) and the SBT age-at-length relationship (Anon (1994)). Table 5.4 shows the weight intervals associated with each age-class. Each sighting is assigned to the age-class for which the weight interval contains the mean of the spotters' estimates of fish size.

There are often multiple patches in a sighting. While in general the multiple patches are of the same age-class, when they are not, this procedure has a drawback — is assigns all patches to the same age-class, overestimating the biomass of the mean age-class and underestimating the biomass of the minority (in terms of tonnes of SBT) age-class. Comparison of the total biomass by age-class determined using this procedure and total biomass by age-class based on the estimated age of each patch suggests that the effect is not great.

There would also be a drawback if we divided the sighting into parts based on the estimated age of each patch and only used the appropriate part in calculating each aged based estimate. The detectability of each part is increased by the rest of the sighting and the correction of size bias would need to be adjusted for this.

Table 5.5 shows the number of sightings in each age-class for 1991 and 1993–1997.

Age	0	1	2	3	4	5
Interval	[0, 0.7)	[0.7, 4.5)	[4.5, 12.2)	[12.2, 20.7)	[20.7, 30.5)	[30.5, 38.2)

Table 5.4: SBT fish weight intervals for each age-class

	Age-class					
	0	1	2	3	4	5
1991	0	10	37	56	3	0
1993	2	1	27	167	69	0
1994	0	8	65	164	48	3
1995	0	3	82	181	28	0
1996	0	1	33	126	24	1
1997	0	10	38	111	29	1

Table 5.5: Total number of sightings in each age-class; entire Bight; 1991 and 1993–1997

Figure 5.3 shows the number of detected patches in each age-class and stratum for 1993–1997.

There are very few sightings of 0, 1 or 5 year-old SBT and therefore we exclude these sightings and give estimates for 2–4 year-olds only. Three year-olds are the most abundant, followed by 2 year-olds. The estimates by age-class are given in Tables 5.6 and 5.7.

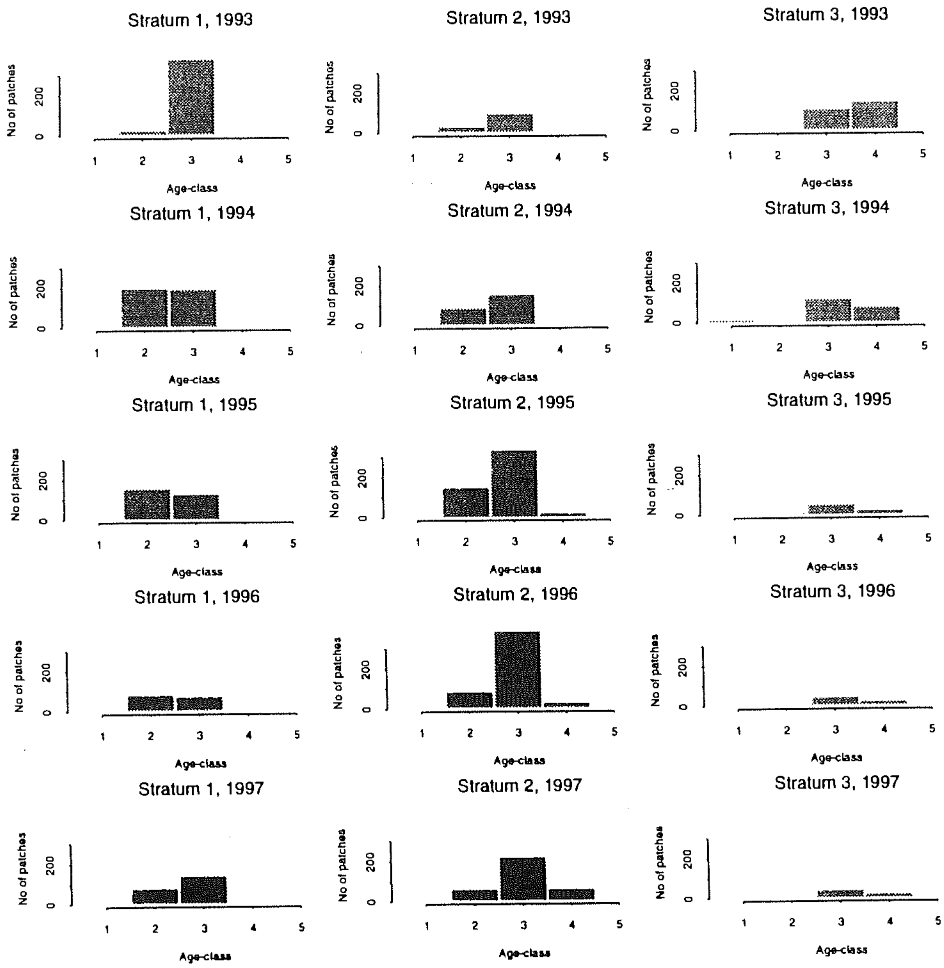

Figure 5.3: Number of detected patches in each age-class; 1993–1997

		Age-class		
		2	3	4
1991	n	37	56	3
	$\widehat{D}_1$	22.5 (14.4)	23.4 (12.6)	1.6 (1.6)
	$\widehat{D}_0$	0.52 (0.32)	0.71 (0.44)	0.01 (0.01)
1993	n	24	114	31
	$\widehat{D}_1$	12.1 (6.9)	139.7 (63.3)	13.7 (8.5)
	$\widehat{D}_0$	0.25 (0.14)	1.62 (0.37)	0.17 (0.10)
1994	n	51	127	35
	$\widehat{D}_1$	29.9 (10.3)	44.5 (7.5)	13.2 (8.1)
	$\widehat{D}_0$	0.19 (0.08)	0.88 (0.27)	0.24 (0.13)
1995	n	63	129	19
	$\widehat{D}_1$	43.6 (13.2)	107.4 (41.3)	9.0 (6.6)
	$\widehat{D}_0$	0.53 (0.19)	1.30 (0.28)	0.09 (0.05)
1996	n	29	98	19
	$\widehat{D}_1$	22.3 (11.3)	89.7 (23.5)	8.1 (5.6)
	$\widehat{D}_0$	0.26 (0.12)	0.72 (0.17)	0.11 (0.09)
1997	n	26	92	24
	$\widehat{D}_1$	14.6 (8.6)	76.9 (26.2)	27.0 (15.1)
	$\widehat{D}_0$	0.22 (0.09)	1.04 (0.30)	0.21 (0.09)

Table 5.6: Estimated surface abundance of juvenile SBT by age-class; entire Bight; 1991 and 1993–1997; equal effort (ee) estimates. The fish size estimates were agreed between the pilot and spotter, D. Hayman and K. White, in 1991, given by the pilot, D. Hayman, in 1993, and by the pilots, D. Hayman, K. Warren and L. Jaensch in 1994–97.

		Age-class		
		2	3	4
1991	n	20	40	2
	$\widehat{D}_1$	25.2 (23.0)	32.3 (14.3)	1.9 (1.9)
	$\widehat{D}_0$	0.39 (0.31)	0.93 (0.51)	0.06 (0.06)
1992	n	10	73	6
	$\widehat{D}_1$	11.7 (3.1)	136.6 (75.5)	17.6 (17.6)
	$\widehat{D}_0$	0.30 (0.17)	1.96 (0.43)	0.12 (0.12)
1993	n	18	92	22
	$\widehat{D}_1$	29.7 (18.6)	83.4 (33.7)	32.1 (23.3)
	$\widehat{D}_0$	0.35 (0.10)	1.65 (0.61)	0.29 (0.17)
1994	n	37	90	22
	$\widehat{D}_1$	19.0 (4.8)	53.1 (13.5)	12.6 (4.9)
	$\widehat{D}_0$	0.27 (0.10)	0.94 (0.43)	0.28 (0.14)
1995	n	29	102	12
	$\widehat{D}_1$	18.0 (5.2)	99.0 (35.4)	13.6 (5.9)
	$\widehat{D}_0$	0.37 (0.10)	1.60 (0.47)	0.18 (0.06)
1996	n	4	35	17
	$\widehat{D}_1$	3.2 (2.6)	28.8 (14.9)	12.2 (7.8)
	$\widehat{D}_0$	0.03 (0.02)	0.30 (0.13)	0.17 (0.14)
1997	n	11	82	15
	$\widehat{D}_1$	18.4 (11.3)	99.1 (30.8)	43.4 (24.6)
	$\widehat{D}_0$	0.13 (0.07)	1.00 (0.19)	0.33 (0.13)

Table 5.7: Estimated surface abundance of juvenile SBT by age-class; eastern Bight; 1991–1997; equal effort (ee) estimates. The fish size estimates were agreed between the pilot and spotter, D. Hayman and K. White, in 1991, given by the pilot, D. Hayman, in 1993, and by the pilots, D. Hayman, K. Warren and L. Jaensch in 1994–97.

6 Effect of environmental conditions during the annual surveys

The aerial survey is conducted in varying environmental conditions, which are thought to affect both the surfacing behaviour of schools and their detectability, thereby affecting the encounter rate and abundance estimates.

6.1 Effect of environmental conditions on surfacing behaviour and detectability

We give graphs showing the relationship between environmental conditions and both the perpendicular distance to a sighting and the pilot's estimate of school size in Appendices A.4 and A.5.

Figure A.10 shows that detected schools are larger in higher air-temperatures, and Figure A.6 shows that sightings are made to greater distances in higher air-temperatures than in low air-temperatures. It appears that in higher air-temperatures sightings are larger (perhaps consisting of more patches) and such larger sightings are therefore detectable at greater distances than when the air-temperature is lower and sightings are smaller.

Figure A.8 shows that detected schools are smaller in higher wind-speeds, and Figure A.4 shows that sightings are made at shorter distances in higher wind-speeds than in lower wind-speeds. It appears that in higher wind-speeds sightings are smaller (perhaps consisting of fewer patches or of smaller patches) and therefore are detectable at shorter distances than when it is less windy and sightings are larger.

Figures A.9 and A.5 show that there is little association between cloud cover and school size or detectability.

To maximise the probability of schools surfacing and being detectable it is vital to conduct the survey in good weather conditions (low wind-speeds and high air-temperatures). Replicates of the survey conducted in poor conditions will have few detections, resulting in poor estimates of abundance, as $f(0)$ and $\beta(0)$ cannot be estimated well from few sightings.

6.2 Effect of environmental conditions on encounter rate

The encounter rate is a raw measure of abundance affected by both surfacing behaviour and detectability.

Figures 6.1 and 6.3 show that the encounter rate (n/L) is highly dependent on wind-speed and air-temperature. In 7 knots or more of wind, the encounter rate is very low, while it is highest in 3 knots or less. In air-temperatures above 24° the encounter rate is much higher than in lower air-temperatures. Figure 6.2 indicates little change in encounter rate with cloud cover.

If the proportion of each year's survey effort spent in these conditions is relatively stable from year to year and if there is little change in abundance from year to year, there will be little change in encounter rate from year to year. However, changes in the proportion of time spent in favourable conditions will obviously result in changes in encounter rate, assuming no change in abundance. Figure 6.4 shows that

1. In 1991, the survey spent much more time in higher wind-speeds than in the later years of the survey, as would be expected from the more relaxed wind restrictions on survey operation. Between 1993 and 1996, there was a 10% decrease in the proportion of the survey effort spent in the most favourable wind conditions and an increase of 10% in 1997. This explains in part the decrease in encounter rate between 1993 and 1996 and increase in 1997.

2. 1997 had the highest proportion of favourable air-temperatures and 1995 had the lowest. 1993 had only slightly less favourable air-temperatures than 1997. Based on air-temperature and wind-speed, if SBT abundance was constant in the survey area, 1997 would be expected to have the highest encounter rate, followed by 1993 and then 1995, but 1993 had the highest encounter rate. We conclude that the affect of environmental variables is more complex—there may be interactions between the effects or other important environmental variables that have not been considered—or that SBT abundance within the Bight has not been constant.

In the eastern Bight, examination of Figure 6.5 leads to the expectation that encounter rate would drop from 1993 to 1996 and rise in 1997 (assuming constant abundance). This was observed to be the case.

6.3 Effect of environmental conditions on abundance estimates

The abundance estimates adjust for differences in the detectability of schools as long as there are sufficient detectable surface schools to estimate $f(0)$ and $\beta(0)$ well, but cannot adjust for differences in school surfacing rates.

If more or larger schools surfaced in high air temperatures and low wind-speeds and if there was no change in abundance, we would expect the surface biomass estimates for the entire Bight to be highest in 1997 and lowest in 1995 or 1996, but the biomass estimate was highest in 1993 and lowest in 1994.

We think that the effect of environmental variables on surfacing rates is more complex, and confounded with changes in true abundance in the survey area over the 7 year period of the survey. There are also other important variables not taken into account—for example, sea surface temperature. There is a need to better account for these effects in the survey estimate.

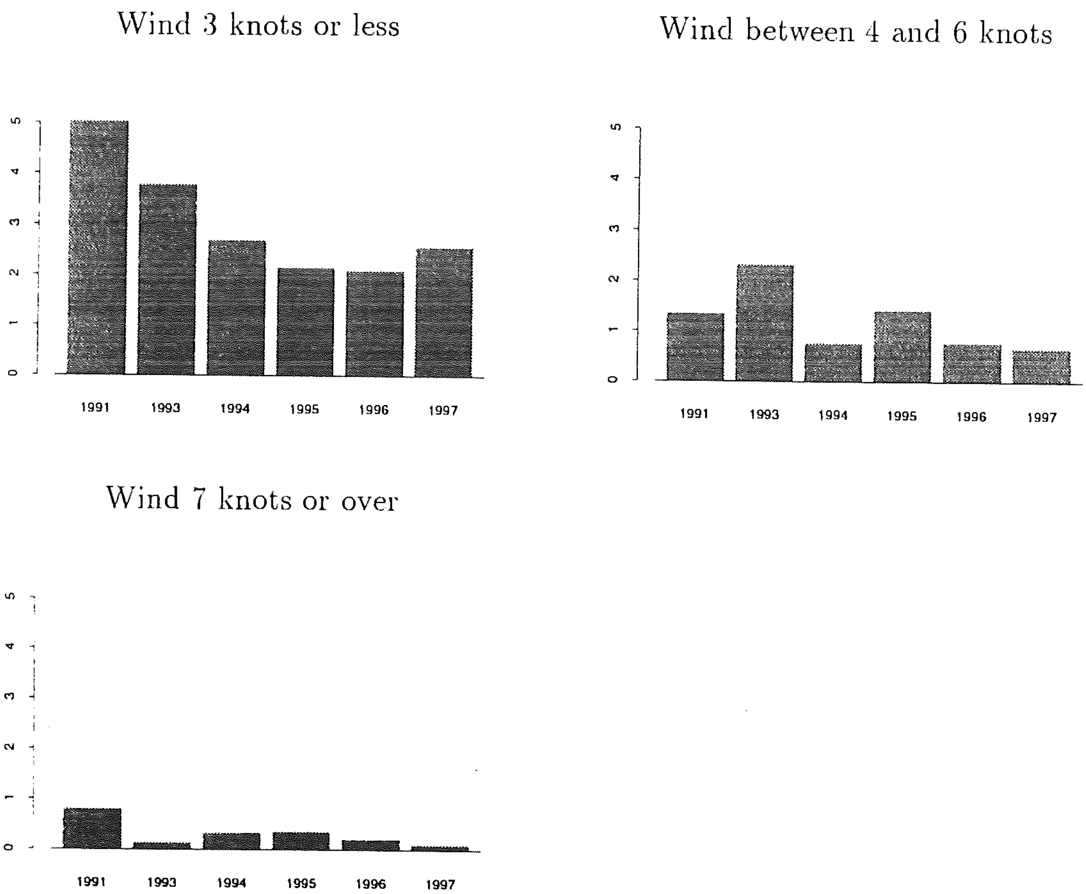

Figure 6.1: Encounter rate $(100n/L)$ in different wind-speeds; entire Bight; 1991 and 1993–1997

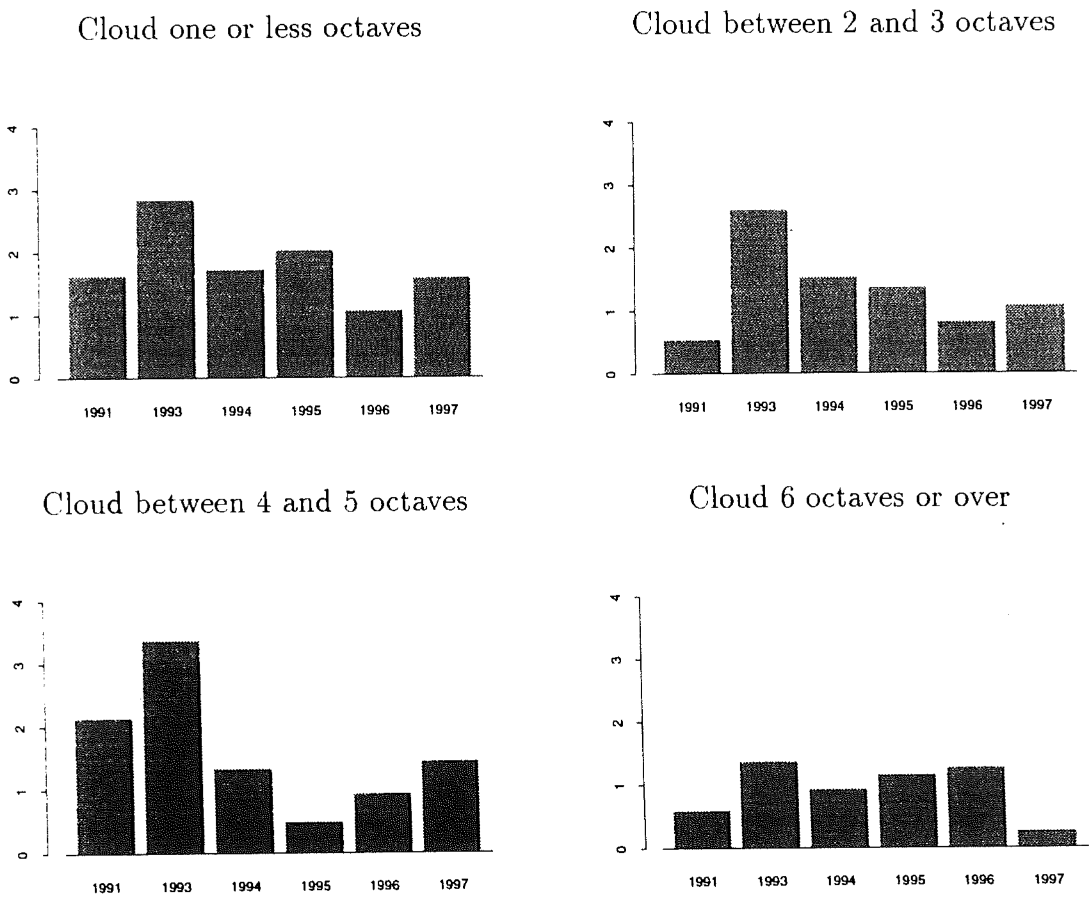

Figure 6.2: Encounter rate ($100n/L$) in different cloud conditions; entire Bight; 1991 and 1993–1997

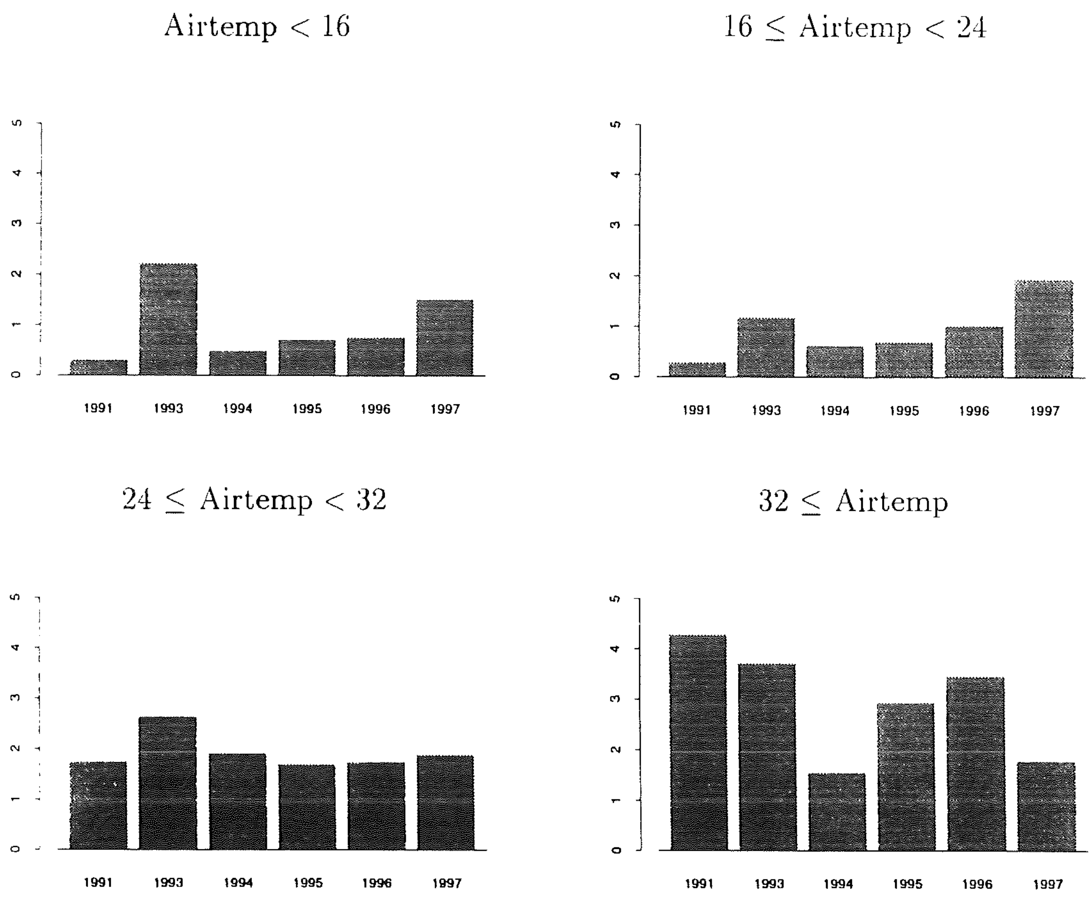

Figure 6.3: Encounter rate ($100n/L$) in different air temperatures; entire Bight; 1991 and 1993–1997

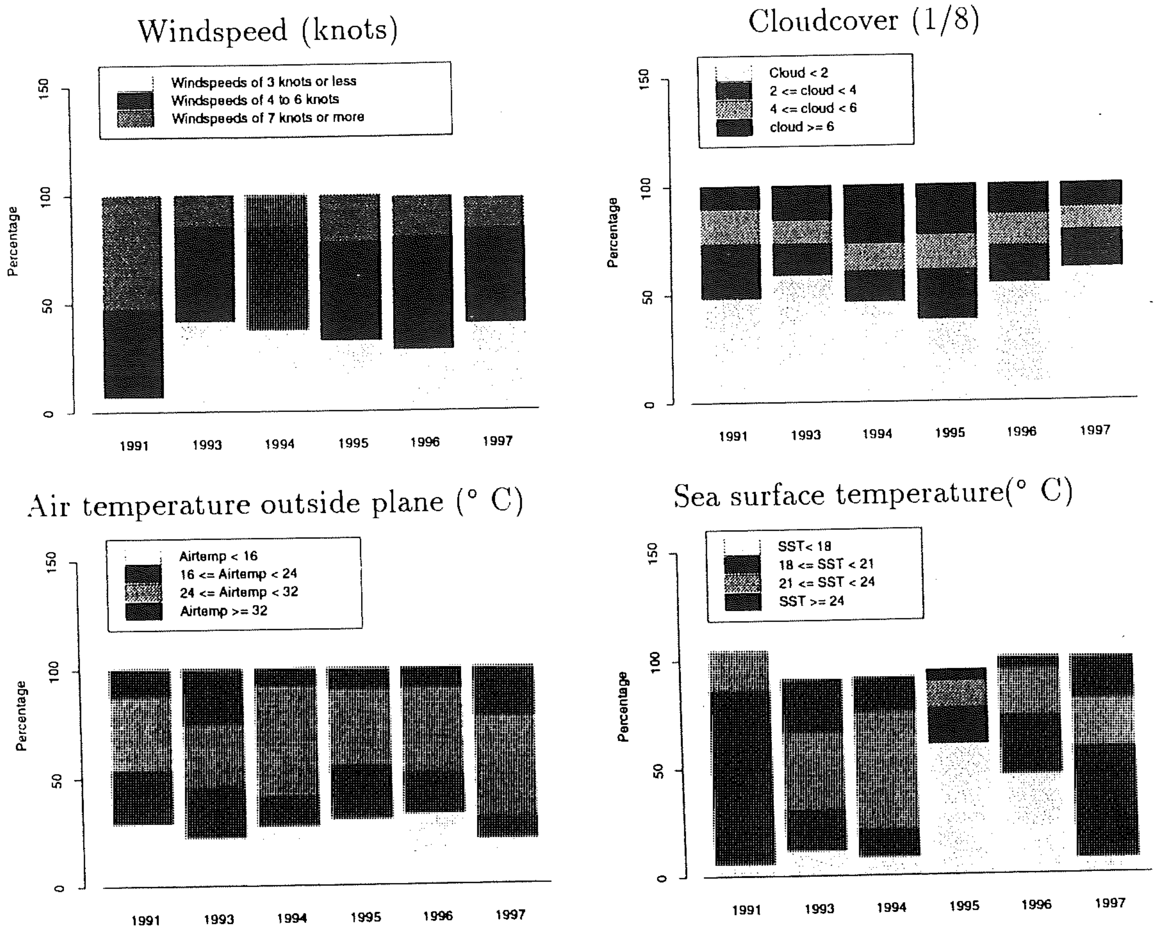

Figure 6.4: Percentage of survey effort spent in various environmental conditions; entire Bight; 1991 and 1993–1997

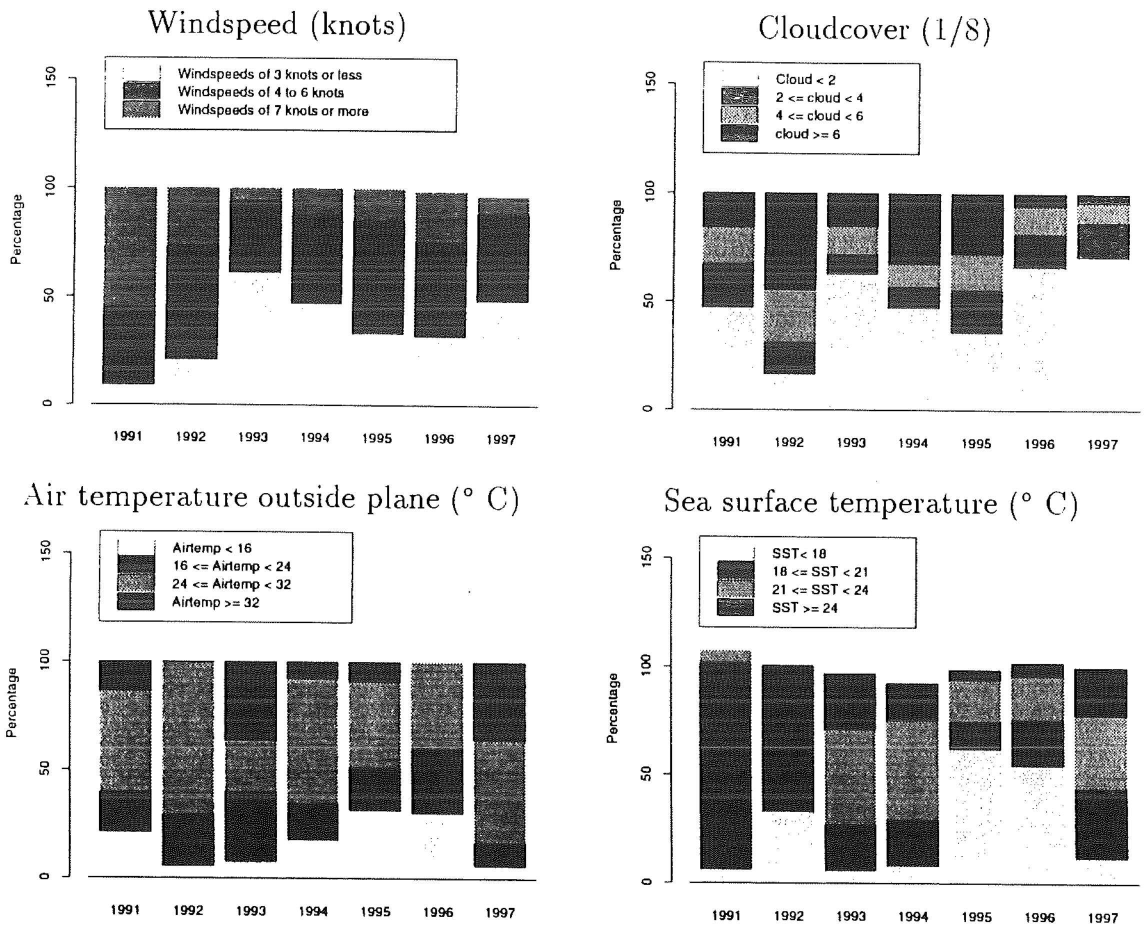

Figure 6.5: Percentage of survey effort spent in various environmental conditions; eastern Bight; 1991–1997

7 Discussion

There is a degree of variation in the annual surface abundance indices but there are no statistically significant differences between the estimates for any two years. No significant trends have appeared as yet.

Generally speaking, the year to year variability in SBT surface abundance estimates is due to one or more of the following four factors:

1. Differences in the survey areas and trackline designs.
2. Differences in the environmental conditions experienced during the surveys.
3. Differences in the proportion of the juvenile population of any age-class entering the survey area.
4. Differences in actual abundance.

We want to minimise the effects of Factors 1 and 2. Then assuming that the variation in the proportion of each age-class that enters the survey area each year is small, the abundance indices will give indices of global abundance.

The data sets were reconfigured as described in Section 2.4 to reduce the effect of differences in survey area and trackline design. However, the 1991 survey was conducted in distinctly higher wind-speeds than the later surveys (Figure 6.4) resulting in a lower encounter rate. The school size estimates for 1991 were also considerably lower than in the later surveys, perhaps due to the higher wind-speeds. The 1991 and 1992 surveys also used different definitions of sightings and patches than those used in the later surveys. Thus the 1991 estimates should be regarded as possibly non-comparable to the later estimates.

The environmental conditions clearly affect the encounter rate (Figures 6.1 to 6.3). The abundance estimators correct for differences in detectability as long as there are sufficient detections in any replicate to estimate $f(0)$ and $\beta(0)$ well. The remaining variation in the estimates is due to differences in surfacing rates with environmental conditions or to Factors 3 or 4 above.

There is considerable variation in the abundance estimates for any replicate in any year, In 1995 for example, $\hat{D}_1$ was very high in replicate 5 and low in Replicate 8 (Table A.1), yet there was little difference in the weather conditions during these replicates (Figures A.1 to A.3). In 1993 $\hat{D}_1$ was high in Replicate 1 and low in Replicate 4. These differences do not seem attributable to weather conditions in a simple way.

The sometimes large variations in estimates between replicates means that it is not clear that increasing the number of replicates in the survey area will decrease the variance of the estimates. While the 1993 biomass estimate (4 replicates) has the highest standard error, the 1997 estimate (5 replicates) has a lower standard error than 1995 or 1996 (8 and 7 replicates respectively).

Acknowledgements

Acknowledgement is made to David Morgan and Song Chen, the scientists in charge of the aerial surveys in 1991–92 and 1993–94 respectively; to Derek Hayman, Lyall Jaensch, Kevin Warren, Andrew Jakobs, Milo Mislov, Kiwi White, Simon Bey, Fiona Fraser, E Hayman, David Heathcote, Iain MacGill, Bob Stanley, R J Treble, Sally Troy, Mardi van der Weilen and D White for their dedicated survey spotting and recording work in the 1991–1997 surveys; to Jeff Cordell and Matt Sherlock of CSIRO Marine Laboratories for providing electronic assistance; and to Kevin Williams and Deirdre Waddington for their support to the survey.

References

Anon (1992). Report of the Southern Bluefin Tuna Aerial Survey Design Workshop. November 25-27, Hobart, Australia.

Anon (1994). Report of the Southern Bluefin Tuna Trilateral Workshop. January 17–February 4, Hobart, Australia.

Buckland, S. T., Anderson, D. R., Burnham, K. P., and Laake, J. L. (1993). *Distance Sampling: Estimating Abundance of Biological Populations.* Chapman and Hall, London.

Burnham, K. P., Anderson, D. R., and Laake, J. L. (1980). Estimation of density from line transect sampling of biological populations. Wildlife Monograph Number 72.

Chen, S. X. (1996a). A kernel estimate for density of a biological population using line transect sampling. *Appl. Statist.* **45**, 135–150.

Chen, S. X. (1996b). Studying school size effects in line transect sampling using the kernel method. *Biometrics* **52**, 1283–1294.

Chen, S. X. and Polacheck, T. (1993). Report on the 1993 aerial survey for juvenile southern bluefin tuna in the Great Australian Bight. MRWS/93/8. 1993 SBT Recruitment Monitoring Workshop. Hobart.

Cowling, A., Polacheck, T., and Millar, C. (1996). Data analysis of the aerial surveys (1991–1996) for juvenile Southern Bluefin Tuna in the Great Australian Bight. RMWS/96/6. 1996 Recruitment Monitoring Workshop. Hobart.

Drummer, T. D. and McDonald, L. L. (1987). Size bias in line transect sampling. *Biometrics* **43**, 13–21.

Morgan, D. G. (1991). A survey of Southern Bluefin Tuna abundance in the Great Australian Bight, 1990-1991. Center for Program Evaluation. University of Melbourne.

Morgan, D. G. (1992). Aerial survey of Southern Bluefin Tuna abundance in the Great Australian Bight, 1992. Education Report. University of Melbourne.

Quang, P. X. (1991). A nonparametric approach to size-biased line transect sampling. *Biometrics* **47**, 269–279.

Ripley, B. D. (1981). *Spatial Statistics.* Wiley, New York.

Robins, J. P. (1963). Synopsis of biological data on bluefin tuna *thunnus thunnus maccoyii* (Castelnau). *FAO Fish. Rep.* **2**, 562–587.

A.1 Tables of surface abundance estimates

Year		Replicate 1	2	3	4	5	6	7	8	Total
1991	n_i	30	2	23	40	1				96
	L_i	1,480	1,418	1,741	1,622	1,327				7,587
	$\widehat{D}_1$	114.7	0.0	25.2	114.3	0.0				50.9
	$\hat{\sigma}_1$	(59.4)	(0.0)	(11.5)	(39.0)	(0.0)				(26.4)
	$\widehat{D}_0$	1.65	0.00	1.13	3.99	0.00				1.35
	$\hat{\sigma}_0$	(0.85)	(0.00)	(0.55)	(1.33)	(0.00)				(0.73)
1993	n_i	72	36	37	24					169
	L_i	1,908	1,847	1,958	1,782					7,495
	$\widehat{D}_1$	329.1	151.6	100.2	73.0					163.5
	$\hat{\sigma}_1$	(121.9)	(48.5)	(34.6)	(28.4)					(57.6)
	$\widehat{D}_0$	2.57	1.81	1.64	2.84					2.21
	$\hat{\sigma}_0$	(0.95)	(0.60)	(0.57)	(1.10)					(0.29)
1994	n_i	14	20	38	25	22	24	44	26	213
	L_i	1,730	1,988	1,885	1,924	1,702	1,789	2,027	2,068	15,112
	$\widehat{D}_1$	57.0	55.0	129.3	99.1	64.1	69.8	154.3	90.0	89.8
	$\hat{\sigma}_1$	(48.1)	(28.9)	(49.3)	(47.8)	(40.1)	(28.4)	(44.6)	(33.8)	(12.8)
	$\widehat{D}_0$	0.49	1.35	1.22	0.50	0.40	1.60	3.70	1.39	1.33
	$\hat{\sigma}_0$	(0.40)	(0.62)	(0.46)	(0.30)	(0.25)	(0.75)	(1.12)	(0.50)	(0.38)
1995	n_i	21	31	31	25	33	31	31	8	211
	L_i	1,914	1,837	1,691	1,805	1,724	1,741	1,846	1,945	14,503
	$\widehat{D}_1$	120.5	133.5	137.9	103.2	397.9	198.0	151.0	33.8	159.5
	$\hat{\sigma}_1$	(52.6)	(49.1)	(44.9)	(31.9)	(151.0)	(101.7)	(72.6)	(17.8)	(37.8)
	$\widehat{D}_0$	1.73	2.60	2.73	2.54	2.85	2.23	1.28	0.76	2.09
	$\hat{\sigma}_0$	(0.82)	(1.01)	(0.94)	(0.82)	(1.14)	(1.09)	(0.64)	(0.50)	(0.27)
1996	n_i	21	11	18	24	44	27	1		146
	L_i	1,688	1,895	1,812	1,750	1,987	2,141	1,930		13,204
	$\widehat{D}_1$	110.1	21.3	96.0	221.1	217.3	122.3	0.0		112.6
	$\hat{\sigma}_1$	(63.6)	(12.5)	(50.0)	(112.4)	(99.2)	(57.8)	(0.0)		(32.4)
	$\widehat{D}_0$	0.81	0.85	1.38	1.27	2.09	0.93	0.00		1.05
	$\hat{\sigma}_0$	(0.43)	(0.49)	(0.73)	(0.66)	(0.99)	(0.42)	(0.00)		(0.24)
1997	n_i	22	46	36	31	7				142
	L_i	1,802	1,949	1,949	1,519	1,872				9,091
	$\widehat{D}_1$	121.5	152.4	92.6	176.4	7.1				110.0
	$\hat{\sigma}_1$	(52.7)	(59.5)	(40.2)	(73.0)	(6.4)				(29.3)
	$\widehat{D}_0$	1.69	2.24	1.30	1.65	0.18				1.41
	$\hat{\sigma}_0$	(0.81)	(0.89)	(0.55)	(0.68)	(0.20)				(0.34)

Table A.1: Estimated surface abundance of 2–4 year olds; entire Bight; 1991 and 1993–1997. Equal effort estimates. n_i is the number of sightings in replicate i, L_i is the transect length flown in nm, $\widehat{D}_1$ is the estimated biomass (tonnes/1000 sq nm), $\widehat{D}_0$ is the estimated school density (schools/1000 sq nm). $\hat{\sigma}_1$ and $\hat{\sigma}_0$ are the standard deviations of the estimation error estimates of $\widehat{D}_1$ and $\widehat{D}_0$. The school size estimates were given by the pilot.

Year		Replicate 1	2	3	4	5	6	7	8	Total
	n_i	111	62	59	31					263
	L_i	2,748	2,514	2,627	2,286					10,174
1993	$\widehat{D}_1$	254.3	129.2	193.1	54.6					157.8
	$\hat{\sigma}_1$	(68.1)	(35.2)	(51.6)	(17.9)					(42.8)
	$\widehat{D}_0$	2.69	1.74	2.37	1.98					2.20
	$\hat{\sigma}_0$	(0.70)	(0.51)	(0.66)	(0.66)					(0.21)
	n_i	18	24	50	30	32	34	56	33	277
	L_i	2,283	2,633	2,460	2,604	2,319	2,369	2,802	2,722	20,191
1994	$\widehat{D}_1$	45.1	34.6	93.3	96.9	69.5	80.4	157.8	72.8	81.3
	$\hat{\sigma}_1$	(24.8)	(16.4)	(29.4)	(42.0)	(29.1)	(29.4)	(46.5)	(21.8)	(13.3)
	$\widehat{D}_0$	0.37	0.86	0.78	0.52	0.94	1.75	3.56	1.49	1.28
	$\hat{\sigma}_0$	(0.20)	(0.34)	(0.26)	(0.26)	(0.44)	(0.70)	(0.94)	(0.43)	(0.36)
	n_i	30	42	39	37	49	44	41	9	291
	L_i	2,739	2,646	2,331	2,640	2,449	2,522	2,690	2,776	20,793
1995	$\widehat{D}_1$	100.3	122.5	107.9	73.9	349.6	158.5	146.0	33.1	136.5
	$\hat{\sigma}_1$	(33.3)	(40.3)	(39.1)	(24.8)	(108.3)	(64.4)	(60.5)	(14.3)	(33.5)
	$\widehat{D}_0$	1.60	2.25	2.21	2.61	2.98	2.58	1.43	0.79	2.05
	$\hat{\sigma}_0$	(0.60)	(0.78)	(0.83)	(0.90)	(1.00)	(0.99)	(0.60)	(0.43)	(0.26)
	n_i	23	13	20	33	57	34	3		183
	L_i	2,262	2,576	2,486	2,501	2,820	2,910	2,709		18,265
1996	$\widehat{D}_1$	126.8	20.9	101.6	207.9	201.7	90.3	4.0		107.6
	$\hat{\sigma}_1$	(67.8)	(11.1)	(47.7)	(86.4)	(66.7)	(40.1)	(2.8)		(30.0)
	$\widehat{D}_0$	0.80	0.96	1.71	1.29	2.46	0.69	0.12		1.15
	$\hat{\sigma}_0$	(0.40)	(0.50)	(0.82)	(0.55)	(0.85)	(0.29)	(0.09)		(0.29)
	n_i	29	55	43	41	10				178
	L_i	2,563	2,786	2,814	2,121	2,561				12,845
1997	$\widehat{D}_1$	148.5	185.0	58.2	156.1	12.6				112.1
	$\hat{\sigma}_1$	(62.2)	(61.5)	(25.8)	(56.0)	(7.2)				(32.7)
	$\widehat{D}_0$	1.50	2.35	0.81	1.37	0.48				1.30
	$\hat{\sigma}_0$	(0.69)	(0.77)	(0.36)	(0.44)	(0.30)				(0.32)

Table A.2: Estimated surface abundance of 2–4 year olds; entire Bight; 1993–1997; ue estimates. n_i is the number of sightings in replicate i, L_i is the transect length flown in nm, $\widehat{D_1}$ is the estimated biomass (tonnes/1000 sq nm), $\widehat{D_0}$ is the estimated school density (schools/1000 sq nm). $\hat{\sigma}_1$ and $\hat{\sigma}_0$ are the standard deviations of the estimation error estimates of $\widehat{D_1}$ and $\widehat{D_0}$. The school size estimates were given by the pilot.

Year		Replicate 1	2	3	4	5	6	7	8	Total
1991	n_i	18	1	20	22	1				62
	L_i	742	385	677	990	648				3,442
	$\widehat{D}_1$	147.8	0.0	70.8	88.3	0.0				61.4
	$\hat{\sigma}_1$	(103.5)	(0.0)	(34.8)	(49.4)	(0.0)				(28.1)
	$\widehat{D}_0$	2.00	0.00	2.23	3.35	0.00				1.52
	$\hat{\sigma}_0$	(1.38)	(0.00)	(1.15)	(1.87)	(0.00)				(0.66)
1992	n_i	17	31	10	6					64
	L_i	823	835	598	577					2,833
	$\widehat{D}_1$	26.6	441.3	101.3	82.3					162.9
	$\hat{\sigma}_1$	(20.3)	(233.7)	(64.5)	(64.2)					(94.1)
	$\widehat{D}_0$	2.01	3.10	1.56	1.40					2.02
	$\hat{\sigma}_0$	(1.61)	(1.58)	(1.03)	(1.11)					(0.38)
1993	n_i	41	24	12	17					94
	L_i	969	913	897	714					3,494
	$\widehat{D}_1$	425.5	187.8	41.4	53.9					177.2
	$\hat{\sigma}_1$	(212.4)	(66.9)	(25.1)	(19.3)					(89.2)
	$\widehat{D}_0$	1.84	2.31	0.75	5.30					2.55
	$\hat{\sigma}_0$	(0.93)	(0.85)	(0.42)	(2.00)					(0.97)
1994	n_i	13	14	21	11	12	5	26	16	118
	L_i	765	920	924	846	751	712	948	952	6,817
	$\widehat{D}_1$	126.1	142.7	159.8	28.0	117.5	15.0	194.5	125.9	113.7
	$\hat{\sigma}_1$	(113.8)	(78.2)	(63.9)	(25.6)	(93.4)	(12.3)	(72.8)	(48.6)	(21.9)
	$\widehat{D}_0$	1.10	2.45	1.26	0.03	0.78	0.52	4.75	2.49	1.67
	$\hat{\sigma}_0$	(0.95)	(1.35)	(0.42)	(0.03)	(0.62)	(0.50)	(1.78)	(0.82)	(0.54)
1995	n_i	10	13	11	12	7	25	10	2	90
	L_i	935	766	715	754	786	744	773	869	6,343
	$\widehat{D}_1$	51.7	139.0	67.9	204.1	261.4	472.7	158.3	33.1	173.5
	$\hat{\sigma}_1$	(18.1)	(64.6)	(31.9)	(95.8)	(212.1)	(270.7)	(131.6)	(21.3)	(50.9)
	$\widehat{D}_0$	1.69	3.10	1.31	3.04	2.09	5.00	0.79	1.08	2.26
	$\hat{\sigma}_0$	(0.61)	(1.46)	(0.75)	(1.47)	(1.66)	(2.77)	(0.62)	(1.00)	(0.49)
1996	n_i	0	0	3	3	18	17	0		41
	L_i	736	841	860	934	934	1,104	928		6,337
	$\widehat{D}_1$	0.0	0.0	10.6	54.0	101.8	204.6	0.0		53.0
	$\hat{\sigma}_1$	(0.0)	(0.0)	(9.6)	(60.4)	(96.8)	(124.2)	(0.0)		(29.1)
	$\widehat{D}_0$	0.00	0.00	0.56	0.32	1.97	1.03	0.00		0.55
	$\hat{\sigma}_0$	(0.00)	(0.00)	(0.61)	(0.35)	(1.87)	(0.61)	(0.00)		(0.28)
1997	n_i	10	16	25	26	7				84
	L_i	779	886	947	704	802				4,117
	$\widehat{D}_1$	207.0	106.6	163.6	295.5	16.7				157.9
	$\hat{\sigma}_1$	(132.8)	(52.0)	(77.3)	(114.1)	(15.0)				(46.9)
	$\widehat{D}_0$	1.24	2.28	2.24	2.20	0.43				1.68
	$\hat{\sigma}_0$	(0.86)	(1.11)	(0.94)	(0.82)	(0.46)				(0.37)

Table A.3: Estimated surface abundance of 2–4 year olds; eastern Bight; 1991–1997; ee estimates. n_i is the number of sightings in replicate i, L_i is the transect length flown in nm, $\widehat{D}_1$ is the estimated biomass (tonnes/1000 sq nm), $\widehat{D}_0$ is the estimated school density (schools/1000 sq nm). $\hat{\sigma}_1$ and $\hat{\sigma}_0$ are the standard deviations of the estimation error estimates of $\widehat{D}_1$ and $\widehat{D}_0$. The school size estimates were given by the pilot.

Year		Replicate 1	2	3	4	5	6	7	8	Total
1993	n_i	54	41	15	22					132
	L_i	1,285	1,199	1,185	893					4,562
	$\widehat{D}_1$	360.7	148.0	37.1	43.9					147.4
	$\hat{\sigma}_1$	(116.5)	(52.2)	(20.1)	(15.0)					(75.5)
	$\widehat{D}_0$	2.78	1.65	1.09	3.87					2.35
	$\hat{\sigma}_0$	(0.89)	(0.61)	(0.55)	(1.37)					(0.62)
1994	n_i	17	18	26	11	15	6	34	22	149
	L_i	1,021	1,189	1,196	1,102	953	925	1,269	1,242	8,896
	$\widehat{D}_1$	77.9	62.2	108.7	19.9	108.5	12.5	184.2	99.2	84.1
	$\hat{\sigma}_1$	(45.5)	(34.8)	(45.4)	(18.1)	(61.2)	(14.2)	(53.7)	(36.8)	(19.5)
	$\widehat{D}_0$	0.65	1.50	0.85	0.02	0.87	0.25	5.64	2.20	1.50
	$\hat{\sigma}_0$	(0.36)	(0.70)	(0.31)	(0.02)	(0.51)	(0.31)	(1.67)	(0.69)	(0.64)
1995	n_i	17	20	16	21	16	34	16	3	143
	L_i	1,378	1,087	1,009	1,123	1,088	1,145	1,187	1,229	9,245
	$\widehat{D}_1$	65.6	163.2	27.0	151.6	133.4	363.9	104.6	24.6	129.2
	$\hat{\sigma}_1$	(21.8)	(61.0)	(13.8)	(71.6)	(72.2)	(168.5)	(69.7)	(17.2)	(38.4)
	$\widehat{D}_0$	1.75	3.19	0.55	3.46	1.29	4.84	0.86	1.11	2.13
	$\hat{\sigma}_0$	(0.59)	(1.21)	(0.34)	(1.62)	(0.68)	(2.18)	(0.49)	(0.96)	(0.54)
1996	n_i	0	1	3	8	26	18	0		56
	L_i	993	1,064	1,190	1,357	1,330	1,408	1,235		8,577
	$\widehat{D}_1$	0.0	0.0	8.0	41.8	81.8	165.5	0.0		42.5
	$\hat{\sigma}_1$	(0.0)	(0.0)	(6.8)	(40.7)	(42.9)	(98.7)	(0.0)		(23.5)
	$\widehat{D}_0$	0.00	0.00	0.42	0.28	1.85	0.84	0.00		0.48
	$\hat{\sigma}_0$	(0.00)	(0.00)	(0.44)	(0.25)	(0.95)	(0.48)	(0.00)		(0.26)
1997	n_i	17	17	31	35	8				108
	L_i	1,122	1,308	1,351	982	1,033				5,796
	$\widehat{D}_1$	269.4	100.0	97.5	285.8	20.2				154.6
	$\hat{\sigma}_1$	(145.3)	(45.1)	(44.5)	(105.4)	(15.3)				(52.3)
	$\widehat{D}_0$	1.57	2.14	1.30	1.92	0.46				1.48
	$\hat{\sigma}_0$	(0.89)	(0.96)	(0.56)	(0.65)	(0.36)				(0.29)

Table A.4: Estimated surface abundance of 2–4 year olds; eastern Bight; 1993–1997; ue estimates. n_i is the number of sightings in replicate i, L_i is the transect length flown in nm, $\widehat{D}_1$ is the estimated biomass (tonnes/1000 sq nm), $\widehat{D}_0$ is the estimated school density (schools/1000 sq nm). $\hat{\sigma}_1$ and $\hat{\sigma}_0$ are the standard deviations of the estimation error estimates of $\widehat{D}_1$ and $\widehat{D}_0$. The school size estimates were given by the pilot.

Year		Replicate								$\frac{ee(\hat{D}_1)}{te(\hat{D}_1)}$	$\frac{ee(\hat{D}_0)}{te(\hat{D}_0)}$
		1	2	3	4	5	6	7	8		
1991	n_i	30	2	23	40	1				29.7	20.8
	L_i	1,480	1,418	1,741	1,622	1,327					
	$\hat{f}(0)$	163.2	0	171.3	323.5	0					
	$\hat{\beta}(0)$	11318	0	3815	9276	0					
	cv$\{\hat{f}(0)\}$	0.25	0.0	0.30	0.16	0.0					
	cv$\{\hat{\beta}(0)\}$	0.26	0.0	0.24	0.17	0.0					
	cv(n/L)	0.45	1.09	0.38	0.29	0.92					
1993	n_i	72	36	37	24					36.3	207.3
	L_i	1,908	1,847	1,958	1,782						
	$\hat{f}(0)$	136.3	186.0	173.2	421.0						
	$\hat{\beta}(0)$	17440	15557	10607	10838						
	cv$\{\hat{f}(0)\}$	0.22	0.23	0.25	0.20						
	cv$\{\hat{\beta}(0)\}$	0.22	0.21	0.24	0.21						
	cv(n/L)	0.30	0.24	0.25	0.33						
1994	n_i	14	21	38	25	22	24	44	26	128.1	32.6
	L_i	1,730	1,988	1,885	1,924	1,702	1,789	2,027	2,068		
	$\hat{f}(0)$	122.0	269.3	121.4	76.5	62.2	239.2	340.9	221.7		
	$\hat{\beta}(0)$	14089	10936	12832	15248	9922	10400	14216	14316		
	cv$\{\hat{f}(0)\}$	0.34	0.26	0.26	0.56	0.39	0.36	0.17	0.24		
	cv$\{\hat{\beta}(0)\}$	0.43	0.37	0.26	0.42	0.41	0.27	0.15	0.26		
	cv(n/L)	0.72	0.38	0.28	0.23	0.48	0.30	0.25	0.27		
1995	n_i	21	31	31	25	33	31	31	8	51.3	139.7
	L_i	1,914	1,837	1,691	1,805	1,724	1,741	1,846	1,945		
	$\hat{f}(0)$	314.9	307.8	297.7	367.5	297.5	250.8	152.7	370.0		
	$\hat{\beta}(0)$	21963	15820	15049	14896	41583	22247	17987	16422		
	cv$\{\hat{f}(0)\}$	0.29	0.26	0.23	0.24	0.26	0.24	0.39	0.49		
	cv$\{\hat{\beta}(0)\}$	0.22	0.22	0.20	0.22	0.22	0.29	0.37	0.29		
	cv(n/L)	0.38	0.29	0.26	0.22	0.31	0.42	0.31	0.44		
1996	n_i	21	11	18	24	44	27	1		63.2	89.1
	L_i	1,688	1,895	1,812	1,750	1,987	2,141	1,930			
	$\hat{f}(0)$	130.6	293.9	277.4	185.5	188.7	147.9	0			
	$\hat{\beta}(0)$	17704	7351	19335	32254	19622	19393	0			
	cv$\{\hat{f}(0)\}$	0.34	0.33	0.31	0.28	0.27	0.28	0.0			
	cv$\{\hat{\beta}(0)\}$	0.42	0.34	0.28	0.26	0.25	0.32	0.0			
	cv(n/L)	0.40	0.47	0.44	0.43	0.38	0.35	1.06			
1997	n_i	22	46	36	31	7				61.8	76.5
	L_i	1,802	1,949	1,949	1,519	1,872					
	$\hat{f}(0)$	276.2	189.8	140.8	162.0	98.4					
	$\hat{\beta}(0)$	19894	12915	10027	17287	3819					
	cv$\{\hat{f}(0)\}$	0.39	0.22	0.33	0.28	0.89					
	cv$\{\hat{\beta}(0)\}$	0.33	0.21	0.35	0.29	0.66					
	cv(n/L)	0.28	0.33	0.25	0.30	0.61					

Table A.5: Equal effort estimates of $f(0)$, $\beta(0)$ and other components of abundance estimates; entire Bight; 1991 and 1993–1997.

Year		Replicate								$\frac{ee(\widehat{D}_1)}{te(\widehat{D}_1)}$	$\frac{ee(\widehat{D}_0)}{te(\widehat{D}_0)}$
		1	2	3	4	5	6	7	8		
	n_i	111	62	59	31					30.2	230.2
	L_i	2,748	2,514	2,627	2,286						
1993	$\hat{f}(0)$	140.0	180.8	222.4	378.8						
	$\hat{\beta}(0)$	13217	13431	18120	10418						
	$cv\{\hat{f}(0)\}$	0.20	0.20	0.21	0.20						
	$cv\{\hat{\beta}(0)\}$	0.20	0.17	0.20	0.19						
	$cv(n/L)$	0.17	0.22	0.18	0.27						
	n_i	18	24	50	30	32	34	56	33	69.1	24.3
	L_i	2,283	2,633	2,460	2,604	2,319	2,369	2,802	2,722		
1994	$\hat{f}(0)$	120.2	240.9	96.3	91.1	134.4	245.0	403.2	265.9		
	$\hat{\beta}(0)$	14506	9690	11533	16884	9948	11279	17883	12993		
	$cv\{\hat{f}(0)\}$	0.34	0.27	0.26	0.45	0.35	0.28	0.15	0.22		
	$cv\{\hat{\beta}(0)\}$	0.37	0.38	0.24	0.37	0.29	0.23	0.20	0.23		
	$cv(n/L)$	0.40	0.29	0.20	0.22	0.30	0.29	0.22	0.19		
	n_i	30	42	39	37	49	44	41	9	34.2	117.9
	L_i	2 ,739	2,646	2,331	2,640	2,449	2,522	2,690	2,776		
1995	$\hat{f}(0)$	287.9	277.6	265.0	341.7	284.5	295.5	163.9	418.8		
	$\hat{\beta}(0)$	18040	15119	12933	9676	33370	18178	16778	17601		
	$cv\{\hat{f}(0)\}$	0.28	0.25	0.24	0.27	0.25	0.20	0.32	0.41		
	$cv\{\hat{\beta}(0)\}$	0.22	0.22	0.21	0.26	0.21	0.24	0.30	0.24		
	$cv(n/L)$	0.25	0.24	0.29	0.22	0.23	0.32	0.28	0.36		
	n_i	23	13	20	33	57	34	3		46.4	53.8
	L_i	2,262	2,576	2,486	2,501	2,820	2,910	2,709			
1996	$\hat{f}(0)$	137.2	314.5	324.6	170.7	217.8	120.6	308.0			
	$\hat{\beta}(0)$	21626	6855	19276	27549	17836	15703	10416			
	$cv\{\hat{f}(0)\}$	0.31	0.30	0.26	0.31	0.24	0.29	0.41			
	$cv\{\hat{\beta}(0)\}$	0.36	0.33	0.24	0.30	0.22	0.33	0.27			
	$cv(n/L)$	0.39	0.42	0.40	0.29	0.24	0.30	0.65			
	n_i	29	55	43	41	10				43.0	57.9
	L_i	2,563	2,786	2,814	2,121	2,561					
1997	$\hat{f}(0)$	275.2	198.7	115.8	164.2	245.9					
	$\hat{\beta}(0)$	27222	15649	8302	18723	6378					
	$cv\{\hat{f}(0)\}$	0.35	0.20	0.36	0.25	0.45					
	$cv\{\hat{\beta}(0)\}$	0.29	0.20	0.36	0.30	0.38					
	$cv(n/L)$	0.30	0.26	0.26	0.20	0.43					

Table A.6: Unequal effort estimates of $f(0)$, $\beta(0)$ and other components of abundance estimates; entire Bight; 1993–1997.

Year		Replicate 1	2	3	4	5	6	7	8	$\frac{ee(\widehat{D}_1)}{te(\widehat{D}_1)}$	$\frac{ee(\widehat{D}_0)}{te(\widehat{D}_0)}$
1991	n_i	18	1	20	22	1				72.7	61.8
	L_i	742	385	677	990	648					
	$\hat{f}(0)$	165.1	0.0	150.7	301.8	0.0					
	$\hat{\beta}(0)$	12185	0	4792	7948	0					
	$\mathrm{cv}\{\hat{f}(0)\}$	0.26	0.00	0.31	0.18	0.00					
	$\mathrm{cv}\{\hat{\beta}(0)\}$	0.29	0.00	0.27	0.19	0.00					
	$\mathrm{cv}(n/L)$	0.64	1.70	0.41	0.53	1.11					
1992	n_i	17	31	10	6					44.6	317.5
	L_i	823	835	598	577						
	$\hat{f}(0)$	275.0	189.8	243.6	290.6						
	$\hat{\beta}(0)$	3646	27050	15795	17043						
	$\mathrm{cv}\{\hat{f}(0)\}$	0.32	0.23	0.30	0.26						
	$\mathrm{cv}\{\hat{\beta}(0)\}$	0.20	0.30	0.20	0.20						
	$\mathrm{cv}(n/L)$	0.39	0.32	0.54	0.59						
1993	n_i	41	24	12	17					39.8	38.2
	L_i	969	913	897	714						
	$\hat{f}(0)$	86.8	176.1	112.6	445.4						
	$\hat{\beta}(0)$	20124	14285	6196	4529						
	$\mathrm{cv}\{\hat{f}(0)\}$	0.30	0.24	0.44	0.18						
	$\mathrm{cv}\{\hat{\beta}(0)\}$	0.28	0.22	0.49	0.14						
	$\mathrm{cv}(n/L)$	0.41	0.28	0.35	0.33						
1994	n_i	13	14	21	11	12	5	26	16	131.2	40.2
	L_i	765	920	924	846	751	712	948	952		
	$\hat{f}(0)$	129.2	322.3	110.8	5.3	97.0	148.2	346.2	295.9		
	$\hat{\beta}(0)$	14837	18759	14063	4299	14708	4274	14181	14983		
	$\mathrm{cv}\{\hat{f}(0)\}$	0.34	0.26	0.30	0.82	0.49	0.85	0.19	0.23		
	$\mathrm{cv}\{\hat{\beta}(0)\}$	0.42	0.25	0.37	0.87	0.48	0.70	0.19	0.30		
	$\mathrm{cv}(n/L)$	0.80	0.49	0.16	0.27	0.63	0.42	0.32	0.24		
1995	n_i	10	13	11	12	7	25	10	2	90.8	109.3
	L_i	935	766	715	754	786	744	773	869		
	$\hat{f}(0)$	315.4	365.8	169.9	382.6	469.7	297.7	121.6	941.0		
	$\hat{\beta}(0)$	9654	16384	8834	25655	58708	28132	24469	28790		
	$\mathrm{cv}\{\hat{f}(0)\}$	0.27	0.26	0.48	0.27	0.22	0.26	0.65	0.71		
	$\mathrm{cv}\{\hat{\beta}(0)\}$	0.26	0.25	0.35	0.25	0.28	0.30	0.70	0.25		
	$\mathrm{cv}(n/L)$	0.24	0.39	0.31	0.40	0.76	0.49	0.45	0.59		
1996	n_i	0	0	3	3	18	17	0		68.8	116.3
	L_i	736	841	860	934	934	1,104	928			
	$\hat{f}(0)$	0.0	0.0	321.3	198.3	204.3	134.3	0.0			
	$\hat{\beta}(0)$	0	0	6104	33593	10562	26567	0			
	$\mathrm{cv}\{\hat{f}(0)\}$	0.00	0.00	0.91	0.86	0.35	0.33	0.00			
	$\mathrm{cv}\{\hat{\beta}(0)\}$	0.00	0.00	0.68	0.88	0.36	0.37	0.00			
	$\mathrm{cv}(n/L)$	0.00	0.00	0.59	0.69	0.88	0.48	0.00			
1997	n_i	10	16	25	26	7				72.0	111.0
	L_i	779	886	947	704	802					
	$\hat{f}(0)$	193.3	252.9	169.7	119.1	98.4					
	$\hat{\beta}(0)$	32244	11802	12392	15990	3819					
	$\mathrm{cv}\{\hat{f}(0)\}$	0.56	0.25	0.34	0.32	0.89					
	$\mathrm{cv}\{\hat{\beta}(0)\}$	0.50	0.26	0.40	0.34	0.66					
	$\mathrm{cv}(n/L)$	0.41	0.42	0.25	0.19	0.61					

Table A.7: Equal effort estimates of $f(0)$, $\beta(0)$ and other components of abundance estimates; eastern Bight; 1991–1997.

Year		Replicate 1	2	3	4	5	6	7	8	$\frac{ee(\widehat{D}_1)}{te(\widehat{D}_1)}$	$\frac{ee(\widehat{D}_0)}{te(\widehat{D}_0)}$
	n_i	54	41	15	22					18.6	54.7
	L_i	1,285	1,199	1,185	893						
1993	$\hat{f}(0)$	136.6	130.9	179.9	389.0						
	$\hat{\beta}(0)$	17706	11772	6153	4406						
	cv$\{\hat{f}(0)\}$	0.25	0.23	0.36	0.22						
	cv$\{\hat{\beta}(0)\}$	0.25	0.20	0.41	0.20						
	cv(n/L)	0.20	0.29	0.36	0.28						
	n_i	17	18	26	11	15	6	34	22	57.1	16.6
	L_i	1,021	1,189	1,196	1,102	953	925	1,269	1,242		
1994	$\hat{f}(0)$	127.2	297.2	106.4	5.3	119.8	112.1	462.0	295.3		
	$\hat{\beta}(0)$	15264	12369	13591	4299	14950	5587	15087	13292		
	cv$\{\hat{f}(0)\}$	0.33	0.28	0.28	0.82	0.44	0.92	0.16	0.21		
	cv$\{\hat{\beta}(0)\}$	0.37	0.41	0.34	0.87	0.41	0.77	0.15	0.28		
	cv(n/L)	0.45	0.38	0.24	0.24	0.39	0.83	0.25	0.24		
	n_i	17	20	16	21	16	34	16	3	51.0	58.7
	L_i	1,378	1,087	1,009	1,123	1,088	1,145	1,187	1,229		
1995	$\hat{f}(0)$	318.5	342.8	133.6	380.1	386.4	299.9	152.4	889.4		
	$\hat{\beta}(0)$	11954	17517	6552	16652	39915	22522	18589	19647		
	cv$\{\hat{f}(0)\}$	0.26	0.27	0.52	0.27	0.26	0.22	0.45	0.68		
	cv$\{\hat{\beta}(0)\}$	0.25	0.26	0.40	0.28	0.30	0.25	0.57	0.45		
	cv(n/L)	0.22	0.27	0.33	0.38	0.45	0.39	0.35	0.53		
	n_i	0	1	3	8	26	18	0		48.9	43.8
	L_i	993	1,064	1,190	1,357	1,330	1,408	1,235			
1996	$\hat{f}(0)$	0.0	0.0	321.3	122.8	192.1	127.0	0.0			
	$\hat{\beta}(0)$	0	0	6104	18430	8500	25137	0			
	cv$\{\hat{f}(0)\}$	0.00	0.00	0.91	0.75	0.29	0.34	0.00			
	cv$\{\hat{\beta}(0)\}$	0.00	0.00	0.68	0.85	0.31	0.37	0.00			
	cv(n/L)	0.00	1.25	0.51	0.48	0.43	0.47	0.00			
	n_i	17	17	31	35	8				53.3	119.5
	L_i	1,122	1,308	1,351	982	1,033					
1997	$\hat{f}(0)$	238.0	236.3	143.2	127.7	113.3					
	$\hat{\beta}(0)$	40924	11018	10722	18967	5024					
	cv$\{\hat{f}(0)\}$	0.39	0.26	0.36	0.30	0.62					
	cv$\{\hat{\beta}(0)\}$	0.34	0.26	0.39	0.34	0.58					
	cv(n/L)	0.42	0.37	0.23	0.15	0.49					

Table A.8: Unequal effort estimates of $f(0)$, $\beta(0)$ and other components of abundance estimates; eastern Bight; 1993–1997.

A.2 School size estimates; 1991 and 1993–97

Year		Replicate 1	2	3	4	5	6	7	8	Total
1991	$\widehat{SS}$	66.8	NA	22.0	26.8	NA				38.6
		(23.2)	NA	(7.0)	(6.5)	NA				(14.2)
	$\bar{y}$	76.9	54.0	36.3	35.0	15.0				50.5
1993	$\widehat{SS}$	124.9	80.0	59.4	23.9					72.0
		(39.1)	(20.3)	(13.8)	(8.7)					(21.1)
	$\bar{y}$	158.8	99.9	65.1	46.2					110.9
1994	$\widehat{SS}$	100.0	27.8	96.2	158.3	171.8	43.0	41.7	60.6	87.4
		(61.6)	(36.3)	(38.6)	(173.1)	(30.5)	(19.2)	(8.0)	(25.6)	(19.2)
	$\bar{y}$	114.9	71.4	106.2	139.8	120.1	79.5	65.2	107.1	97.8
1995	$\widehat{SS}$	61.8	52.3	51.5	39.6	138.7	78.7	123.8	47.0	74.2
		(22.6)	(8.5)	(5.4)	(15.2)	(32.7)	(41.0)	(50.0)	(19.3)	(13.2)
	$\bar{y}$	149.0	85.8	67.4	59.6	244.5	139.1	121.1	79.0	123.4
1996	$\widehat{SS}$	124.6	24.4	66.4	174.8	97.5	123.4	NA		101.9
		(82.2)	(6.9)	(28.6)	(51.8)	(34.0)	(46.1)	NA		(21.3)
	$\bar{y}$	177.0	34.0	96.7	260.2	144.6	139.0	100.0		152.2
1997	$\widehat{SS}$	67.3	69.4	67.7	107.6	32.4				68.9
		(47.6)	(14.4)	(31.7)	(34.3)	(55.1)				(11.9)
	$\bar{y}$	89.5	104.7	82.3	109.2	38.4				95.1

Table A.9: Size-bias corrected school size estimates ($\widehat{SS}$) and unadjusted estimates $\bar{y}$; entire Bight; 1991 and 1993–1997; using all sightings from north/south transects (ee data).

	Stratum				Overall
	Inshore	Middle	Shelf	Hot	
1991	3.4	1.4	1.1	3.5	2.4
1992	3.6	4.4	1.7	1.0	2.9
1993	7.1	3.3	1.8	2.3	3.1
1994	4.1	3.0	2.3	3.0	3.1
1995	3.5	3.8	1.6	2.4	3.2
1996	5.9	4.5	2.0	4.0	4.2
1997	4.5	4.1	1.9	6.8	3.8
Overall	4.4	3.7	1.9	3.2	3.3

Table A.10: Average number of patches per sighting by year and stratum

	Replicate								Overall
	1	2	3	4	5	6	7	8	
1991	4.2	1.0	1.6	1.5	1.0				2.4
1992	1.7	3.9	3.9	1.8	2.3				2.9
1993	4.4	2.6	2.3	1.2					3.1
1994	2.9	3.1	2.7	5.2	3.2	2.2	2.4	4.0	3.1
1995	4.8	2.8	2.1	1.6	5.7	2.7	3.0	2.4	3.2
1996	5.3	1.5	2.5	6.5	3.7	4.3	2.3		4.2
1997	5.1	3.9	3.0	3.7	2.2				3.7

Table A.11: Average number of patches per sighting by year and replicate

	Inshore	Middle	Shelf	Hot	Overall
1991	19.5 NA	26.0 NA	21.1 NA	9.3 NA	20.4 NA
1992	30.9 29.9	29.0 26.7	28.0 20.2	6.0 10.0	29.4 26.3
1993	30.0 30.7	33.0 32.2	36.6 35.0	38.7 38.6	33.1 32.6
1994	35.4 33.4	26.7 27.2	26.3 22.5	26.1 22.7	30.4 28.5
1995	33.6 32.7	34.5 35.1	27.7 27.6	44.9 48.0	34.1 34.3
1996	29.5 26.3	34.3 32.5	31.3 30.8	26.8 27.1	32.5 30.5
1996	18.9 14.0	29.8 29.1	32.2 32.8	36.6 32.0	27.2 25.0
Overall	29.3 28.7	32.0 31.6	30.6 28.5	35.1 34.9	30.8 30.1

Table A.12: Estimated mean patch size by year and stratum. Mean of pilots' estimates followed by mean of spotters' estimates. NA: not available

	Inshore	Middle	Shelf	Hot	Overall
1991	9.2 NA	13.1 NA	16.8 NA	18.4 NA	10.8 NA
1992	16.2 15.7	13.7 14.5	15.1 15.6	12.0 13.7	15.1 15.3
1993	16.0 17.2	16.3 17.1	21.5 22.5	16.9 17.6	17.8 18.8
1994	12.8 13.4	14.1 14.5	19.4 19.5	16.9 16.0	15.0 15.4
1995	12.7 13.5	15.1 14.8	17.8 17.9	16.5 16.3	14.7 14.7
1996	13.1 12.5	15.8 15.1	18.7 19.3	14.7 13.4	15.3 14.8
1997	15.5 11.4	16.2 15.6	17.9 17.4	17.3 16.4	16.3 14.5
Overall	13.7 14.0	15.3 15.2	19.1 19.5	16.8 16.3	15.4 15.6

Table A.13: Estimated mean size of fish within a patch by year and stratum. Mean of pilots' estimates followed by mean of spotters' estimates. NA: not available

A.3 Environmental conditions during the surveys 1991 and 1993–1997 by replicate

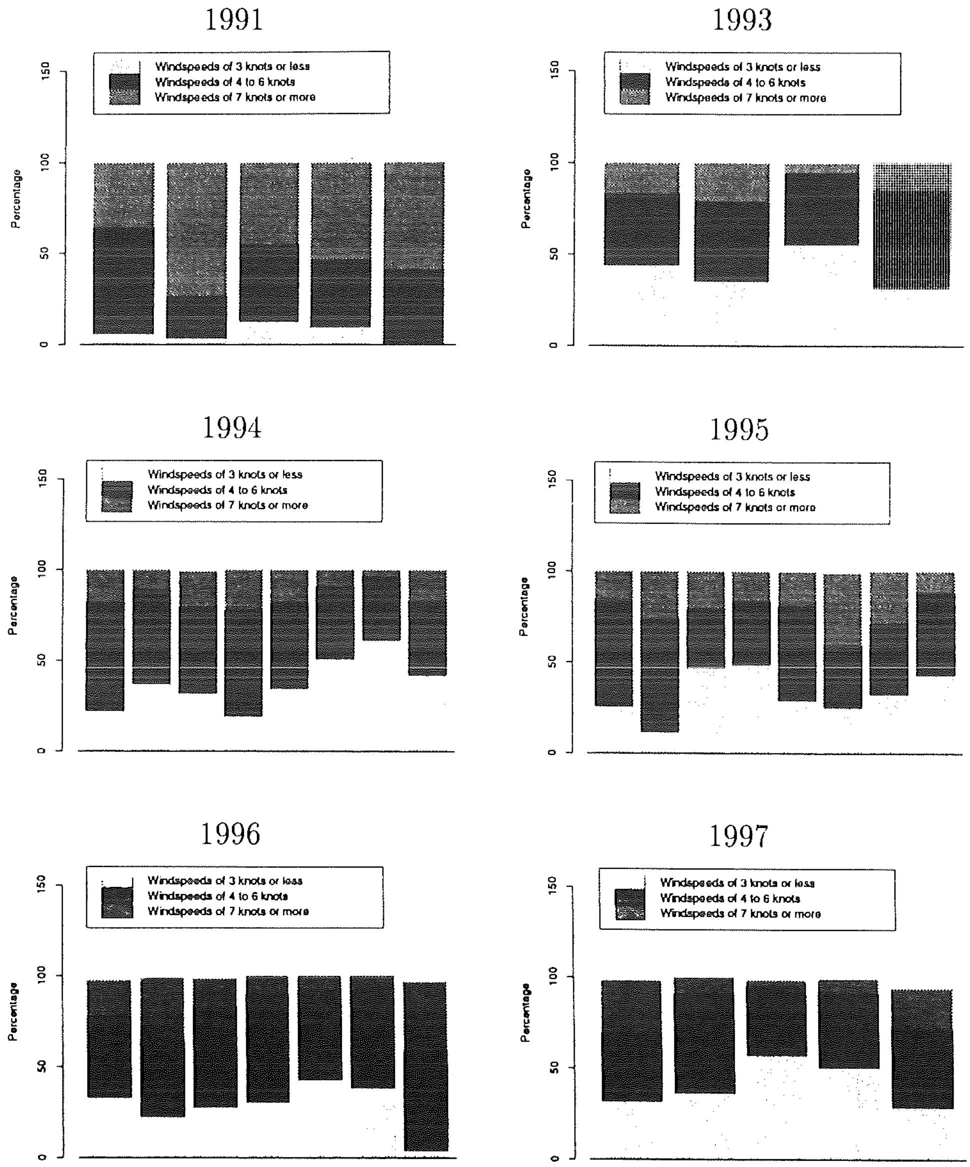

Figure A.1: Percentage of survey effort spent in different windspeeds by replicate; entire Bight; 1991 and 1993–1997

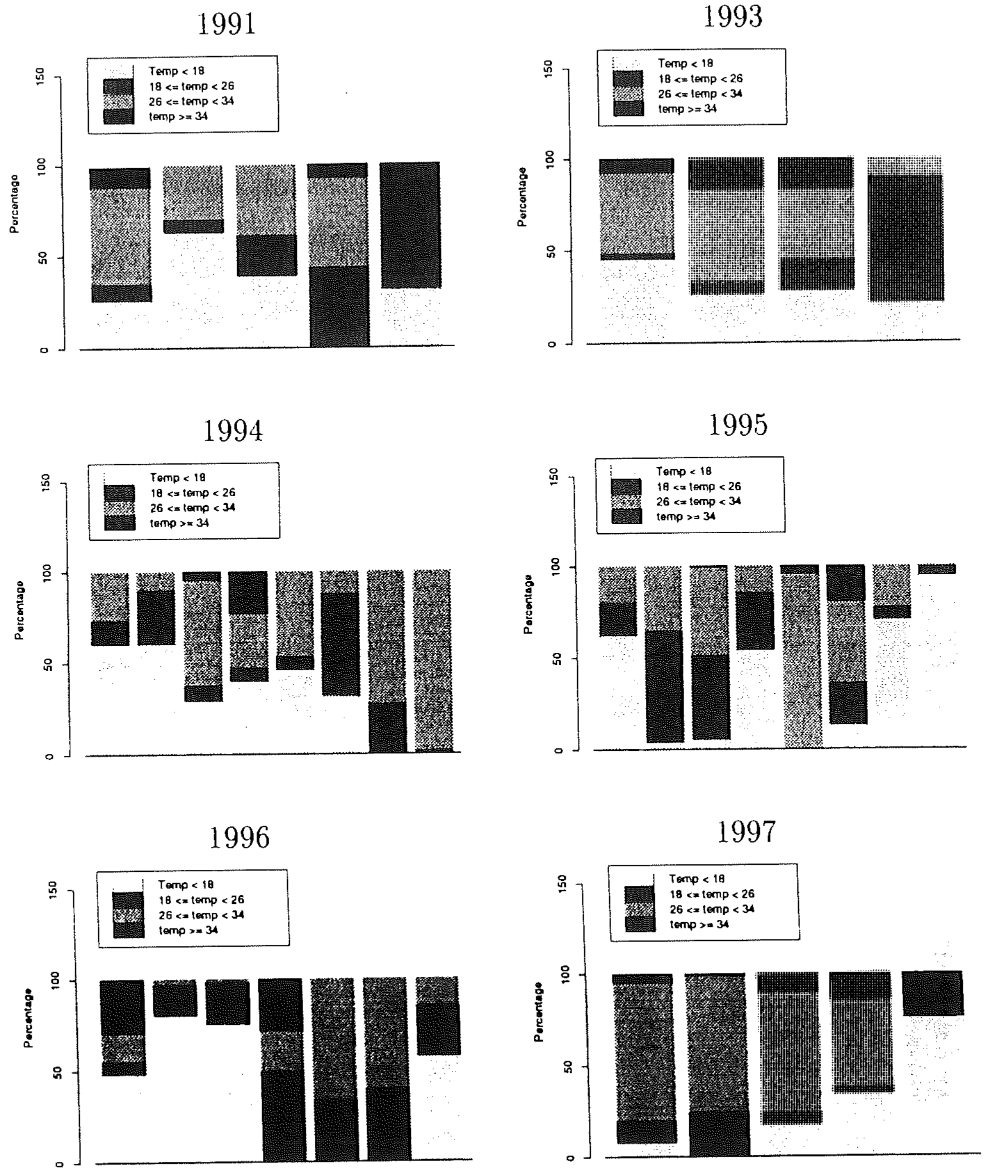

Figure A.2: Percentage of survey effort spent in different air temperatures by replicate; entire Bight; 1991 and 1993–1997

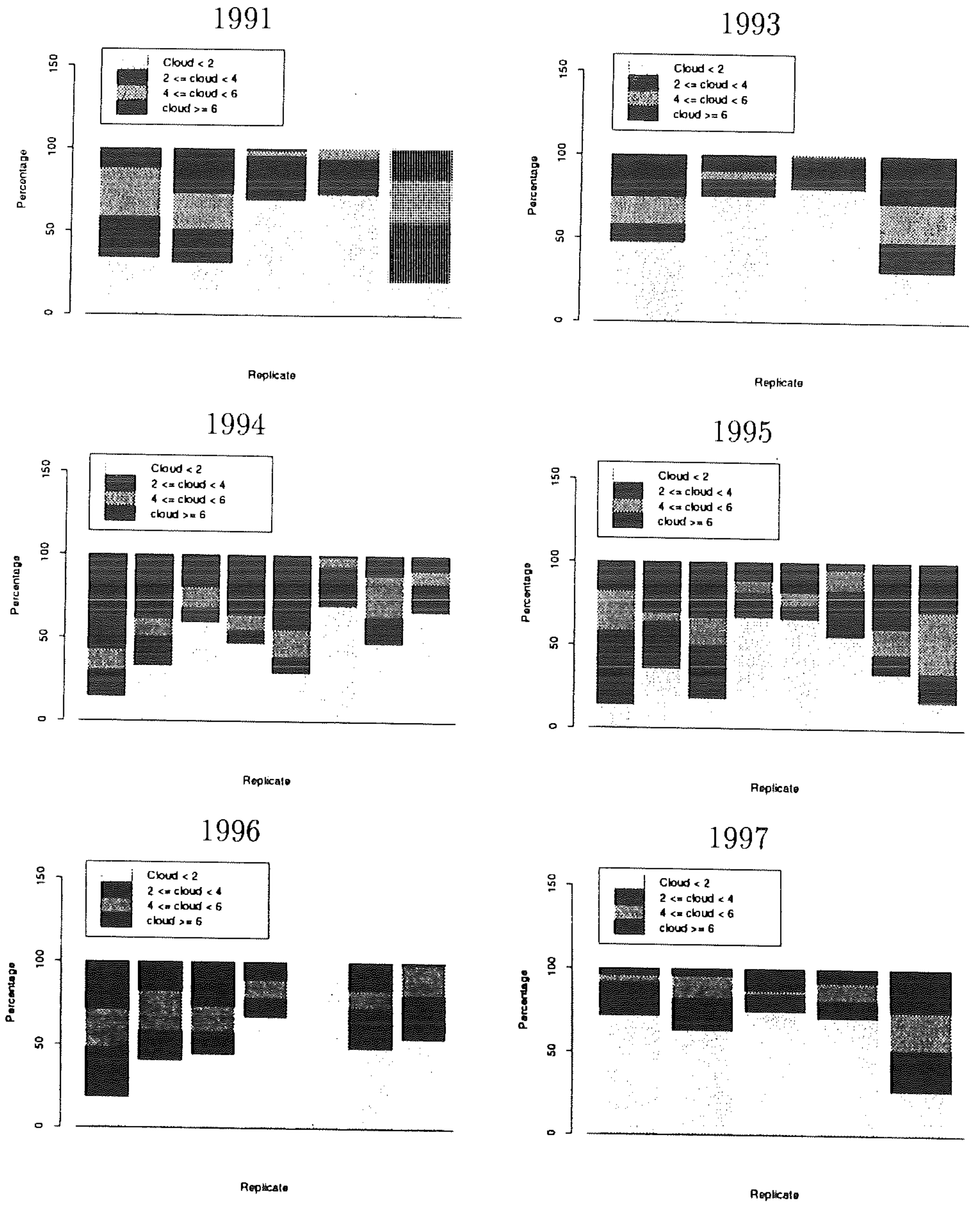

Figure A.3: Percentage of survey effort spent in different cloud conditions by replicate; entire Bight; 1991 and 1993–1997

A.4 Relationship between perpendicular sighting distance and environmental conditions

A non-parametric repression curve is shown on each plot (obtained using **supsmu** in Splus), together with the (maximum likelihood) estimate of the correlation, and the P-value of the test of the null hypothesis $\rho = 0$.

Figure A.4: Perpendicular distance versus windspeed

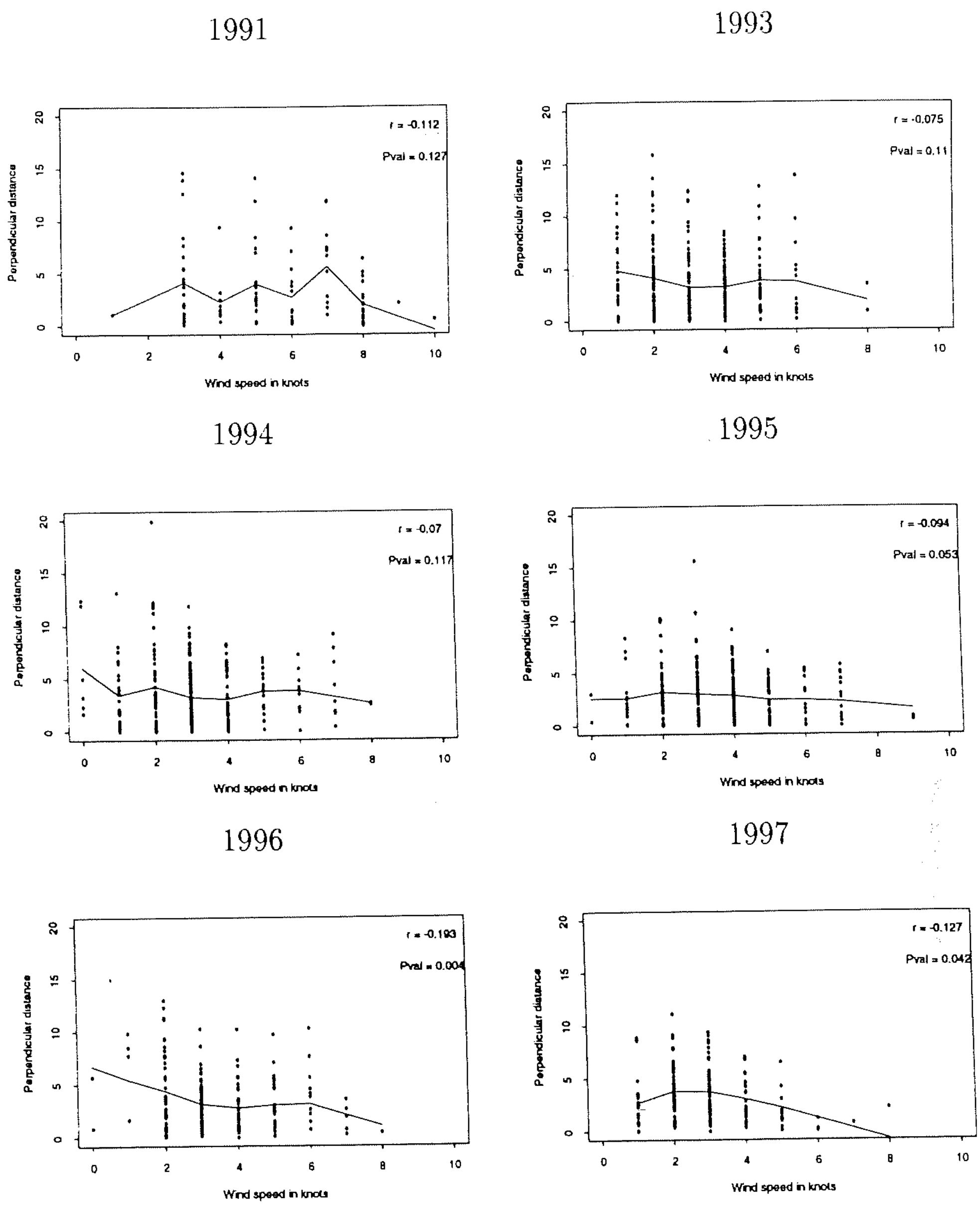

Figure A.5: Perpendicular distance versus cloudcover

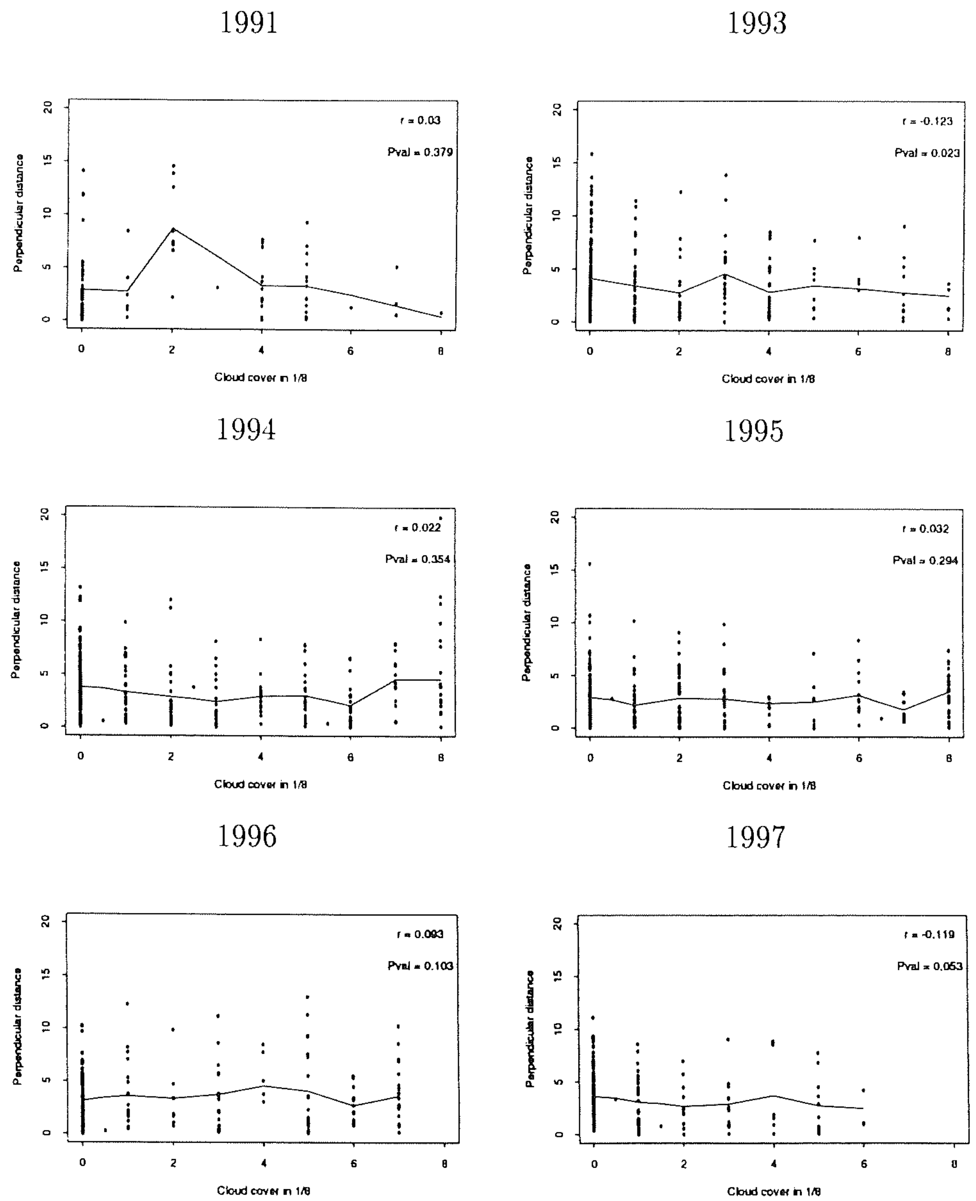

Figure A.6: Perpendicular distance versus air temperature

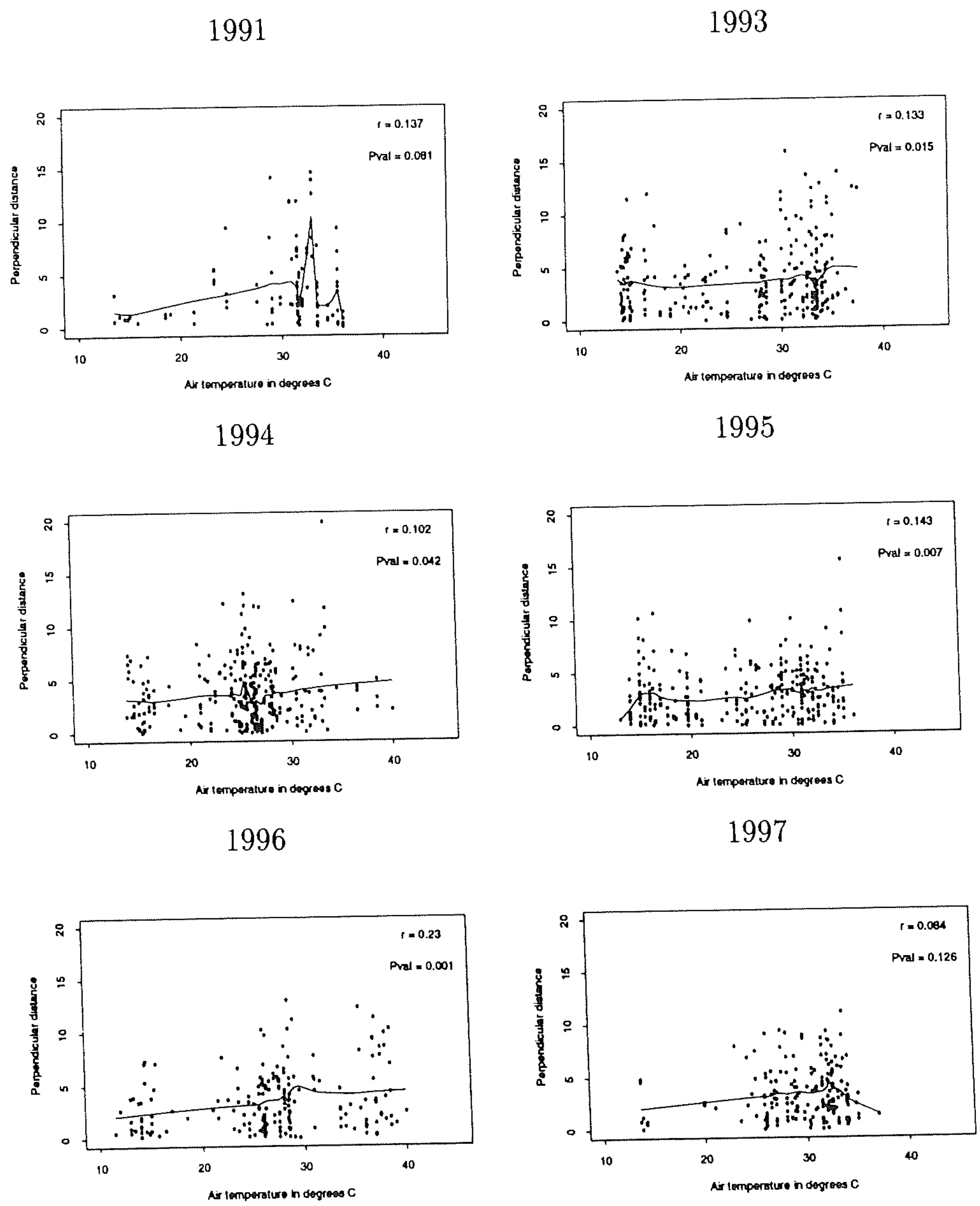

Figure A.7: Perpendicular distance versus sea surface temperature

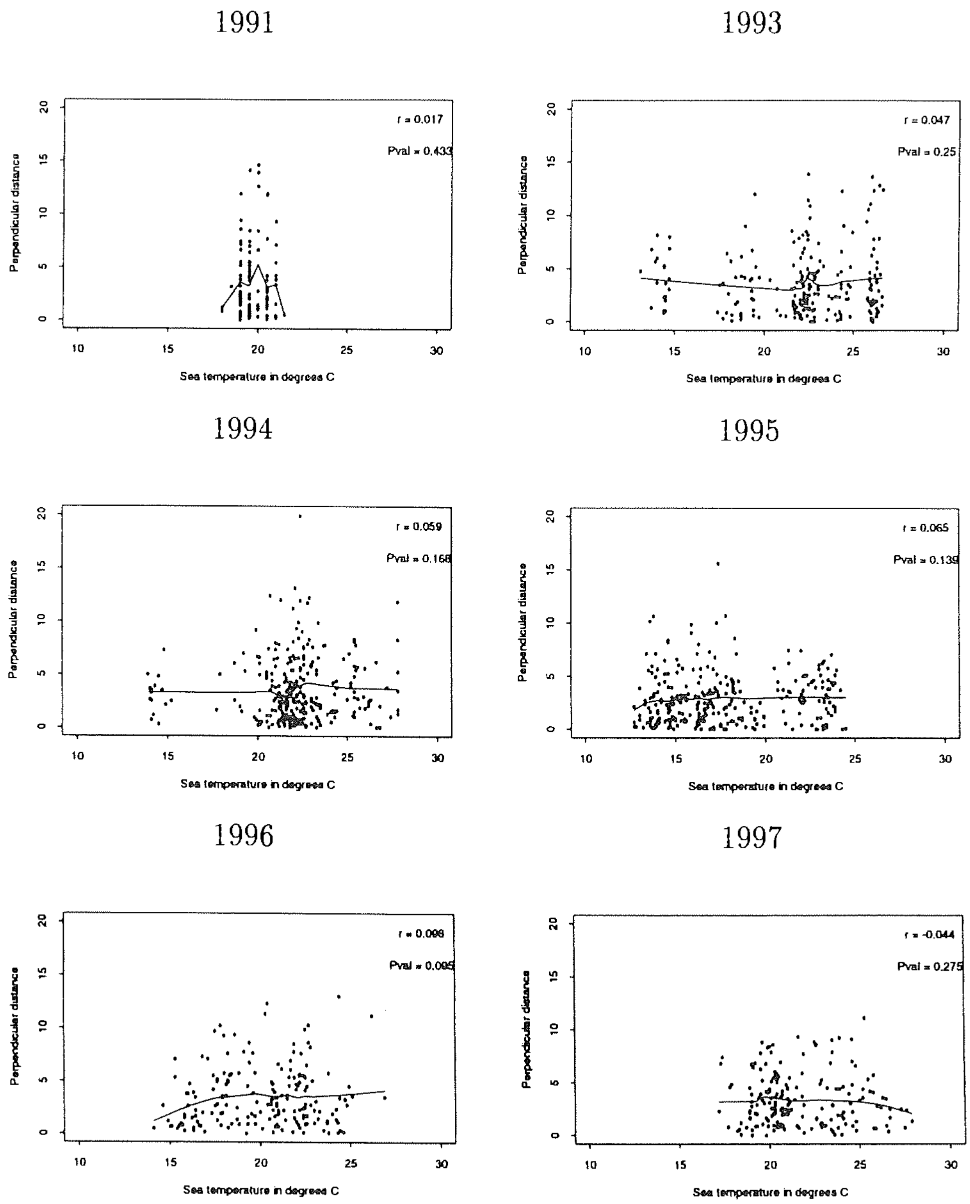

A.5 Relationship between pilot's estimate of school size and environmental conditions

Figure A.8: Pilot's estimate of school size versus windspeed

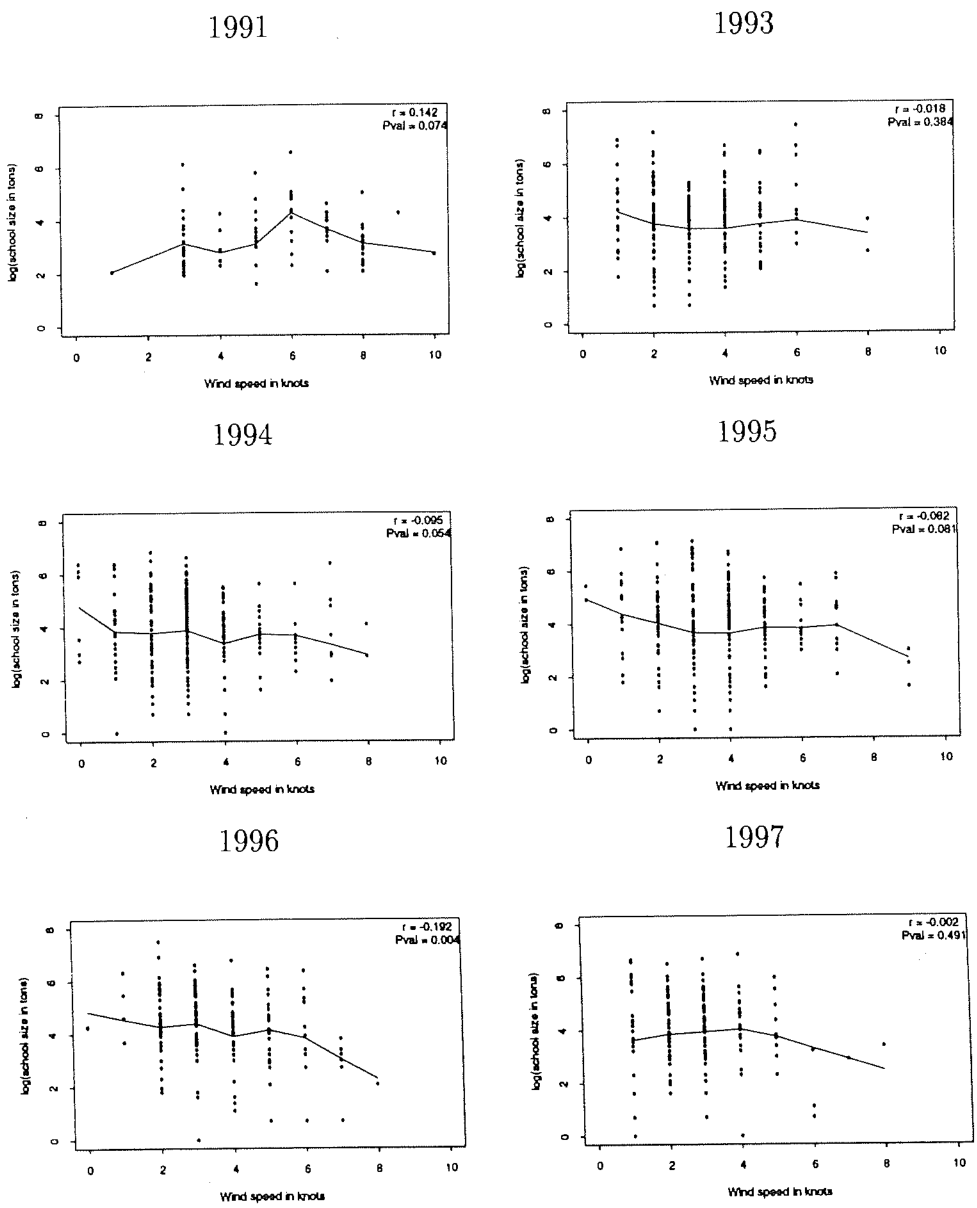

Figure A.9: Pilot's estimate of school size versus cloudcover

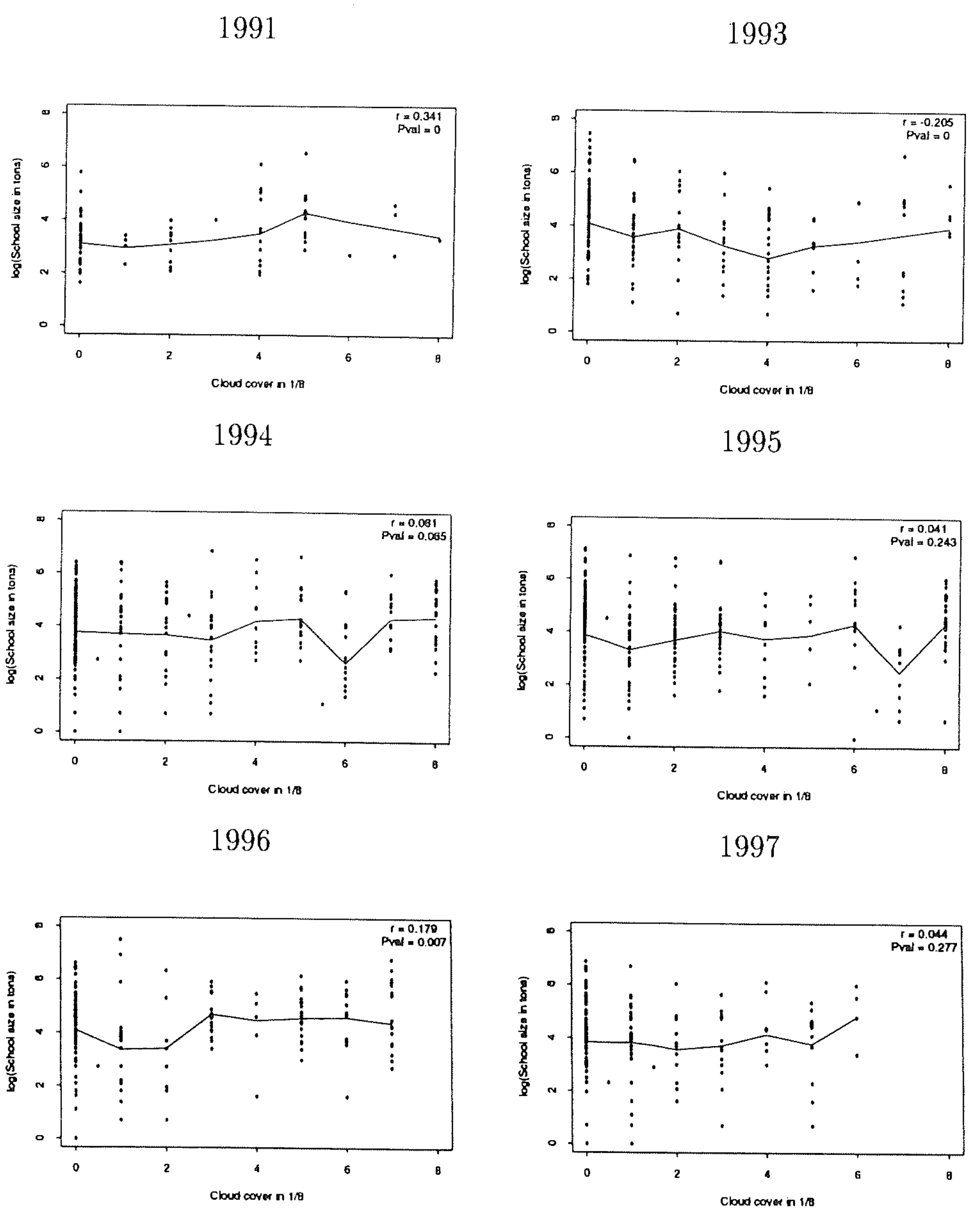

Figure A.10: Pilot's estimate of school size versus air temperature

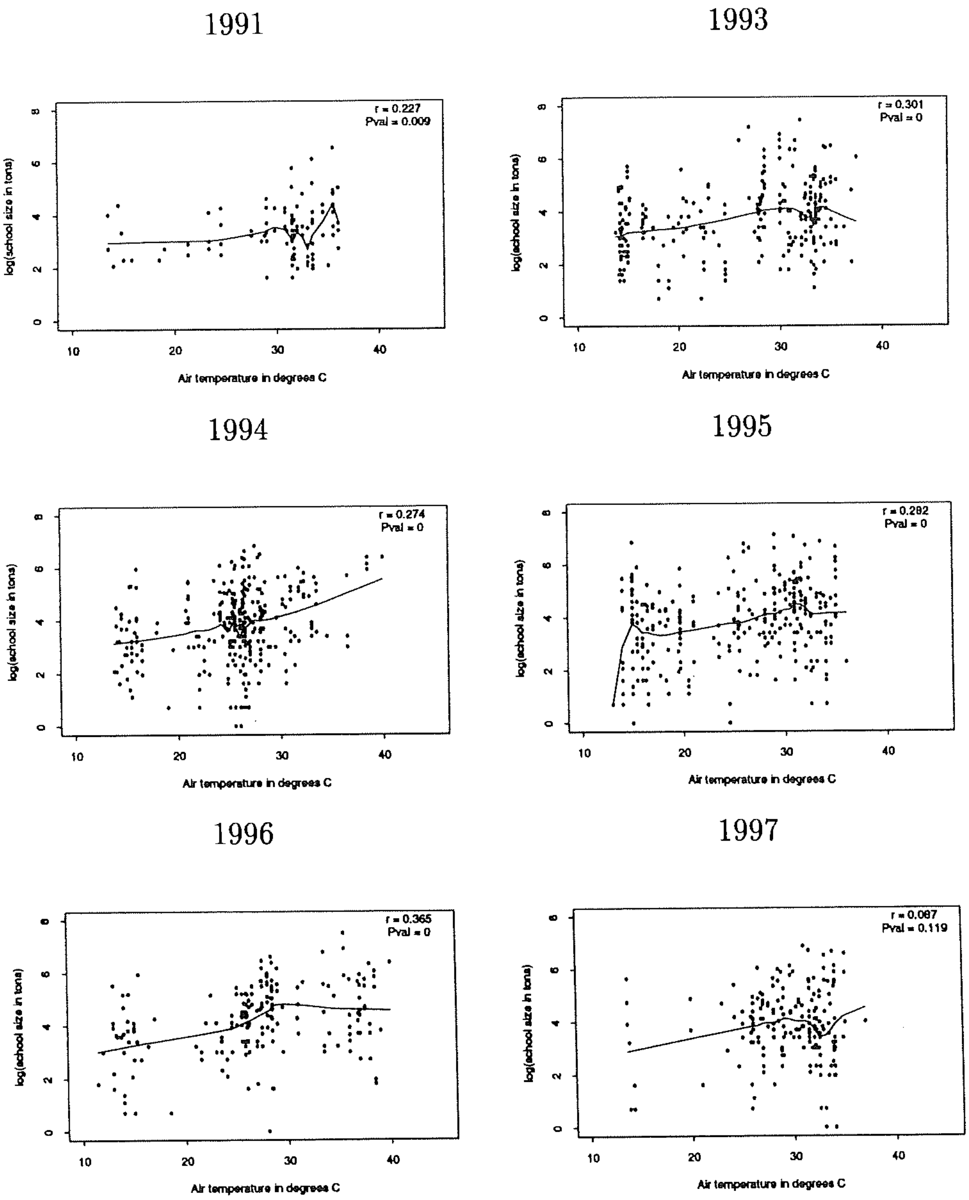

Figure A.11: Pilot's estimate of school size versus sea surface temperature

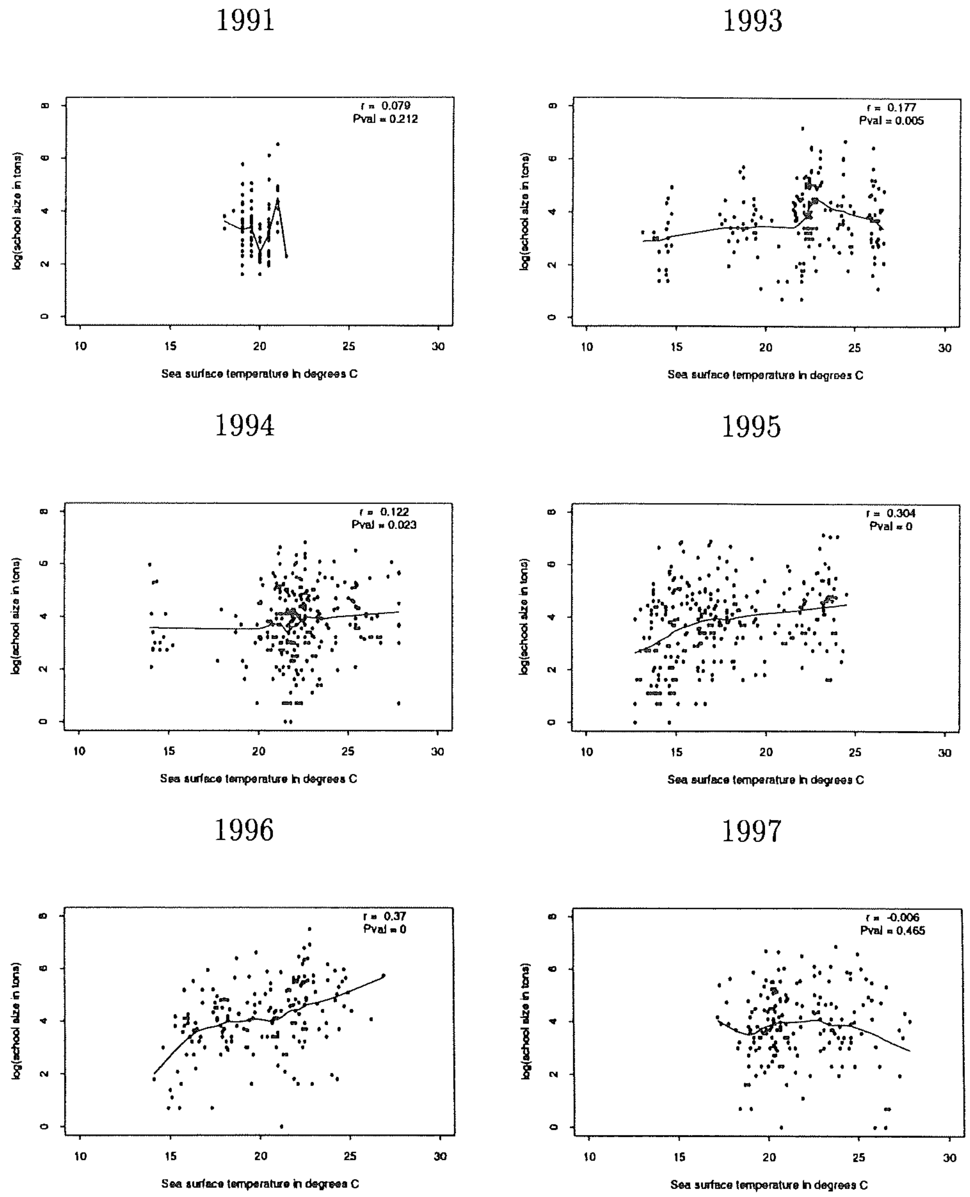

RMWS/97/24

SBT Surfacing Behaviour

Colin Millar and Ann Cowling
CSIRO Division of Marine Research
GPO Box 1538
Hobart, Tasmania 7001

SBT Surfacing Behaviour - Colin Millar, Ann Cowling.

The indices of abundance from the aerial survey are surface measures. To estimate absolute abundance, we need to adjust these indices for the proportion of schools at the surface. From experience gained through many years of commercial fishing and aerial spotting of tuna schools, it is believed that tuna surfacing behaviour is influenced by weather conditions.

Archival tags record tuna depth and sea temperature every 4 minutes. By matching this data with weather data from Bureau of Meteorology weather stations, it may be possible to identify patterns of surfacing behaviour in response to environmental conditions. These could then be used to provide surfacing probabilities for use in the aerial survey analysis.

Methods :

The main sources of data were 5 archival tags and the Bureau of Meteorology's weather station at Ceduna. Ceduna was chosen because it is located at about the central longitude of the survey area.

From each tag, sea surface temperature (SST) and depth recordings (which were at 4 minute intervals) were grouped into 24 'hours'. First the dawn and dusk times were calculated using the light levels from the tags, and then the data grouped into 6 periods before dawn, 12 between dawn and dusk, and 6 after dusk in order to standardise the days for changes in day length. For each of these periods the average SST was calculated along with the number of sample times the fish was at the surface, and beneath the surface. A fish was defined to be at the surface if it was at a depth of 2 metres or less. The average SST for each period was calculated by using the average sea temperature of all samples where the fish was at the surface

The Ceduna weather station data provided 3-hourly readings of air temperature (AT), barometric pressure (BP), and wind speed (WS). These readings were interpolated to match the midpoint of the fish 'hourly' intervals using smoothing splines. Missing data for the tags and Ceduna weather station was replaced in a similar manner.

The data was restricted to the period from the 25th January to 31st March 1994, as this period was fully covered by all of the tags.

The explanatory variables used in statistical models of surfacing behaviour were AT, BP, WS, SST, 'hour' of day (H) and several variables representing the day in the study period. The most general of these was simply the day of the period. A question examined during the analysis was whether this could be replaced by moon phase. Moon phase (MP), was defined as the day of the lunar cycle with the range of 1 to 29, and the full moon corresponding to day 1 of the cycle. MP was further split into 4 categories, 3 of 7 days duration, and one of 8 days which corresponded to the full moon, last quarter, new moon, and first quarter. The actual event (such as the full moon), occurred in the middle of the period.

Generalised additive models (GAMs) and generalised linear models (GLMs) were used in the analysis. GAMs were used first because of the flexibility of splines in fitting the response variables. However the distribution theory of GAM's is not yet known, and the usual tests based on deviance for including or excluding terms from models are at best approximate, but serve as guidelines.

The fitted splines were used to indicate the degree of the appropriate polynomial required in a GLM. Tests based on deviance for GLM's are asymptotically exact.

Binomial models were used with the number of sampling times the fish was at the surface and the total number of sampling times in each hour as the response variables.

Results :

Model 1 :
Explanatory variables : day, hour, SST, AT, WS, BP

Trends by variable :
- day - two patterns can be seen in response to day, a cycle with a frequency of about a month, and a cycle of smaller magnitude with a frequency of roughly 10 days.
- hour - fish tend to surface more in the first half of the day from midnight to noon.
- AT - surfacing decreases as AT increases
- SST - surfacing increases as SST increases
- WS - surfacing decreases as WS increases, but seems to increase again when WS > 15 knots.
- BP - There is no strong pattern apparent except for a small bump at 1005 hectoPascals where surfacing activity increases.

Model 2:
Explanatory variables : moon, hour, SST, AT, WS, BP

The moon variable was added in response to the lunar cycle seen in the day variable in Model 1. There appears to be a decrease in surfacing activity around the full moon, with a couple of smaller troughs at day 14 and 21 of the moon phase period. All of the other variables that were in Model 1 had the same patterns as described under Model 1.

Model 3:
Explanatory variables : hr1, hr2, hr3, hr4, SST, AT, WS, BP

The previous models fitted the same hourly pattern throughout the survey period. To allow for different hourly surfacing patterns in different phases of the lunar cycle, moon phase was divided into 4 periods and a separate hour variable fitted (see method section for more detail). These became the most important. Three of the hour variables (hr2..hr4) showed similar patterns with higher surfacing rates around mid-morning and the least after about 3PM, while hr1 (the full moon period) shows the opposite effect with the least amount of surfacing between 10AM and 4PM.

The effects of the environmental variables remained much the same as with Model 1.

Model 4:

Explanatory variables : fish, hr1, hr2, hr3, hr4, SST, AT, WS, BP, + interaction terms

The objective of this model was to test the extent to which the 5 fish behaved similarly. It is essentially the same model as Model 3, with terms added to allow each fish to respond differently to each variable.

The main effects of the explanatory variables from Model 3 are unchanged. The additional terms are all significant, and shows that the individual fish are behaving differently. The plots for the interaction effects for each fish show the different behaviour of the fish, with some fish showing exactly the opposite response to a variable.

Tables:

Model	df	deviance	change in df	change in deviance
Null	7919	66107		
Model 1	7882	54927		
Model 2	7885	55162	3	235
Model 3	7879	52995		
Model 4	7715	46549	164	6446

Variable	Df	Deviance
Null	7919	66107
hr1	5	3856
hr2	5	1356
hr3	5	1614
hr4	5	1963
SST	5	2383
AT	5	1705
WS	5	167
BP	5	69
Model residual	7879	52995

Anova table for Model 3.

Conclusions :

Of the models fitted, Model 3 was the most effective at explaining SBT surfacing patterns. The hour of day by moon phase variable had a larger deviance (more explanatory power) than any environmental variable. SST had the largest deviance of the environmental variables. During the full moon, SBT are more likely to be at the surface after dusk when the SST is high. During the other phases, SBT are more likely to be at the surface during mid-morning, again when the SST is high.

Model 4 shows that the individual SBT had significantly different responses to each factor in the model, including the hour of day by moon phase variable.

The models fitted to date do not have very high explanatory or predictive power. The AT, BP and WS data fitted to date comes from Ceduna, which may differ to the corresponding weather at sea. The lowest cost source of such data is currently being sought. Wind direction has not been used in the analysis to date but can be expected to be influential. With more relevant environmental data, the fit of the corresponding model may well improve. Other models of diurnal behaviour may also provide a better fit. Following further discussions with fisheries ecologists, other models will be attempted.

To date, only 5 archival tags have been returned with daily data collected during the aerial survey period, all for 1994. While the observed lunar behavioural response is consistent with what has been observed in longline catch data, data from at least one more year is required for confirmation. Thus more returns of archival tags are needed.

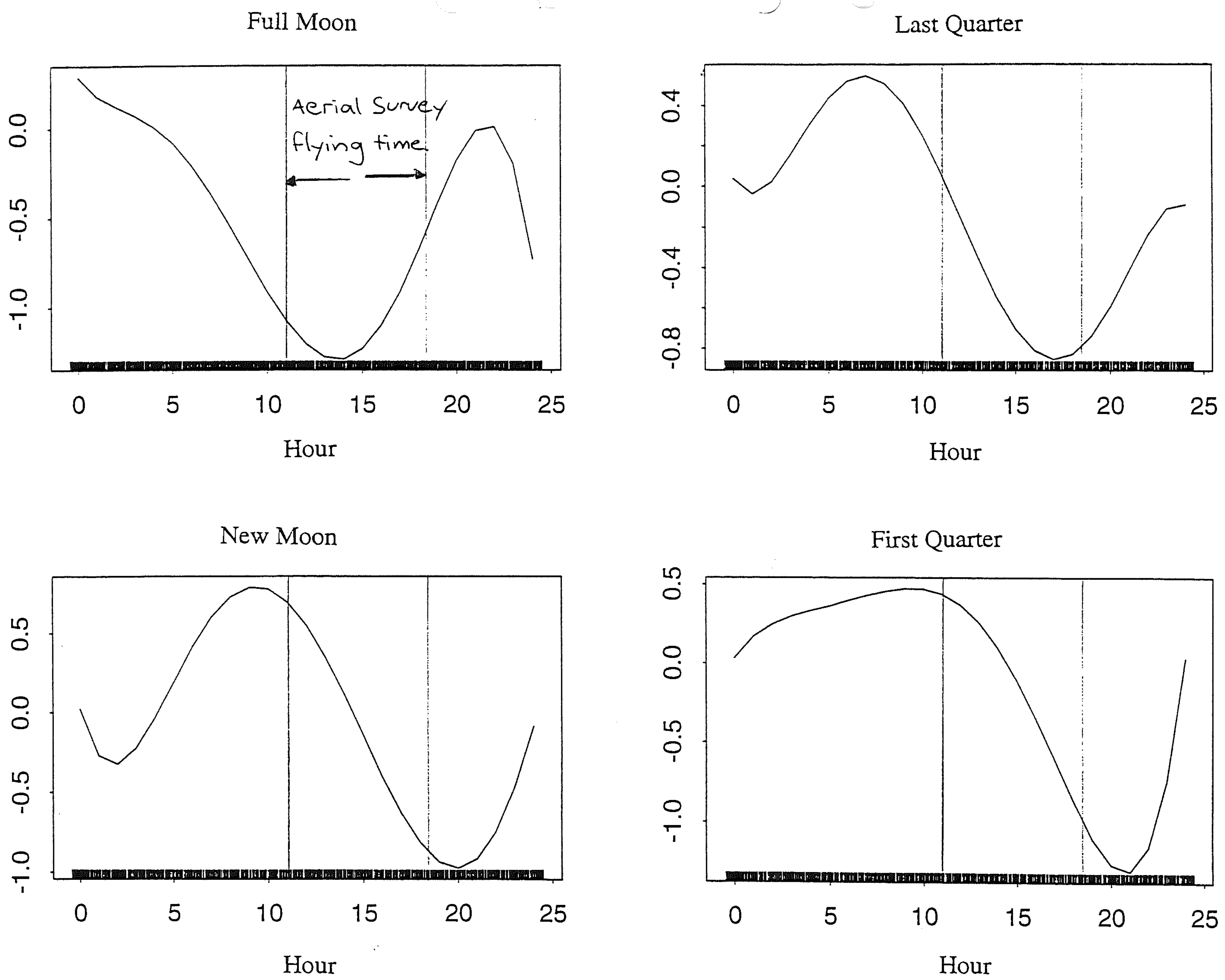

Full Moon
Aerial Survey flying time
0.0
-0.5
-1.0
0
5
10
15
20
25
Hour
Last Quarter
0.4
0.0
-0.4
-0.8
0
5
10
15
20
25
Hour
New Moon
0.5
0.0
-0.5
-1.0
0
5
10
15
20
25
Hour
First Quarter
0.5
0.0
-0.5
-1.0
0
5
10
15
20
25
Hour

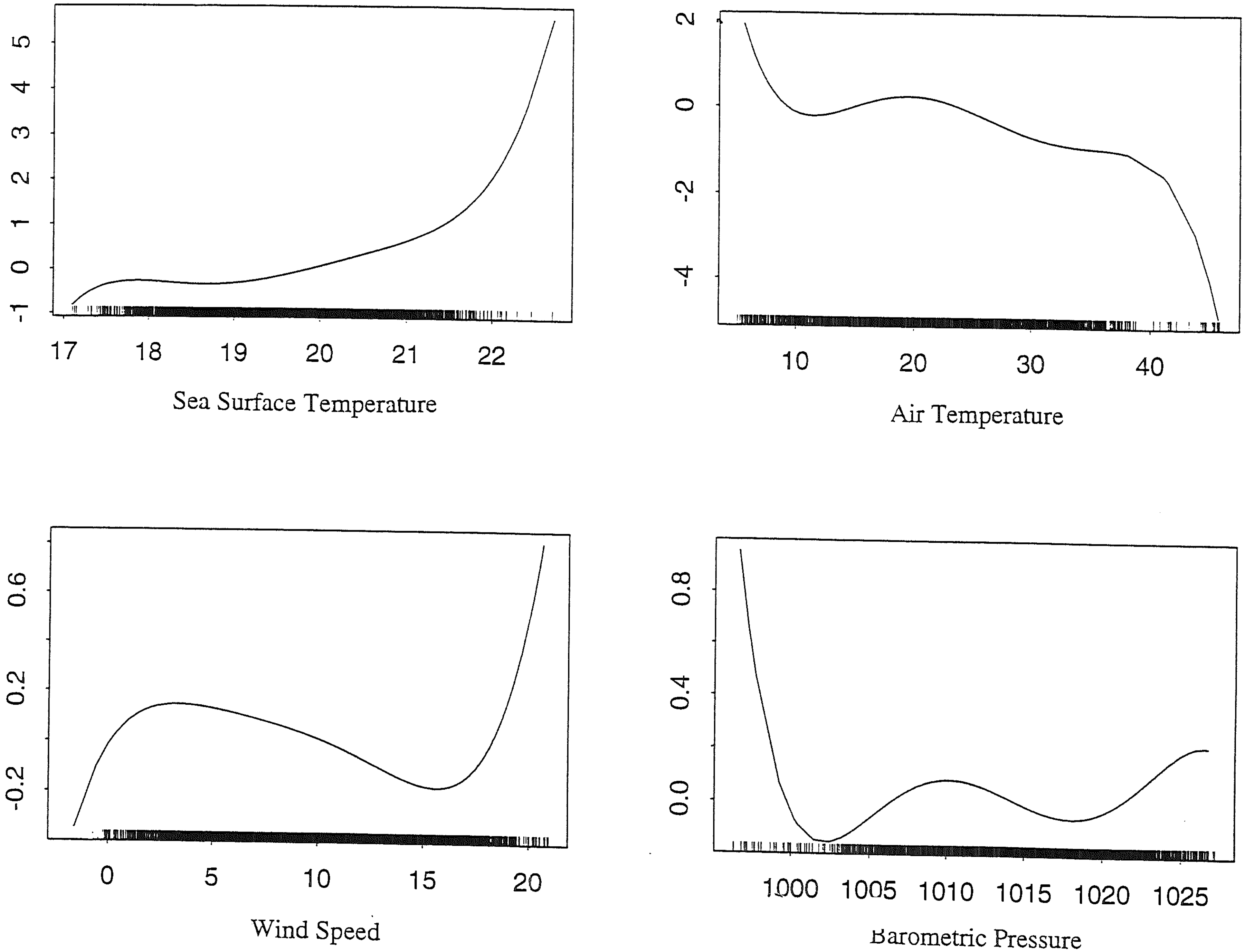

5
4
3
2
1
0
-1
17
18
19
20
21
22
Sea Surface Temperature
2
0
-2
-4
10
20
30
40
Air Temperature
0.6
0.2
-0.2
0
5
10
15
20
Wind Speed
0.8
0.4
0.0
1000
1005
1010
1015
1020
1025
Barometric Pressure

RMWS/97/7

Report on the LIDAR Trials for 1997

Ann Cowling
CSIRO Division of Marine Research
GPO Box 1538
Hobart, Tasmania 7001

Report on the 1997 LIDAR trial

Ann Cowling

September 1, 1997

1 Background

Line transect estimation procedures, such as those of the aerial survey, assume that school size is measured without error. If this assumption is not met, there is a systematic bias in the biomass density estimates. The estimation procedure can be corrected, but requires information on the accuracy and precision of the spotters' estimates. It is necessary to collect information to determine whether there is measurement error in their estimates, and if so, assess the size of the error.

The current survey estimates by ageclass are based on the spotters' estimates of fish size, and the assumption that all fish within a single patch are of one age. Catch data suggests that there may be a considerable size range (and hence age range) within a patch. Remote sensing technologies may be able to provide information on the size distribution of fish within each school that would not otherwise be available, allowing improved apportionment of fish to age-class.

Physical ground truthing of the spotters' estimates would involve purse-seining spotted schools and measuring the length or weight of all the fish. The logistics of this appear to be too difficult, and the cost too high (even if quota, boats and crew were available). Since 1993, several remote sensing technologies have been trialled to assess their potential to provide information on fish size and school size.

2 Aims of the trial

The main aim of the trial was to evaluate whether LIDAR technology can be used to

1. estimate the size of schools of SBT (in terms of the number of fish or the school volume),
2. estimate the size of fish within schools of SBT,
3. detect sub-surface schools of SBT that are not detectable to the spotters.

Other aims of the trial were to

4. map the spatial extent of SBT schools,
5. determine appropriate field procedures for collecting LIDAR images of SBT schools,
6. assess the operational feasibility and cost effectiveness of using a LIDAR in the aerial survey.

3 Results

The start of the trial was delayed as Arete had experienced some difficulties with suppliers. The 10 day trial was finally held in late March/early April 1997. It was planned that after installation and testing, data would be collected over the farms in Boston Bay for ground truthing the instrument. The remaining time would be spent on open sea trials. However, during the 10 days, there was only one day with suitable weather for SBT to form surface schools in the GAB. On that day the instrument was being ground tested. Open ocean trials were attempted on 4 days in April, but on each of these days the weather was not suitable for SBT to form surface schools (windy, cold, cloudy, low cloud, big swell).

The Port Lincoln trials were the first time that this instrument had been extensively field tested. Thus it had not been used in attempts to detect fish from a plane before, although laboratory tests using fish in tanks had been made. The data collected during the trial showed that there were a number of design issues which need to be addressed before air-borne LIDAR becomes useful for fisheries applications.

A large number of images were collected over Boston Bay, principally of two of the Lucky S farms and one of Hagan Stehr's farms, in water of about 18m depth. It was intended that the known numbers and sizes of SBT in these farms would be used to ground truth the estimates obtained using the LIDAR. However, it was found that the water in Boston Bay, even on the outer side of Boston Island where these farms are located, was so turbid that the LIDAR could only penetrate to about 10m depth, and so was unable to collect information on all the fish in the cages.

In view of the weather conditions during the trial, the design issues and the water quality in Boston Bay, it was not possible to fully achieve all the aims of the trial. However, some progress was made to achieving the aims, and further progress has been made since the trial.

The results of each aim were

1. Schools size estimates. It was intended that school size would be measured using the volume of the school determined from the LIDAR images and estimates of the packing density of SBT. Because the depth penetration was hampered by the turbidity of the Boston Bay water, it was not possible to measure the full depth extent of the fish in the cages. However, it was possible to measure the lateral extent of the caged SBT, as shown in Figure 1. The lateral extent is consistent with the size of the net. This suggests that the lateral extent of open ocean SBT schools should be measurable.

2. Fish size estimates. Differences in fish signatures can be seen in the images which are related to fish size. Estimates of the size distribution can be developed from these, but it is not known how accurate these estimates will be.

3. Detection of deep schools of SBT. Over open ocean, the LIDAR was able to penetrate to about 25m. It is possible that we detected a school at 25m near a reef but obtaining verification of unobservable schools will obviously remain an issue.

4. Mapping SBT schools. It appears that this will be possible. The lateral extent of caged SBT was measured in Boston Bay. As no surface open ocean schools were detected, it is not known how reliably the lateral extent of the underside of the school can be detected.

5. Field procedures. The Laser swath is fairly narrow (especially at higher altitudes). It was found to be difficult to control a plane sufficiently to hold the pitch and roll steady and fly directly over the cages in Boston Bay, especially in a gusty cross wind. Sometimes several passes were necessary before an observer looking along the path of the laser was able to confirm that we had centered images of the cage. Over Boston Bay, the walls of the cages could be used to judge the location of the fish, but it would have been extremely difficult over the open ocean.

   The operating altitude was varied depending on the operational mode. When searching for schools under the surface greater depth penetration is necessary and an operating altitude of 1000 ft was used. For imaging detected schools, it is necessary to have greater resolution and an operating altitude of 250 ft was used. Some passes were also made at 50ft in the open ocean trials.

   The water clarity data suggest that in the GAB, it should be possible to detect schools to a depth of 20–30m, while in Boston Bay, detections were only made to 10m.

6. Operational feasibility, cost effectiveness. It was shown to be feasible to conduct experiments using LIDAR. If the instrument proves to be useful, this will be a much less costly method of verifying size estimates than purseining schools.

The Arete scientists have shown that over Boston Bay, the presence of a school can be determined by looking at the water turbidity (see Figure 2). There is an increase in turbidity right over the school. It has not yet been shown whether this is also the case in open ocean water, and if so, whether deeper schools can be detected in this way.

4 Design issues identified and subsequent modifications

1. Resolution. The resolution needs to be appropriate for measuring the size of fish within schools. Arete have doubled the resolution in the along track and the depth directions.

2. Reflectance. SBT are not highly reflective fish especially when seen from above. This makes them difficult to detect with a laser. Improving the resolution will give more contrast thus improving the images of the schools.

3. Surface glare. It is important to minimise surface reflection if information on SBT near the surface is to be collected. The solutions appear to be to increase the incidence angle or use a polariser.

4. Real time display. It is essential to have a real time display of the image. This allows the crew to know whether the plane flew directly over a school and would be essential for open ocean trials. Real time processing which removed surface return would also be useful.

5. Weather conditions. As weather conditions in the GAB are so variable, a longer time period should be allowed for any future experiments. A 3 week duration is proposed. Once sufficient data had been collected, the trial would finish and the participants return home. Holding a trial in February would improve the chances of having suitable weather and oceanographic conditions. However, the risk of unsuitable weather will always be a factor that both parties should consider.

5 Future plans

While the results of the Port Lincoln trial suggest that LIDAR has potential, the effectiveness of the instrument for the purposes of the aerial survey have not yet been demonstrated.

Arete plan to hold field trials off Hawaii in late September.

Provided that the Hawaii trial demonstrates that LIDAR can be used to estimate school size, fish size and detect deep schools with reasonable precision, and the estimates have been ground truthed, then we plan to trial the instrument again in the 1998 field season. It is proposed that the trial would be held at the same time as the sonar trial, so that we could cross-verify the images obtained using the two technologies.

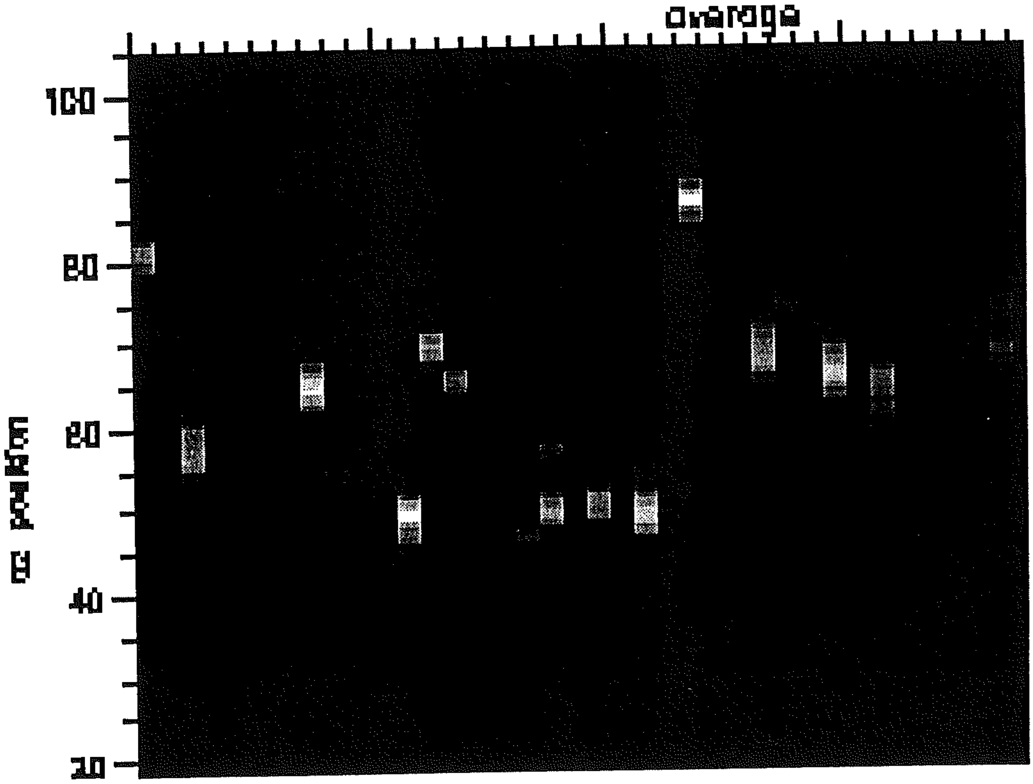

Figure 1: Fish map of SBT at 2.5–4m depth over on Lucky S fish farm

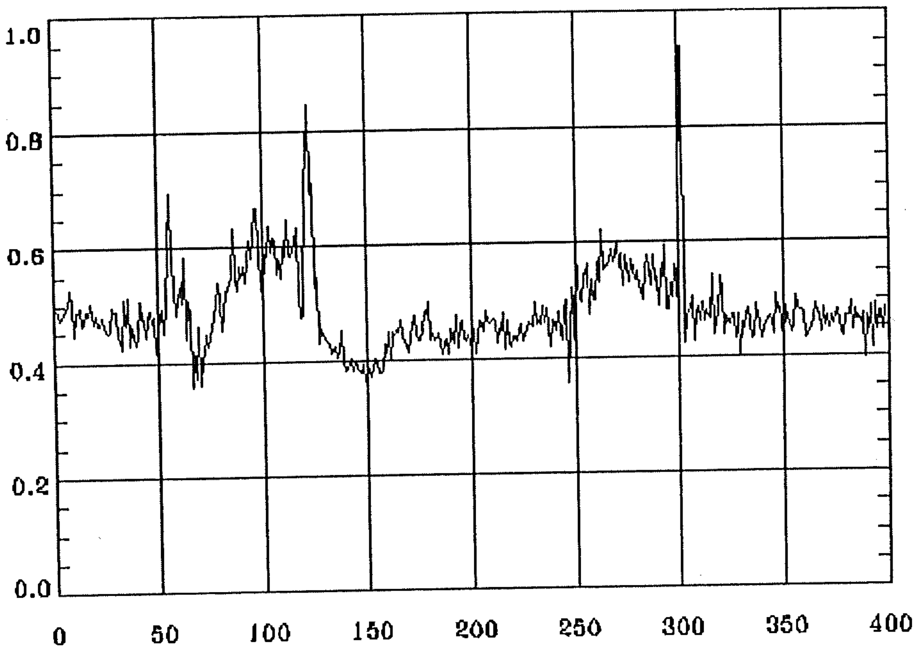

Figure 2: Average per-shot diffuse attenuation: Boston Bay, slit 2

RMWS/97/5

Report on the 1997 LIDAR Trial

Andrew Griffis
ARETE Associates

MEMORANDUM
DRAFT

TO: **Dr. Ann Cowling,** CSIRO Marine Laboratory
FROM: Andrew Griffis, Arete Associates
RE: 1997 South Australia Bluefin Tuna LIDAR Research
DATE: 25 August, 1997
CC: Dr. John McLean, File, Reading

This memo is divided into several parts. The first is a brief description of the sensor hardware configuration, as developed with Arete IR&D funding, the second is a tabulated summary of the experimental data collected, with comments regarding the nature of the data, as appropriate. The third section is a chronolog of the experiment, with annotated photographs. The fourth section shows select experimental data (images) in both processed and raw format. These constitute highlights at the present time of the ongoing analysis effort (funded by ONR and NOAA efforts). The last section is a discussion of issues raised by yourself and Dr. Polachek regarding this experiment.

Sensor Hardware Configuration

The ASTIL system electronic configuration is illustrated in **Figure 1**. The major subassemblies are the host computer (Intel P5-166MHz) with framegrabber and control electronics, the Big Sky Nd:Yag laser, the Hamamatsu C4187 Streak Camera, and the Silicon Mountain Design SMD-60M CCD camera. System timing is facilitated by the Stanford DG535 pulse generator.

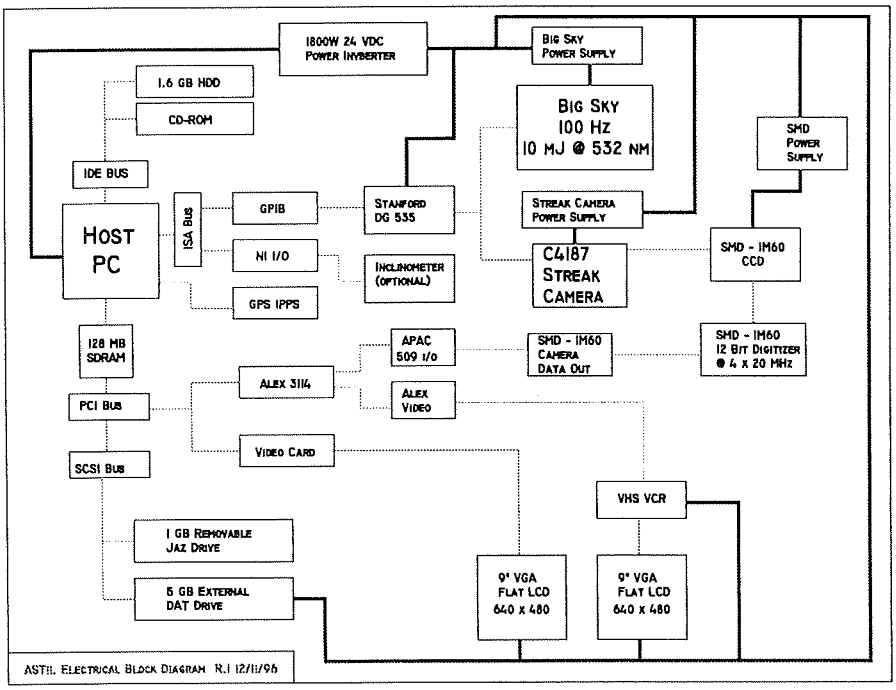

Figure 1. ASTIL System Electrical Layout

These subassemblies are packaged in two groups: 1) receiver/transmitter optics and electronics and 2) data acquisition/control and power supplies. These two packages occupy two ruggedized aircraft racks, as shown in **Figures 3 and 4,** respectively. The general nature of the critical subassemblies that make up the two racks is described below.

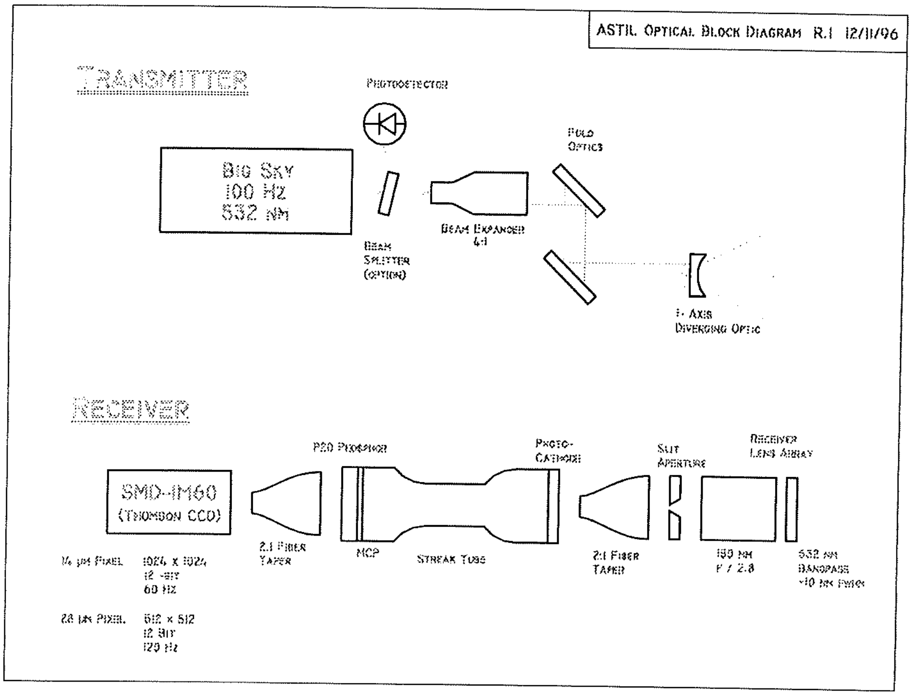

Figure 2. ASTIL Optical Configuration

Receiver/Transmitter Optics

Figure 2 shows the general optical layout of the receiver/transmitter assembly (the only parts not presently in place are the photodiode and associated beam sampler). This is essentially a simplified version of the laboratory system that has been evaluated under the ONR contract, though the receiver has been compacted a bit by the addition of a fiber taper, and the data rate has been increased by changing to the SMD camera. Also, since the sensor is now on a moving platform, the exit mirrors with scanner are not needed, further simplifying the configuration.

The transmitter is a frequency-doubled 100 Hz Big Sky Nd:Yag laser with fundamental at 1064 nm, yielding 8 ns pulses at 532 nm. The nominal output energy is 12.5 mJ per pulse (or 1.25 Watts total power) at 532 nm, which has been confirmed by measurement in the lab and during flight. The transmitted light is expanded 4:1 and steered into a cylindrical lens prior to exiting the transmitter section. This output lens, given collimated light at its input, will provide an output fan beam that is roughly 15 degrees perpendicular to the aircraft track. In the first two flights, the beam is closer to 8 degrees, since the laser beam is not fully collimated in the beam expander (this will be corrected in the near term, though it works out well for other reasons, which will be mentioned later). By using the Q-Switch timing signal from the laser as a reference, the backscattered light from the laser can be confocally imaged with the streak tube receiver, with 5-6 ns of jitter.

The receiver consists of a bandpass filter centered at 532 nm (10 nm total passband) followed by a 180 mm f/1.8 lens that images the received fanbeam through a variable slit onto a 2:1 fiber optic taper, which relays the image to the streak tube photocathode. The resultant photoelectrons are electrostatically deflected across the internal microchannel plate and subsequently accelerated into a phosphor. The image formed on the phosphor is relayed by another 2:1 fiber optic taper to the CCD camera, where the photons are converted to charge, shifted to storage arrays, digitized and then clocked out to the data acquisition electronics..

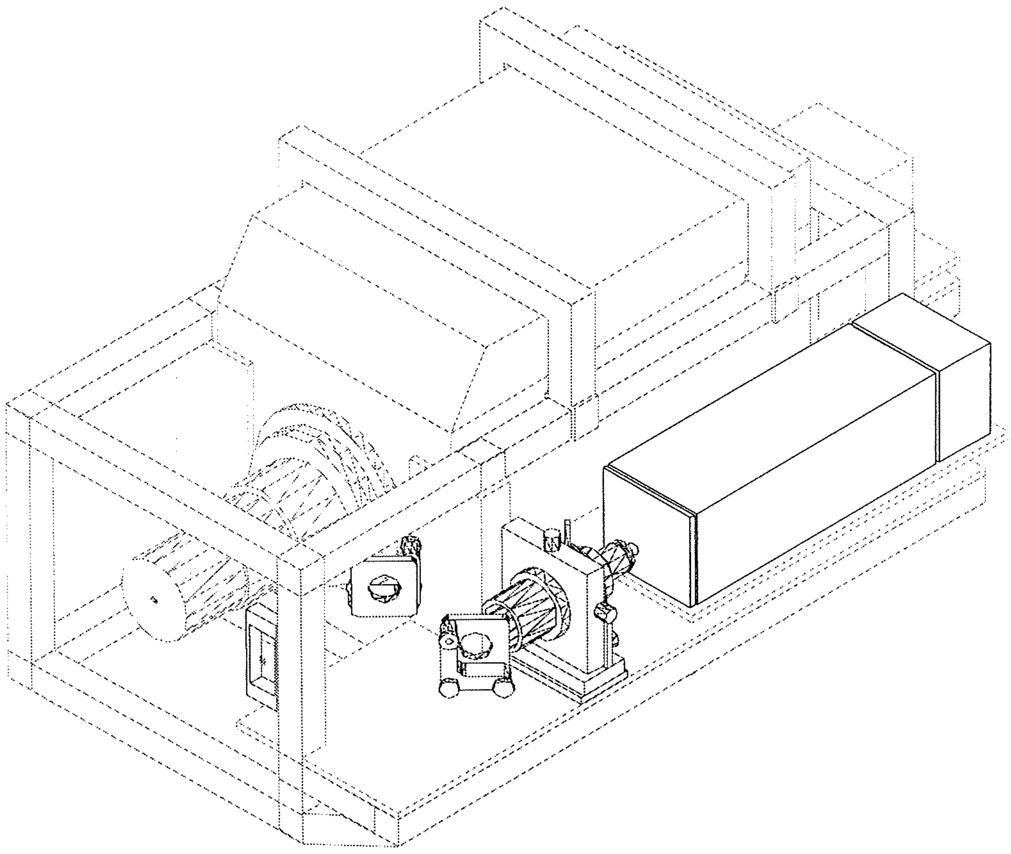

Figure 3. Receiver/Transmitter Cage (outer rack is not shown here)

The fiber taper between the streak tube phosphor and the CCD camera was fabricated by InCom and then custom ground by Joe Apels at Tucson Optical Research Center (over a free weekend he had). The spring-loaded mechanical support for the taper was designed and fabricated by MedOptics, another Tucson company that specializes in compact image formation (for medical imaging) and is quite skilled in bonding tapers to CCDs on intensified cameras. Presently, the fiber taper is permanently bonded to the CCD, but only grease-coupled to the phosphor, so that the CCD camera can be easily decoupled for shipment and remounted prior to experimentation.

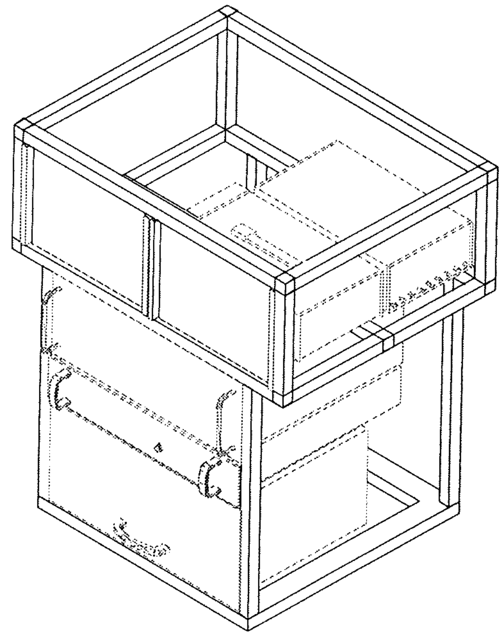

Figure 4. Operator and Sensor Control Rack

Operator Control and Data Acquisition (etc)

The second rack, shown in **Figure 4**, holds the control computer (Pentium-based PC), the laser power supply and chiller, camera power supplies (streak tube and CCD), displays (1 presently), DGPS modules, and aircraft attitude sensor (inclinometer). The control computer is principally concerned with data acquisition via dedicated DSP boards, but also allows for operator interaction and collection of some ancillary data.

The data acquisition was a major part of the IR&D effort, since the peak data rate is 120 MB/sec, as opposed to 3 or so MB/sec (peak) in the laboratory system. Since there are no commercial framegrabbers that can accommodate this pace (ours is the first that I know of, based on input from camera manufacturers and data acquisition board manufacturers – the oft-repeated phrase has been "Really? Let me know if it works!"), we were forced to enlist the support of some seasoned designers and jointly design our own framegrabber subsystem. Also, since radiometric considerations mandated that we get as much of the light out of the streak tube as possible, it was necessary to incorporate a fiber taper at the back end of the streak tube as well as the front end, so the mechanical interface for that had to be designed, integrated and tested (again, this was achieved through local talent that was familiar with the issues and could respond quickly). So the back end of the streak tube, and especially the framegrabber, constituted a significant amount of the IR&D effort. The hardware needed to accommodate the data acquisition is described in the next paragraph, though there are some software-related issues discussed concurrently.

Signal/Data Flow

The data flow after the photons are converted to charge on the (Thomson) CCD inside the SMD-1M60 is as follows:

1. clock charge off CCD along the 4 sections of the CCD, leading to 4 12-bit data channels, each running at 10 MHz (binned 512x512, which is our nominal configuration) or 20 MHz (1024x1024, which is not presently used).
2. convert differential (RS422) signals from each (4 x 12 = 48) digital signal line to single-ended TTL levels; the custom interface board to facilitate this was designed/fab'd by Ken Crocker.
3. synchronously read the data into an FPGA (field programmable gate array) that is designed to a) bin along readout direction, reducing the incoming data to 512x256, b)

serialize the 4x parallel data stream into sequential 32-bit words, with pixel data on 16-bit boundaries; the baseline FPGA design was also provided by Ken Crocker, and we tested/debugged and modified it after the camera was delivered.

4. read the 32-bit data directly from the FIFO that resides between the FPGA and the DSP data bus, and then a) bin perpendicular to the readout direction, yielding a 256x256 image, and b) descramble the pixels so that the stored image can be viewed with minimal post-process manipulation.
5. DMA (direct memory access) the data from the first SHARC down to the root SHARC on the PCI motherboard (which carries the daughtercard that holds the FPGA and 1st DSP); this DMA uses 2 link ports to assure timely completion on a per-row basis.
6. DMA the data from the root SHARC across the PCI bus using an absolute host DRAM address (the host is the PC) obtained with Windriver.
7. after accumulating an image set (presently about 450 images or less, though this will increase to about 900 images if we can get the dedicated DRAM board to work properly), copy the data from host DRAM to JAZZ drive (a removable hard drive medium) for later use.

Data Collection Summary

The following table summarizes the data collected during flights made in Port Lincoln and Ceduna (SA).

Table 1. Summary of Collected Digital Data

Prefix	Images	Sweep	MCP	Polarizer	Slit	Comments
3/27						
bf1	450	2000	10	out	5	1000', open water; half image missing
bf2	400	2000	10	out	5	1000', open water;" "
bf3	200	2000	10	out	5	1000',...
3/28						
bf4	200	2000	10	out	5	1000',fixed SMA cable, Data1 cable pins on SMD were straightened (had been crossed)
bf5	150	500	10	out	5	1000', tweaked for best delay w/ 4 degree tilt
bf6	200	500	10	out	5	1000', more delay tweaking
bf7	200?	500	10	out	5	1000',1990ns delay looks good
bf8	450	500	10	out	5	1000', surface still a bit high in image
bf9	?	500	10	out	5	1000',2000ns delay; character dump to display began after this data set was recorded (this turned out to be temperature driven)
3/28						a 2x4 was placed under the forward part of the rcvr/xmtr rack to add about 4 degrees tilt, so that we could get up to 8 degrees total, leading to further glint reduction
bf10	450	500	10	out	5	1000', Lucky S farm
bf11	450	500	10	out	5	1000', Lucky S farm
bf12	450	500	10	out	3	1000', Lucky S farm
bf13	450	500	10	out	3	1000', Lucky S farm – missed slightly
bf14	450	500	10	out	3	1000', bottom data, land→water
bf15	450	500	10	out	3	1000', bottom data, land→water
bf16	450	500	10	out	5	1000', bottom data, land→water
bf17	450	500	10	out	5	1000', bottom data, land→water
bf18	450	500	10	out	3	500', Lucky S farm
bf19	450	500	10	out	3	500', Lucky S farm
bf20	450	500	10	out	5	500', Lucky S farm

bf21	450	500	10	out	5	500', Lucky S farm
bf22	450	500	10	out	3	500', reef area
bf23	450	500	10	out	5	500', bottom data, land→water
fffm1	450	500	10	out	5	1000, focus mode over fish farm to test alignment
amb1	50	500	10	out	5	ambient data over bay area
amb1	50	500	10	out	3	ambient data over bay area
						after the 2nd flight on 3/28 it was determined that focus was still an issue, and that perhaps a polarizer should be tried to further aid in reducing the surface glint; but the timing of the data collection was successfully addressed, and we determined that the first data sets had little chance of being taken over the fish farms.
3/29						the focus was found, in ground tests, to be significantly off; a Hama M72 polarizer was tested (ajg stood at 400' and found the null with the laser on) and taped in place; the final focus was at 0.52" threads on the 180/f1.8 lens mount. We flew immediately after spending nearly all afternoon tweaking.
Bf24	400	500	10	in	3	500', Haygen's farm
bf25	400	500	10	in	3	500', Haygen's farm
bf26	400	500	10	in	3	500', Lucky S farm
bf27	400	500	10	in	3	500', Lucky S farm, off to right a bit
bf28	400	500	10	in	5	800', Haygen's farm
bf29	400	500	10	in	5	1000', Haygen's farm
bf30	400	500	10	in	5	1000', Haygen's farm
						again, after about an hour of operation, the character dump to the screen occurred repeatedly during DMA to host DRAM; this terminated the flight.
3/30						after reviewing the 3/29 data, it appeared that water clarity might be an issue, so a flight was planned for the open ocean S. of Pt Lincoln; part of the flight was to try to tweak the polarizer, in case the null was close to the present setting and some significant improvement could be made thus.
Comp1		500	10	in	5	500',present setting for polarizer; data over open ocean (still inside shelf, though)
Comp2		500	10 I	in	5	500',90 degrees rotation of polarizer (very approximate eyeball estimation)
wc1		500	10	in	5	500',nominal polarizer, open ocean inside shelf
wc2		500	10	in	5	" "
wc3		500	10	in	5	" "
wc4		500	10	in	3	bad data
wc5		500	10	in	3	500',over continental shelf
pw1		500	10	in	3	500',pilot whale attempt
pw2		500	10	in	3	500',pilot whale attempt
wc6		500	10	out	3	500',removed polarizer (for good); still outside shelf region (water is blue)
wc7		500	10	out	3	" "
dolphin1		500	10	out	3	500',try to image dolphin school (very large – hundreds of dolphin across a few

						football fields)
dolphin2		500	10	out	3	" "
qt1	50	500	10	out	3	500',try to align laser by adjusting output mirror upper/inside knob, ¼ turn CW
qt2	50	500	10	out	3	500'," ", ¼ turn additional
qt3	50	500	10	out	3	500'," ", ¼ turn CCW
qt4	50	500	10	out	3	500'," ", ¼ turn additional CCW
amb3		500	10	out	3	500',ambient data set over open ocean
bf32	400	500	10	out	3	500',Lucky S farm
bf33	400	500	10	out	3	500',Lucky S farm
beach1	400	500	10	out	3	land→water boundary for bottom signature
3/31						after some analysis it was determined that some quantitative data on the fish signature would be very helpful; following a morning visit to the local fish factory, where we were lent (given?) a reject bluefin (weighing in at a mere 16kg, or 35 lb) to use for scientific experiments. Specifically, we were going to image the little guy with ASTIL in ground based experiments. The tuna was suspended from a pole supported by two vertical poles, all at about 80' or so from the sensor (we tried 400' initially, but the alignment was impossible, even with a MilSpec bathroom mirror), and the sensor fov was aligned to the wider portion of the tuna cross-section.
Tuna1	50	10000	3+	out	none	tuna top view (90 degrees from broadside) between the 1" galvanized support poles
t90a	50	10000	2	out	3	tuna top view
t90b	50	10000	2+	out	3	tuna top view; we added a white (dirty white – hanger stuff, so yellow might be a better description) sheet approximately 12" wide down one side of the 2-pole stand, to provide a more reflective target to compare with the tuna.
t30	50	10000	2	out	3	tuna 45 degrees from broadside (never mind the name)
t00	50	10000	2	out	3	tuna at broadside (lotsa white showing)
t00a	50	10000	2	out	3	tuna at broadside, but after Dr. Cowling dowsed the specimen with water
t45a	50	10000	2	out	3	repeat of above
t90c	50	10000	2	out	3	tuna at 90 degrees from broadside, again dowsed with water (starting to feel like home, one would presume)
3/31						following the tuna experiments, one flight was made over the fish farms near Boston Island (as usual); previous analysis had shown that more resolution was better, so it was decided that 250' would be tried); it was also surmised that a slower sweep might improve the image SNR at depth, so this was emphasized as well.
bf40	400	500	10	out	3	250' ASL, Lucky S, delay 1000ns wrt QSW; wind 1-2 knots
bf41	400	500	10	out	3	250' ASL, Lucky S
bf42	400	500	10	out	3	250' ASL, Lucky S
bf43	400	500	10	out	5	250' ASL, Lucky S

bf44	400	500	10	out	5	250' ASL, Lucky S
bf45	400	500	10	out	5	250' ASL, Lucky S
bf46	400	1000	10	out	5	250' ASL, Lucky S, delay 100ns wrt QSW
bf47	400	1000	10	out	5	250' ASL, Lucky S
bf48	400	1000	10	out	5	250' ASL, Lucky S
bf49	400	1000	10	out	3	250' ASL, Lucky S
bf50	400	1000	10	out	3	250' ASL, Lucky S
4/1						the above data were encouraging, so we decided to continue flights over the fish farms to allow the potential for good statistics on the imagery
bf60	400	1000	10	out	3	250' ASL, Lucky S, first cages centered, 2nd to rt of camera, windspeed 3-4 knots
bf61	400	1000	10	out	3	250' ASL, Lucky S, both cages to right of fov
bf62	400	1000	10	out	3	250' ASL, Lucky S, 1st cage centered, 2nd nearly so
bf63	400	1000	10	out	3	250' ASL, Lucky S, both cages centered
bf64	400	1000	10	out	2	250' ASL, Lucky S, first more centered than 2nd
bf65	400	1000	10	out	2	250' ASL, Lucky S, cages to rt of plane; mission aborted after character dump during DMA started.
4/1						2nd mission today
bf66	400	1000	10	out	1	250' ASL, Lucky S, down middle
bf67	400	1000	10	out	1	250' ASL, Lucky S, down middle
bf68	400	1000	10	out	1	250' ASL, Lucky S, down middle
bf69	400	1000	10	out	3	250' ASL, Lucky S, down middle
bf70	400	1000	10	out	3	250' ASL, Lucky S, little left
bot10	400	1000	10	out	3	250' ASL, bottom data, slow drop off
bot11	400	1000	10	out	3	250' ASL, bottom data, quick? Drop off
bot12	400	1000	10	out	5	250' ASL, bottom data, quick drop off
bot13	400	1000	10	out	5	250' ASL, bottom data, slow drop off
bfot14	400	1000	10	out	1	250' ASL, bottom data, quick drop off
bot15	400	1000	10	out	1	250' ASL, bottom data, slow drop off
bf71	400	1000	10	out	1	250' ASL, Haygens
bf72	400	1000	10	out	1	250' ASL, Haygens
bf73	400	1000	10	out	3	250' ASL, Haygens
dolphin3	400	1000	10	out	3	250' ASL, saw these guys during a turn-around, so we imaged them – just a small pod swimming along between a couple of islands – shallow water
bf74	400	1000	10	out	3	250' ASL, Haygens
4/2						more images over farms – this is the last day prior to heading to Ceduna in search of bigger fish (schools, that is); analysis of prior data shows that slit 2 yields a bit better resolution than slit 3 (to a first order, anyway) so we should use it preferentially, and even use slit 1 now and then for comparison. 9AM flight
bf90	400	1000	10	out	2	250' Lucky S; wind 9-10 knots, overcast; farms to left of plane
bf91	400	1000	10	out	2	250' Lucky S; farms well aligned
bf92						wrong delay – bad data
bf93						wrong delay – bad data
bf94	400	1000	10	out	1	500' Lucky S; good alignment
bf95	400	1000	10	out	2	500' Lucky S; good alignment
bf96	400	1000	10	out	2	250' Haygen; good

bf97	400	1000	10	out	2	250' Haygen
4/2						4PM flight; overcast, 10 knots windspeed
bf100	400	1000	10	out	2	250' Lucky S; 1st cage centered, 2nd to left of plane (slightly)
bf101	400	1000	10	out	2	250' Lucky S; both cages little to the left
bf102	400	1000	10	out	2	250' Lucky S; both cages little to the left
bf103	400	1000	10	out	2	250' Lucky S; both cages little to the left
bf104	400	1000	10	out	2	250' Lucky S; both cages little to the left
bf105	400	1000	10	out	2	250' Lucky S; both cages little to the left
bf106	400	1000	10	out	2	250' Lucky S; both cages little to the left
bf107	400	1000	10	out	2	250' Lucky S; both cages little to the left
4/2						ferry flight to Ceduna, SA; stop by for some tuna spotting on the way
dolph10	400	1000	10	out	2	spotted a pod of dolphin en route, so we tried to image them; 250' ASL; plane perpendicular to fish; should be right over them
dolph11	400	1000	10	out	2	plane along fish this time; timing is a bit off this and previous
dolph12	400	1000	10	out	2	250'; same as above
bot20	400	1000	10	out	2	bottom imagery en route to Ceduna
4/3						Tuna spotting flight off G. Aus. Bight near Ceduna; one school spotted and attempted, though operator error missed 1s of data in the middle (ajg)
bf110	400	1000	10	out	2	600' ASL; spotter estimates 20-30 ton school, 22 kg fish; fishermen caught it later, found it to be 25 ton, 25 kg fish.
4/6						ferry flight back to Pt Lincoln; nothing was found on 4/5 (absolutely nothing) during spotting flights near Ceduna; this flight would involve some spotting, some transit, and one last farm-overflight at the end. Some sensor evaluation data was collected over the shelf region in order to measure performance for volume backscatter and bottom imaging (one reef was imaged)
bf111	400	1000	10	out	2	250', near cabbage patch; birds visible, maybe tuna underneath
bf112	400	1000	10	out	2	250', near cabbage patch; birds visible, maybe tuna underneath
reef20						wrong delay; bad data; fair amount of sun glint
reef21	400	1000	10	out	2	250';bottom visible;
reef22	400	1000	10	out	5	bottom not visible; swamped by background (solar)
reef23	400	1000	10	out	2	250'; ok
open10	200	1000	10	out	1	300'; open ocean data for reference;overcase, occasionally passing through low clouds.
open11	200	1000	10	out	2	300'; open ocean data for reference
open12	200	1000	10	out	3	300'; open ocean data for reference
open13	200	1000	10	out	5	300'; open ocean data for reference
back13	50	1000	10	out	5	300'; laser not firing (electronics on)
back12	50	1000	10	out	3	300'; laser not firing (electronics on)
back11	50	1000	10	out	2	300'; laser not firing (electronics on)
back10	50	1000	10	out	1	300'; laser not firing (electronics on)
4/6						last pass over farms for few extra data points

bf113	400	1000	10	out	2	Lucky S; 250'; 1st cage ok; 2nd to left
bf114	400	1000	10	out	2	Lucky S; 250'; " "
bf115	400	1000	10	out	2	Lucky S;1st cage very good; 2nd to right
bf116	400	1000	10	out	2	500' ASL; Lucky S; both well centered
bf117	400	1000	10	out	2	500' ASL; Lucky S; good alignment

Chronolog of the 1997 Aerial Survey Experiments

Following the Tucson airborne testing (to assure the sensor veracity in general), the sensor was crated and shipped directly to Port Lincoln, SA. Arete personnel (A. Griffis, J. Plath) arrived March 25, 1997 and uncrated the hardware on the 26^{th}. Figure 5 below shows the sensor racks in the hangar just prior to aircraft installation.

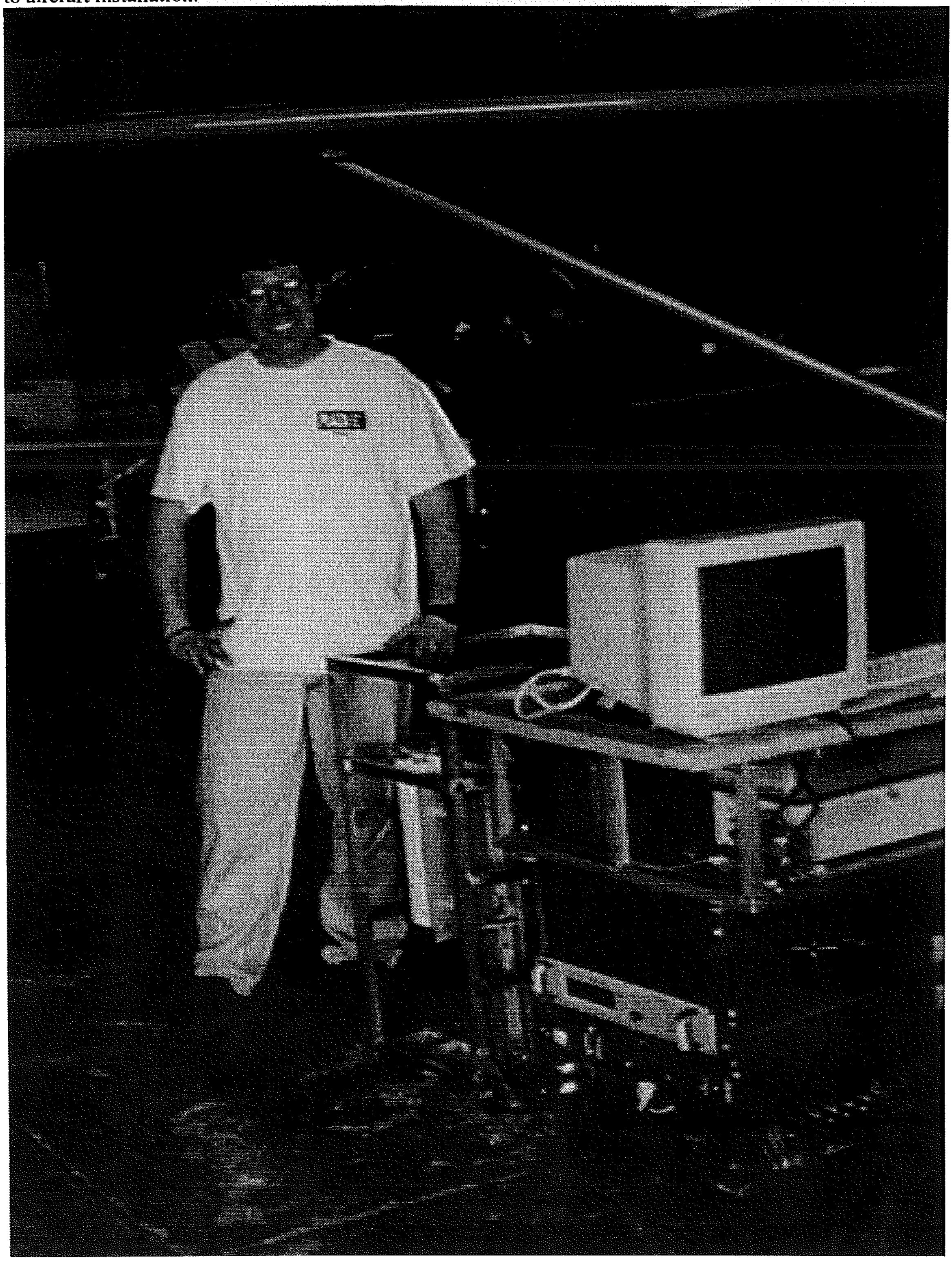

Figure 5. Both sensor racks in the Lincoln Airlines hangar during ground tests prior to aircraft installation.

The Aerocommander was able to accommodate both racks side-by-side, with the transceiver rack installed directly over the floor aperture and the operator rack roughly 0.5 cm away, attaching to the seat mounts. The installation space is shown in Figure 6 below.

Figure 6. Aerocommander sensor installation area (floor aperture is directly aft of the pilot seat).

The installed racks, as viewed from the side, are portrayed in Figure 7 below. As mentioned above, the installation was quite close, allowing only 0.5 cm between the racks, and with foam cushions inserted at the aircraft interior points to prevent abrasion damage to the interior walls.

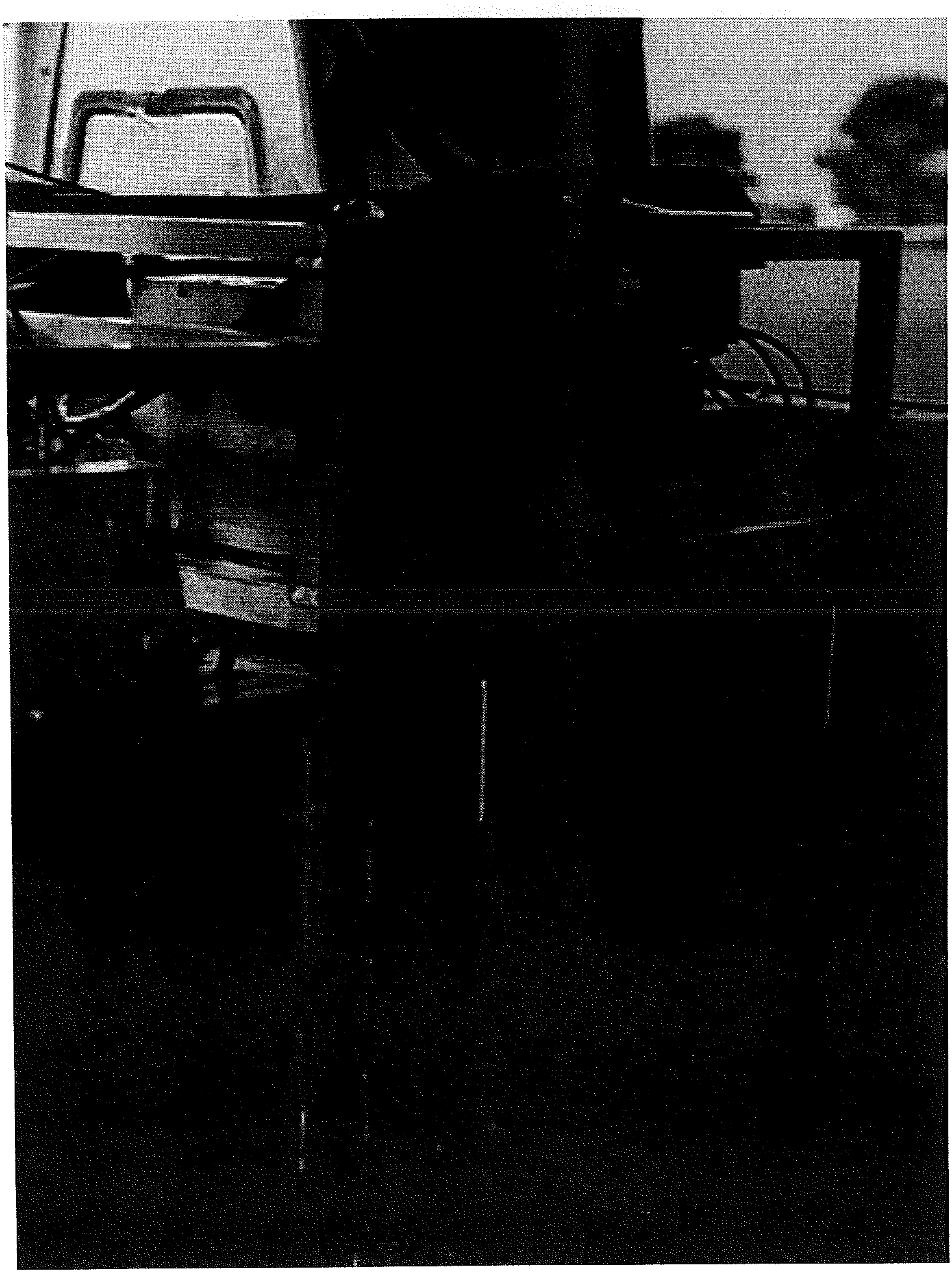

Figure 7. Side view of ASTIL installation aboard the Aerocommander.

Figure 8 shows the installation as viewed through the cockpit entry door. From top to bottom, the operator station components are the Stanford DG535, SMD and HKK power supplies, SVGA monitors (aft of DG535), ruggedized PC with associated electronics, and the laser power supply and chiller assemblies occupy the bottom of the operator station.

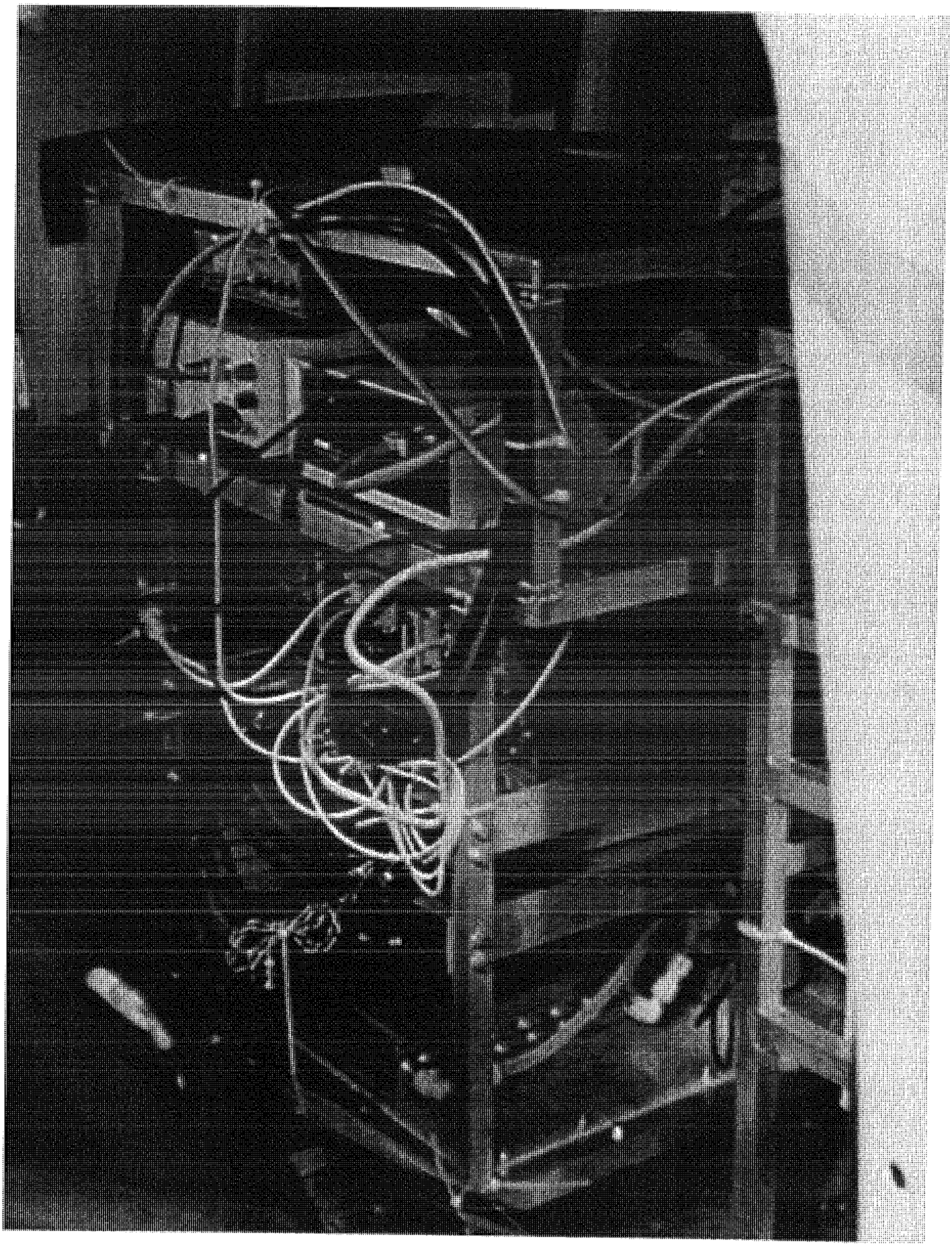

Figure 8. ASTIL installation as viewed from the cockpit area (pilot seat lower left, pushed forward).

Prior to mounting the sensor into the aircraft, ground testing was conducted to assure that the laser, receiver, digital data interface, timing/control and operator displays were all functioning, in addition to verifying the basic lidar operation by ranging on the wall at the rear of the hangar. This allowed the laboratory baseline to be reestablished and provided a means of checking alignment, illumination and energy. After installing the sensor racks in the aircraft, additional ground testing became quite difficult, as there was no auxiliary power unit for use by our host, Lincoln Airlines. However, when ground testing was necessary, a common 2nd-surface mirror was used below the aircraft to project and image distant objects. This arrangement is shown in Figure 9 below. The photograph portrays the same view one would have if the transceiver rack were viewed while lying directly under the belly of the aircraft (the yellow reflection is the bandpass filter on the front of the 180mm f/2.8 receiver lens).

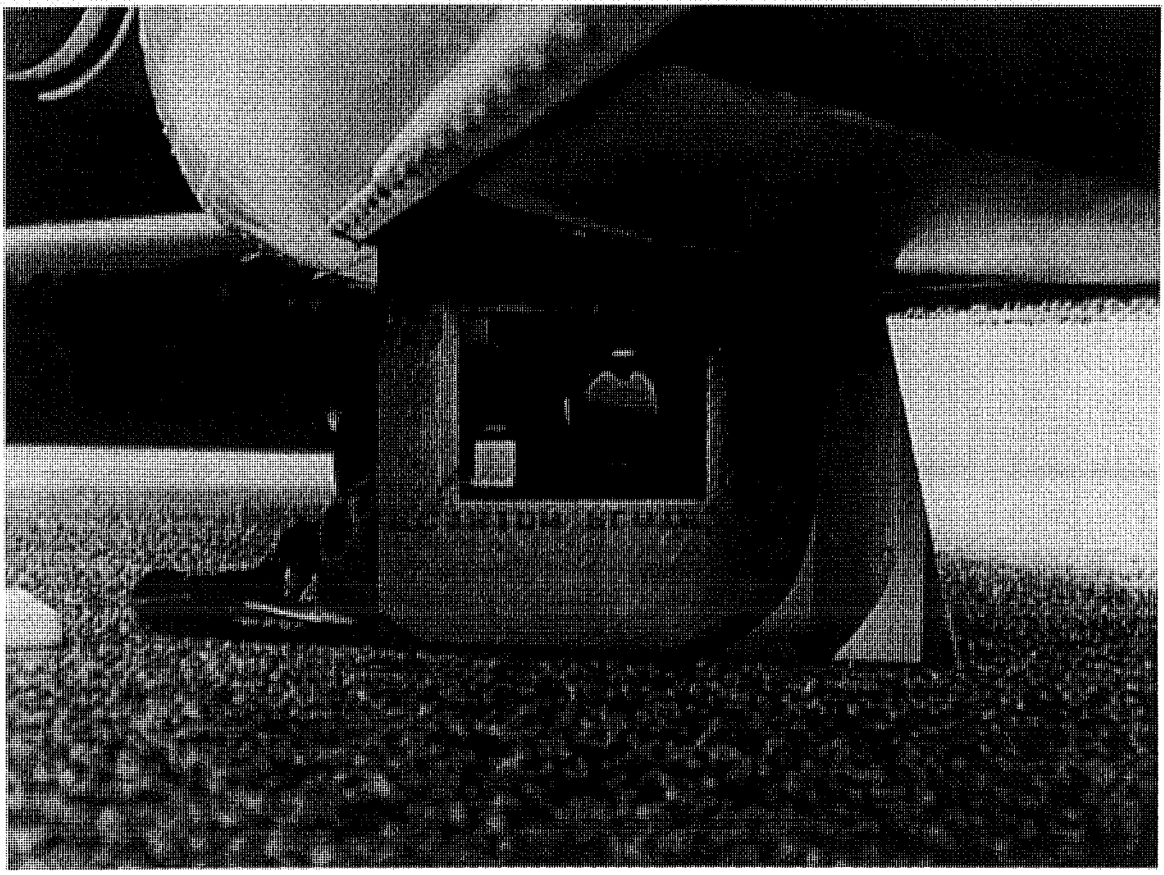

Figure 9. Aft view of ground test apparatus used with Aerocommander.

Subsequent to installation, the sensor was controlled on the ground and in the air by an operator seated on a bench placed directly aft of the two racks. This bench accomodated two passengers comfortably (depending on the length of the flight) and still allowed some flexibility for making in-flight adjustments to the sensor. Figure 10 illustrates the operator seating arrangement.

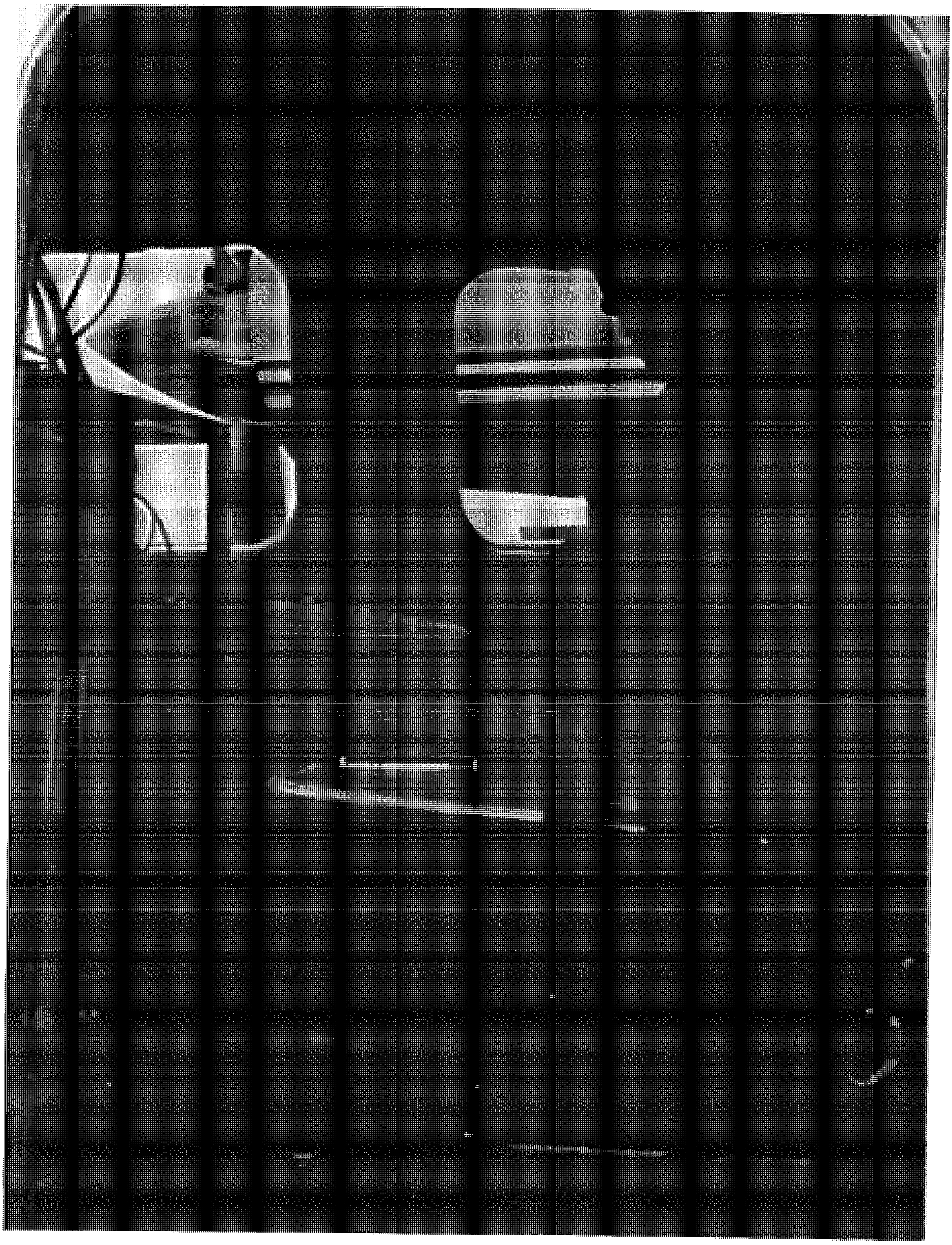

Figure 10. J. Plath operating the sensor from the bench seat during ground tests.

Immediately following the aircraft installation, flights were conducted in the Boston Bay area to evaluate the basic functions of the sensor in the aircraft. Figure 11 shows a photograph of a portion of the Boston Bay region that was flown.

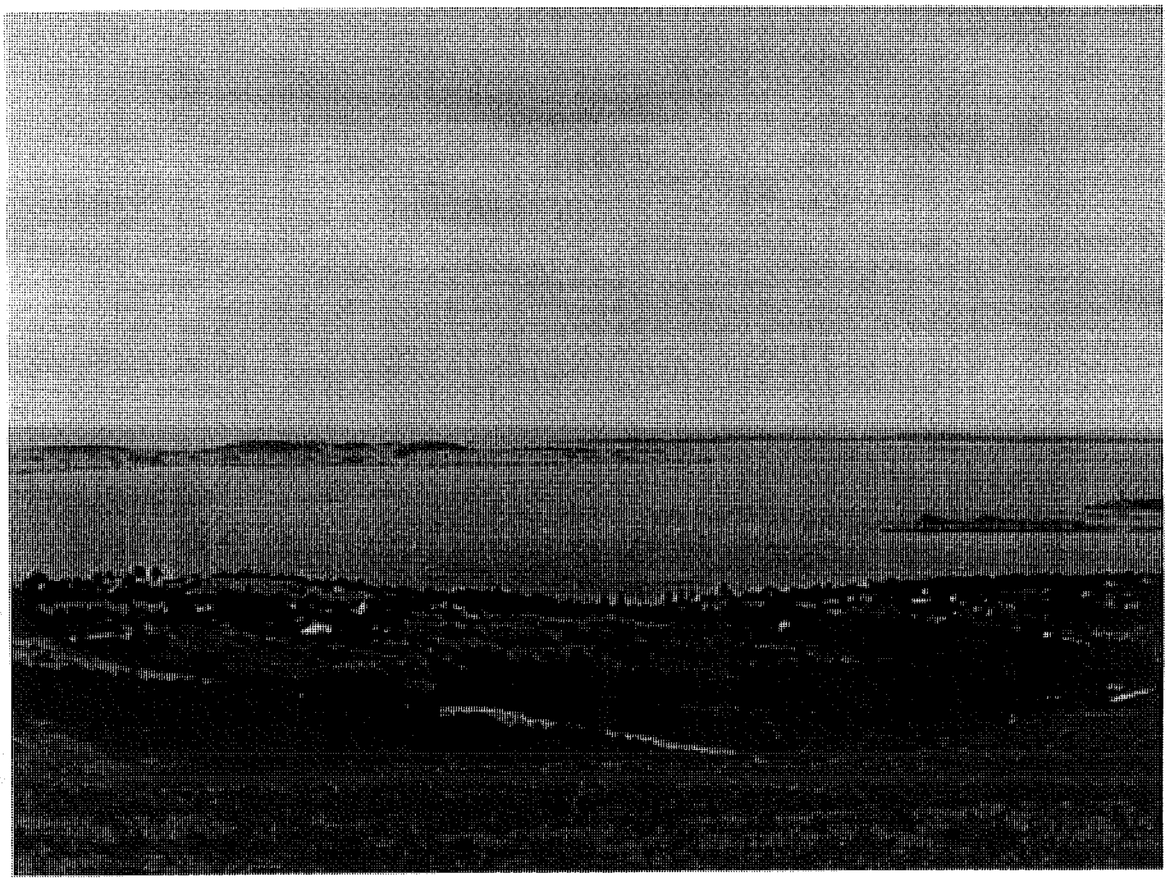

Figure 11. Photograph of Boston Bay from a point above Port Lincoln, SA.

Within Boston Bay, there are many groups of SBT farms. The ASTIL sensor overflew several of these, but concentrated its data collection efforts on two farms. Figure 12 shows a photograph of a single SBT farm in Boston Bay that was overflown in order to collect data on captive tuna.

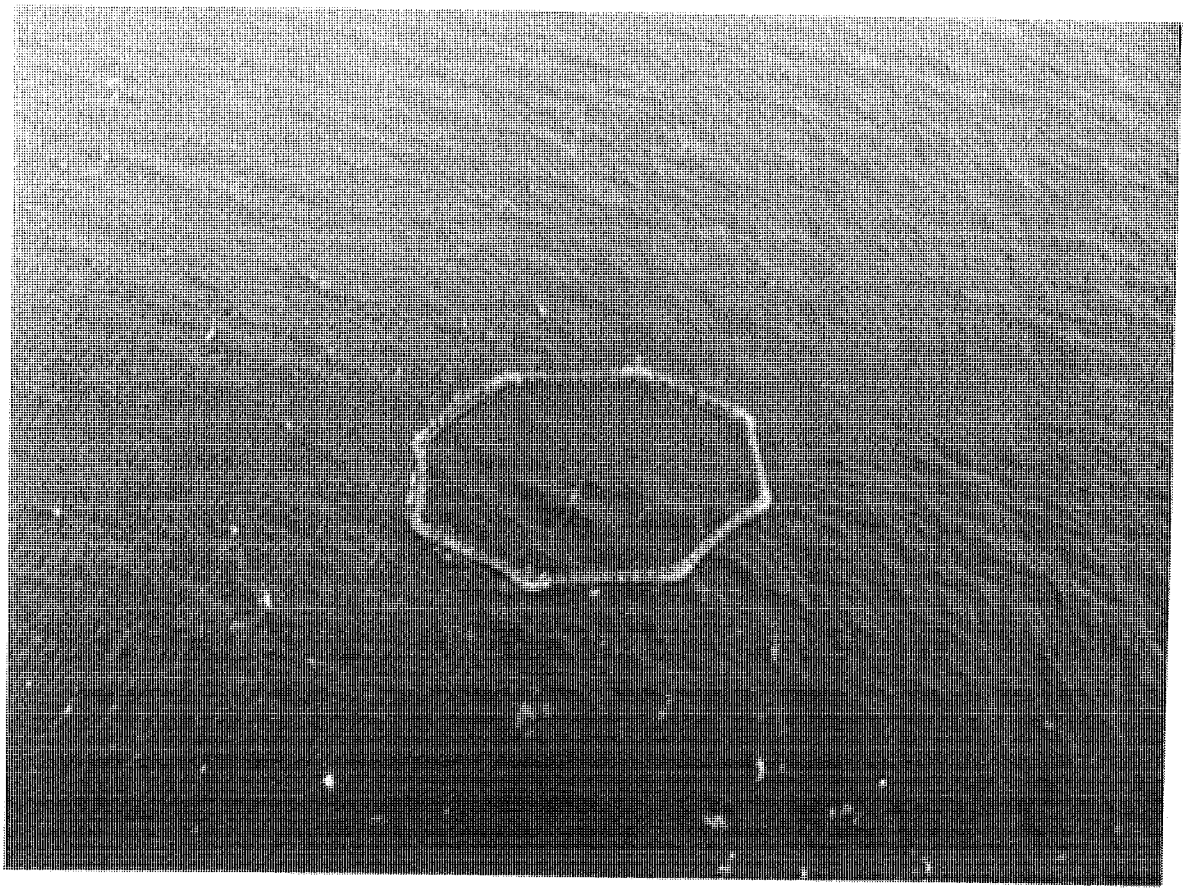

Figure 12. Boston Bay SBT Farm owned by Hayden; this farm is approximately 60m in diameter.

. An additional pair of farms were also overflown in Boston Bay, as shown in Figure 13. Both photographs of the farms show the buoys at the perimeter of the farm that provide support for the net which encompasses the entire water volume of each farm. The farms are serviced daily to provide food for the fish and presumably, minor maintenance on the farm apparatus.

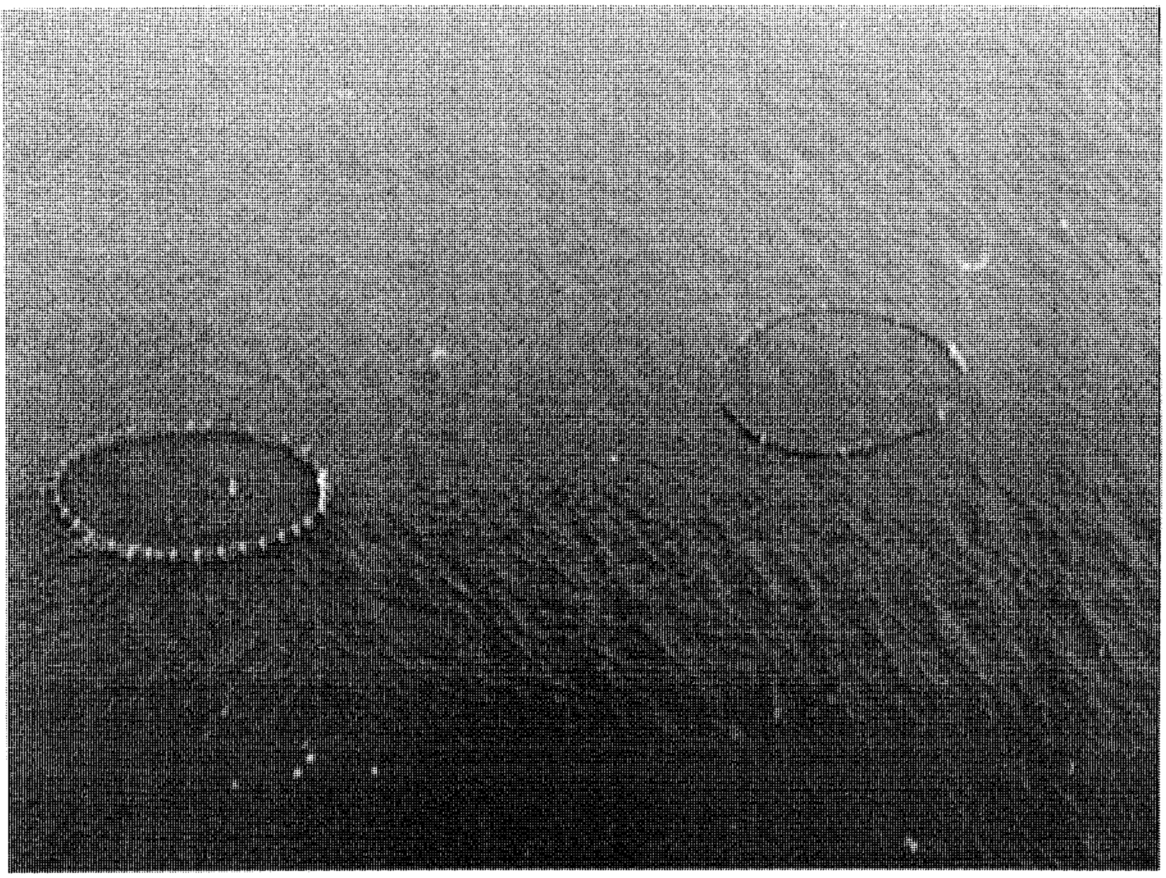

Figure 13. Boston Bay SBT Farms (Lucky S); these farms are approximately 30m in diameter.

Flights were conducted nearly every day after installing the sensor in the aircraft. The data collected on these flights and some of the peculiarities of each day's work were summarized in Table 1. Generally, the sensor performed very well, with a few exceptions:

1. The sensor focus was not set properly for flight altitude, so that several of the early datasets were out of focus.
2. The lack of a realtime display made diagnostics (e.g., discerning the focus problem and correcting it promptly) very difficult to do either on the ground or in the air. As of this writing, a realtime display has been integrated successfully, but it was sorely missed during the SBT experiments.
3. Erratic behavior in the DSP data storage routines that DMA (direct memory access) across the PCI bus caused several of the early flights to be prematurely aborted. This was determined to be a temperature problem, and was promptly corrected (as per our spotter/pilot's suggestion) by using a hose from the aircraft air duct to blow air into the PC chassis, as shown in Figure 14.

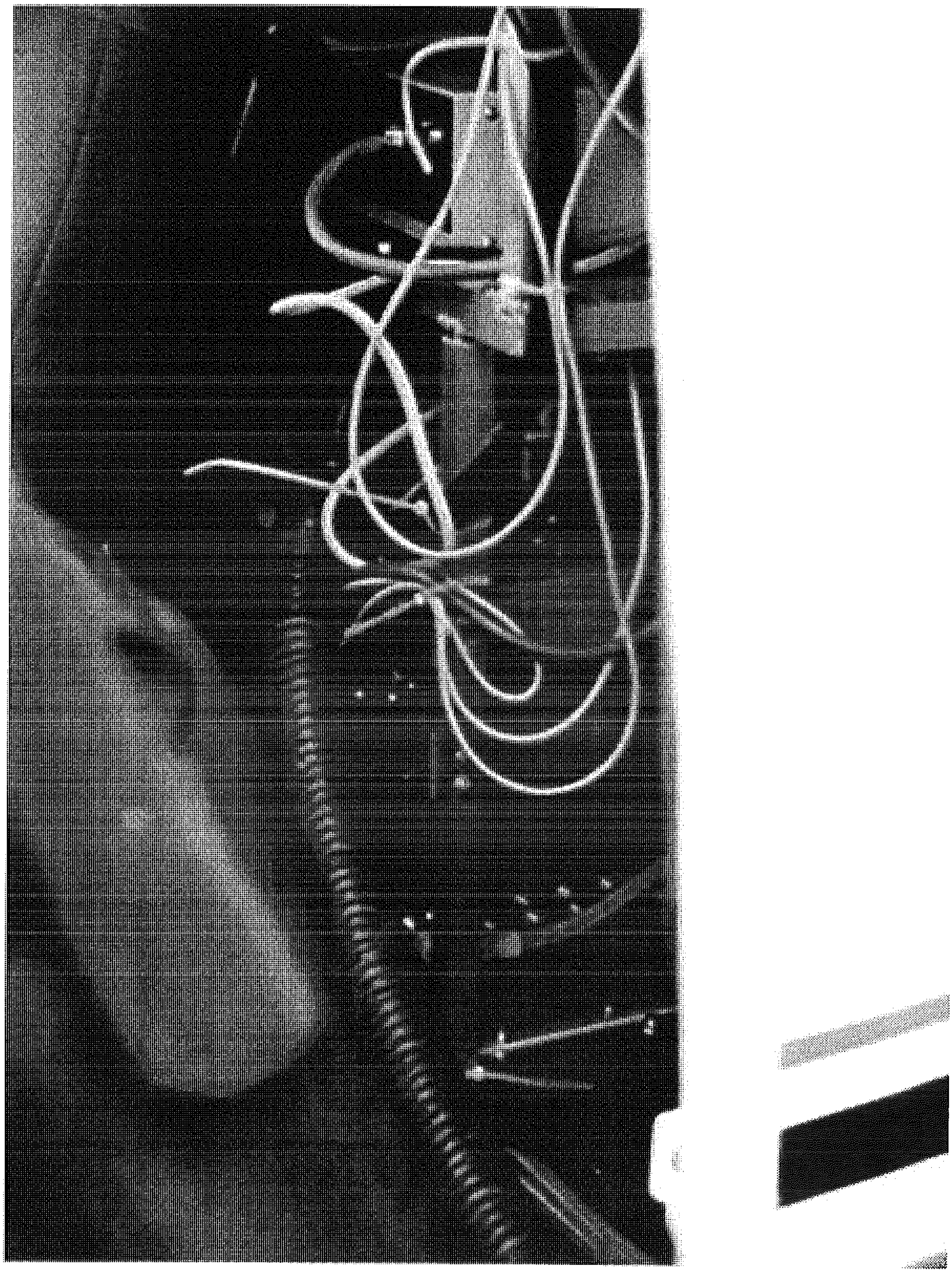

Figure 14. An air hose from a forward aircraft vent was used to cool the PC chassis.

After correcting the focus problem (this was achieved rather painstakingly on the ground with a mirror, much as is depicted in Figure 9), the data quality improved substantially, and the first individual SBT signatures were obtained. However, it was clear from reviewing the data that even at 500 feet altitude, the resolution was marginal. Furthermore, the signatures were obvious in only the first few meters of water, without processing the data.

These analysis observations highlighted the need to obtain some model data on the SBT in order to better understand the difficulties with SBT observation, and to facilitate the separation of sensor issues from target issues. Since very little data has been collected to date on SBT reflectivity, and no quantitative signature data was available, it was decided that some SBT LIDAR signature data be collected to provide estimates of the tuna reflectivity and LIDAR cross-section.

One of the local (Port Lincoln) fisheries was kind enough to donate a 16 kg SBT for use in experiments. It was immediately evident that, as one might suspect, the reflectivity of the upper surface of the tuna was quite low (unlike the bottom side). This is readily observed in Figure 15 and Figure 16 below.

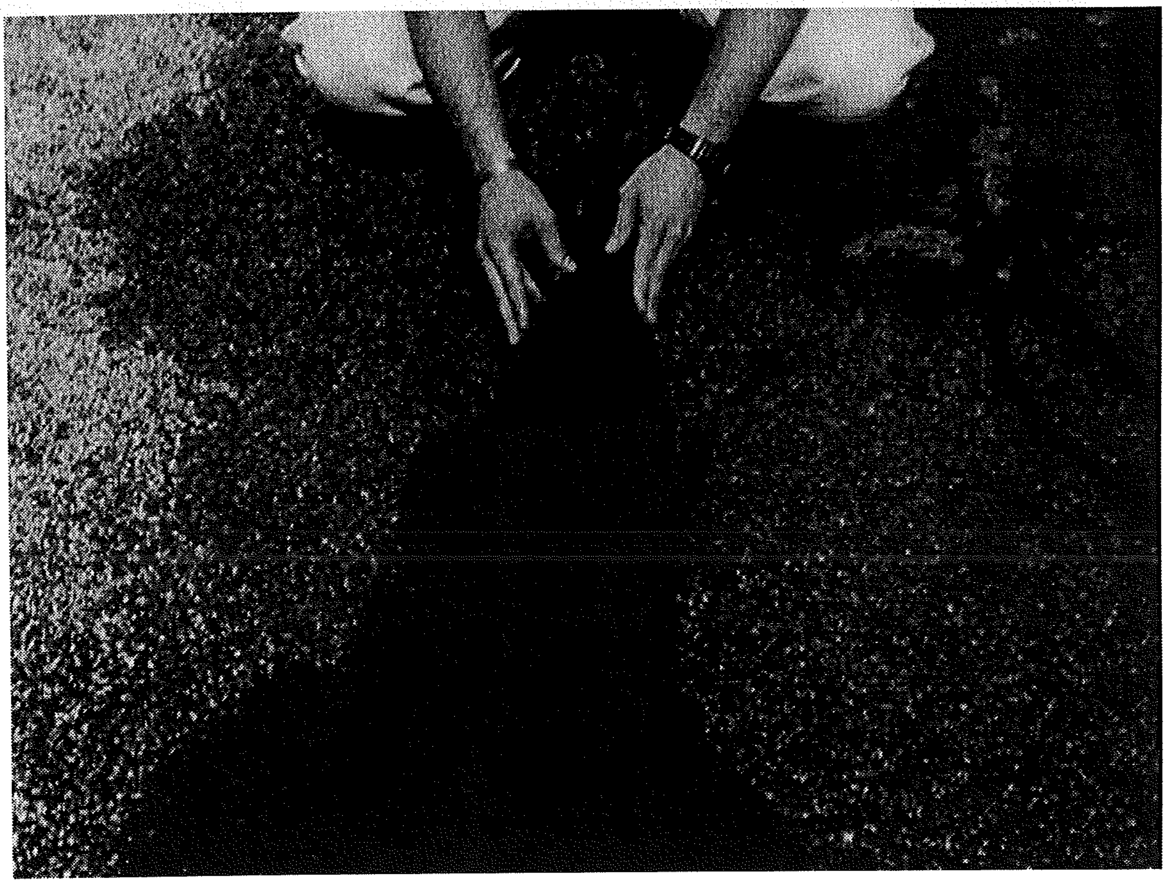

P

Figure 15. Top view of the 16kg SBT as it rests on the pavement outside the hangar.

The physical dimensions of the SBT were approximately 15 x 25 x 99 cm (W x H x L) near the central portion of the tuna body, with the upper 15 cm circumference (of 38 cm half-circumference) having the dark reflectivity.

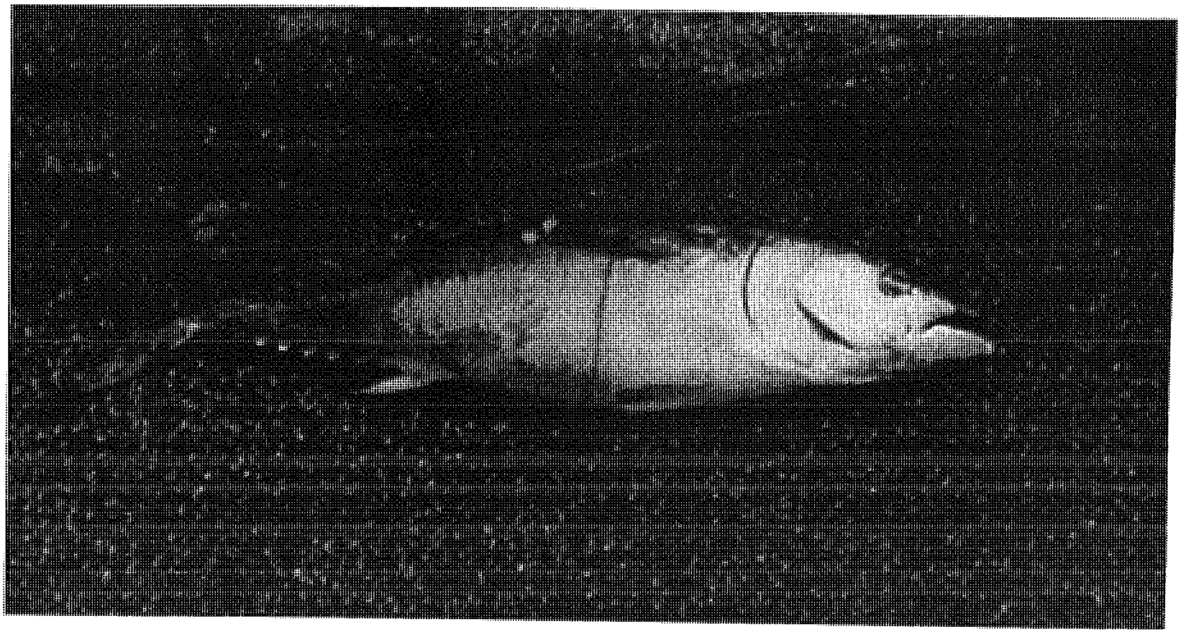

Figure 16. Bottom/side view of the 16kg SBT used for LIDAR signature measurements.

Ground data were collected on the SBT shown above in both dry and wet conditions, and at three orientations (0, 45, 90 degrees with respect to the incident light). The cart used to support the SBT and the reference target (dirty white hangar tarp) placed next to it are shown in Figure 17.

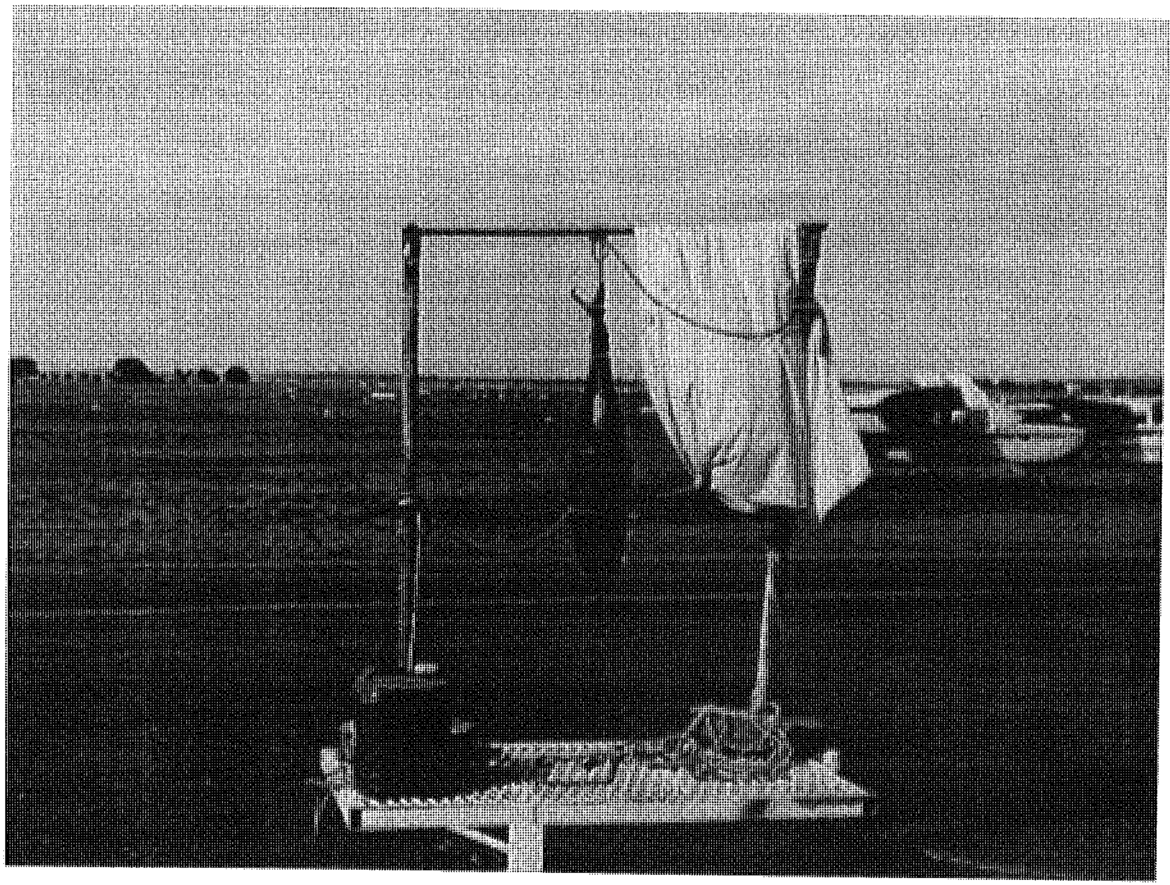

Figure 17. Support stand for the 16kg SBT used to obtain LIDAR signature data.

The data collected on the SBT were consistent with the published literature, which estimated tuna reflectivities in general to be 2-4%; first order estimates of the SBT ground test data indicated reflectivity of approximately 2-3% (for the darkest portion – the light underside of the SBT is not of any particular interest for performance). Also, the measured shape of the tuna indicates that the pre-trial assumptions about the required resolution were too optimistic, which is consistent with the observed performance improvements that were gained when the altitude was changed from 1000' to 500' ASL.

Following the measurement of the tuna signature on the ground, 250' ASL flight altitudes were emphasized, as the resultant sensor resolution was much more amenable to detecting tuna with signatures similar to the tuna used in ground tests. Both reflection and shadow signatures were observed under these conditions, and data analysis is ongoing to assess the performance for the SBT farm overflights.

A few data sets were collected with a polarizer in place to examine the potential of polarization discrimination for reducing the surface return that might obscure near-surface reflection signatures of SBT. This has yet to be fully analyzed, but early analysis indicated that the potential gain could not be realized without fine-adjustment of the polarizer orientation on the ground using a specular target; this required a rotary mount and a realtime display, neither of which were available for the SBT trials.

Data were also collected in the open ocean region to the South of Port Lincoln, since it was also observed in the Boston Bay flights that, even with adequate resolution and lower flight altitudes, the decay of the LIDAR return as a function of depth was greater than one would expect for the open ocean; in some areas it appeared that the diffuse attenuation was as high as 0.7/m, though 0.2-0.4/m were more common. Even so, compared to the open ocean, which is nominally 0.08/m, this represents a substantial loss of performance. Thus, the open ocean data were collected to check this assumption. Only ambient data were collected, but these data did confirm that the penetration depth would be improved in the open ocean and the increased turbidity of Boston Bay was leading to a loss of performance. Further analysis will be conducted to reconcile both types of data with a radiometric model for the sensor, which will aid in the overall assessment of the ASTIL performance.

Once a significant amount of data had been collected near Boston Bay (to enable an adequate analysis of farm SBT signatures), the sensor was flown to Ceduna, SA in order to obtain open ocean data over fish schools. Unfortunately, the end of the SBT season had already arrived and the few schools that were observed were only evident near the surface for a few minutes at a time. Thus, the aircraft could not be positioned over the fish quickly enough once a school had been spotted.

In spite of the lack of open ocean schools, some data were collected over a pod of dolphin (owing mainly to the opportunity – no concerted effort was made to obtain such data). A photograph of this pod is shown (taken from the aircraft) in Figure 18 below. The propeller is visible on the right hand side of the photograph.

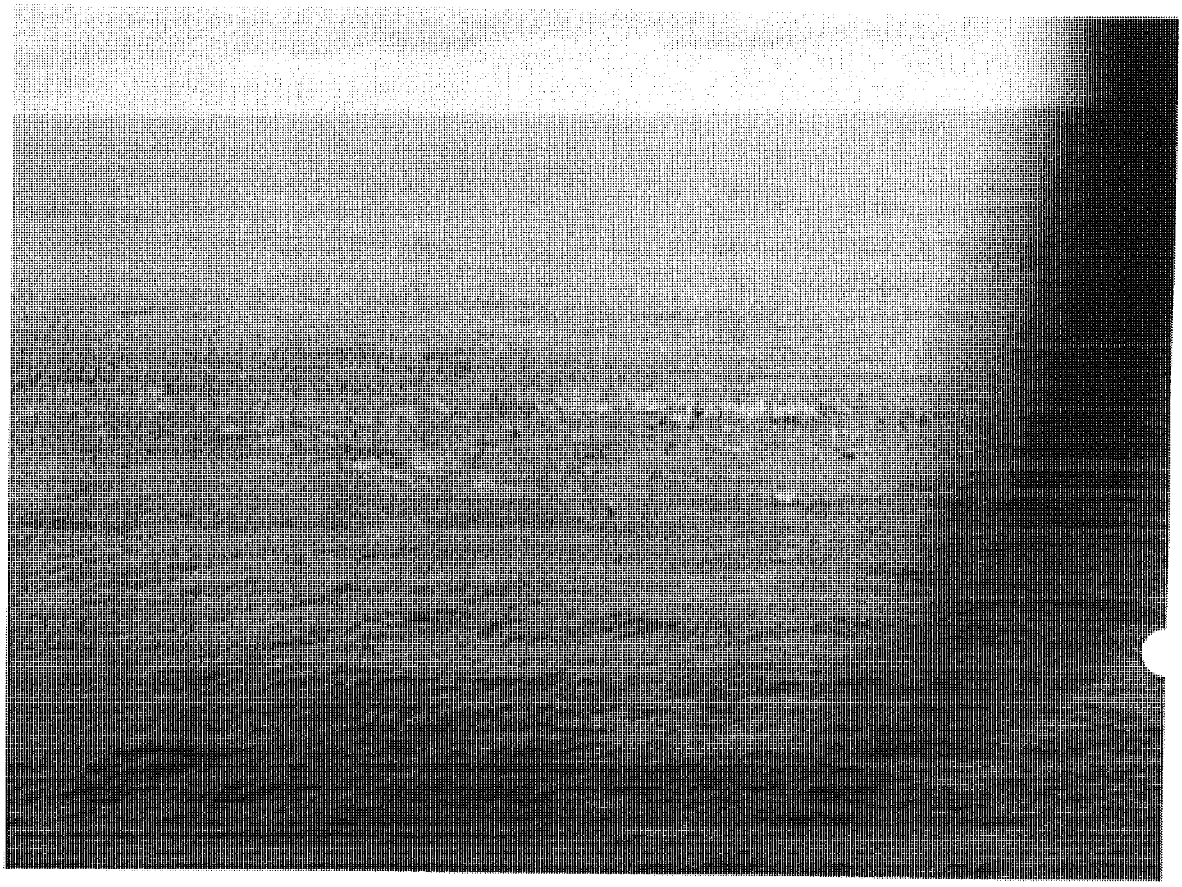

Figure 18. A dolphin pod that was imaged en route to Ceduna, SA.

Some ambient data were also collected to assess open ocean penetration, including some reef data to examine bottom returns in the open ocean. Figure 19 shows a photograph of the reef that was overflown. Bottom data at approximately 20m were obtained, though performance was degraded slightly by the significant air bubbles in the waters adjacent to the reef area. Notice also that there were low-lying clouds in the region that inhibited spotting, creating additional difficulties for finding open ocean fish schools.

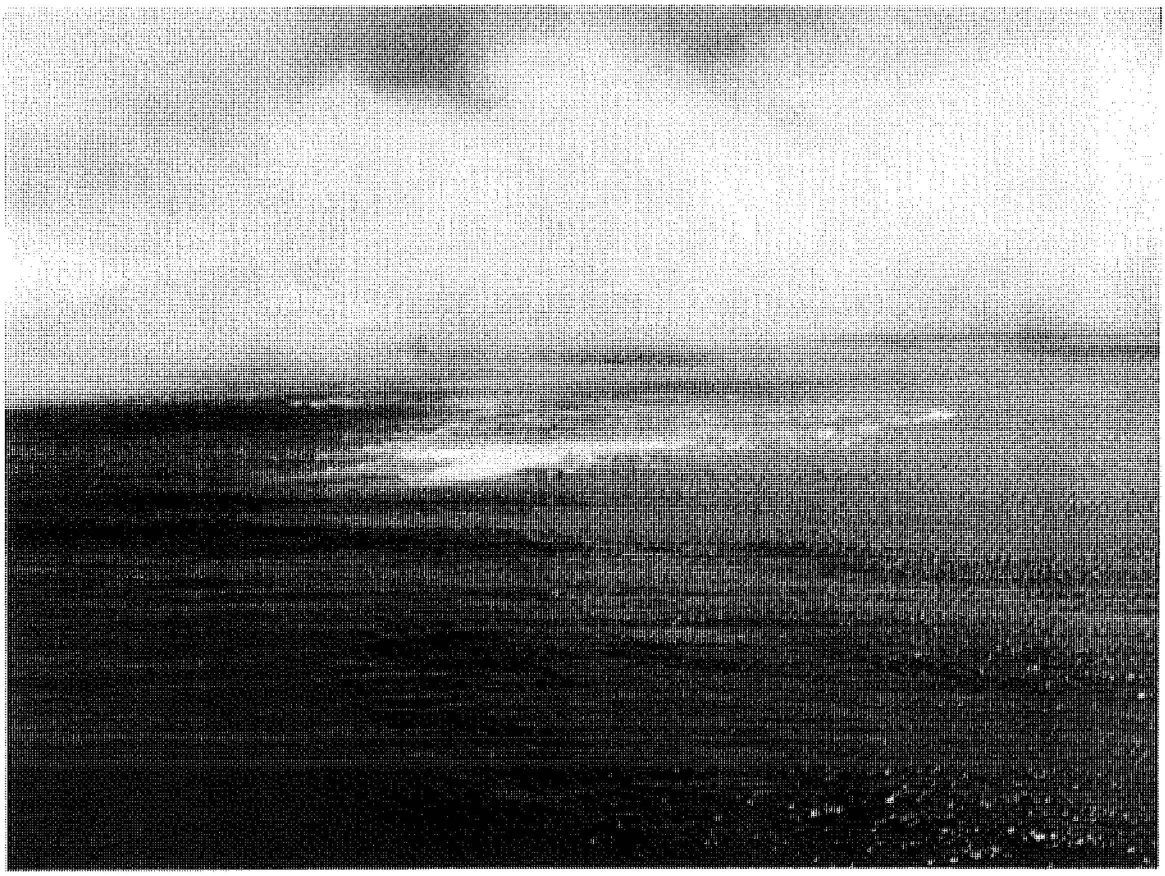

Figure 19. A reef that was imaged during flights near Ceduna, SA.

Following the Ceduna flights, the experiment was brought to a close and the sensor was shipped back to Tucson, AZ. Data analysis is ongoing and is being pursued in order to support ONR and S-K initiatives at Arete. A few processed images are shown here to illustrate the nature of the data obtained, though these images were generated during the trials in Australia and more extensive imagery will be generated in the near-term as part of the on-going analysis effort for airborne and underwater vehicle STIL systems. Figure 20, Figure 21, and Figure 22 all show SBT signatures from Boston Bay farm overflights (bf46.bin, images 215, 217 and 227, respectively). The pseudo-color was used to simplify the identification of the tuna signature, though even on a grayscale image these are easily identified signatures, given some familiarity with the data. Figure 23 shows additional Boston Bay data collected over a small pod of dolphin that were traversing a shallow region between a peninsula and Boston Island. The bottom signature is easily identified, as is the dolphin signature. The surface is rather faint because part of the processing involves a range normalization, that has the effect of removing the depth-dependent light decay; since the surface reflectivity is inherently less than the dolphin or bottom, it appears as a relatively dark signature.

Select Experimental Data

The pseudo-color images shown from Figure 20 to Figure 23 were shown to the Tuna Boat Owner's Association in Port Lincoln based on a review of some early data. Since that time, additional data have been analyzed (albeit briefly, owing to conflicts with ongoing ONR experiments and analysis) and these data are included here as an update of the ongoing analysis work.

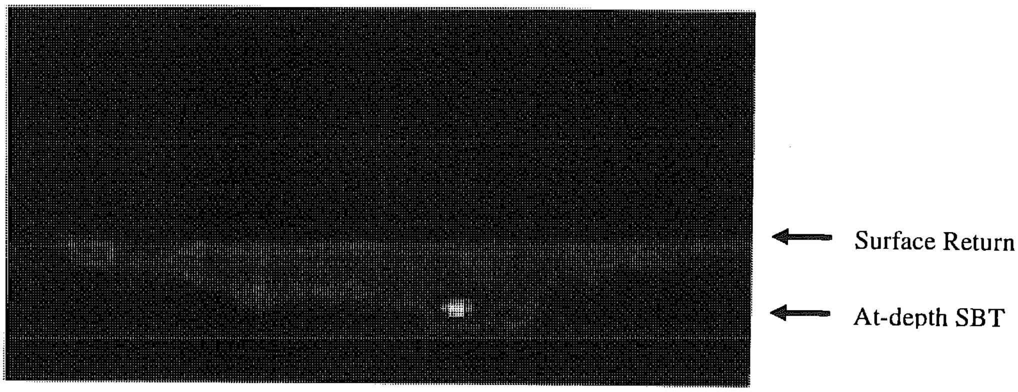

Figure 20. Pseudo-color matched filter image of SBT: 5m depth, Boston Bay

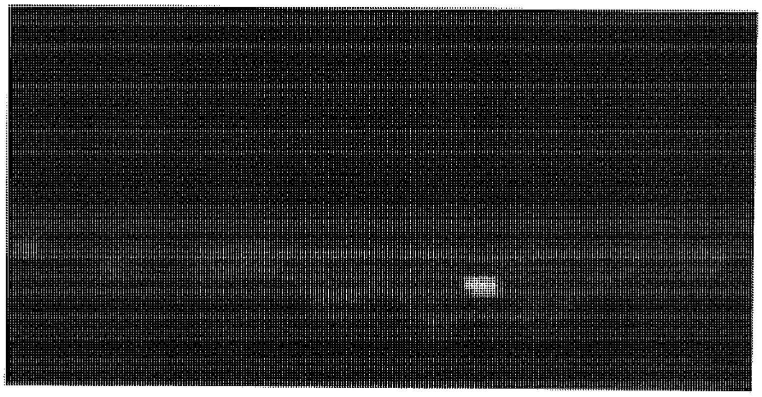

Figure 21. Pseudo-color matched filter image of SBT: 2m depth, Boston Bay

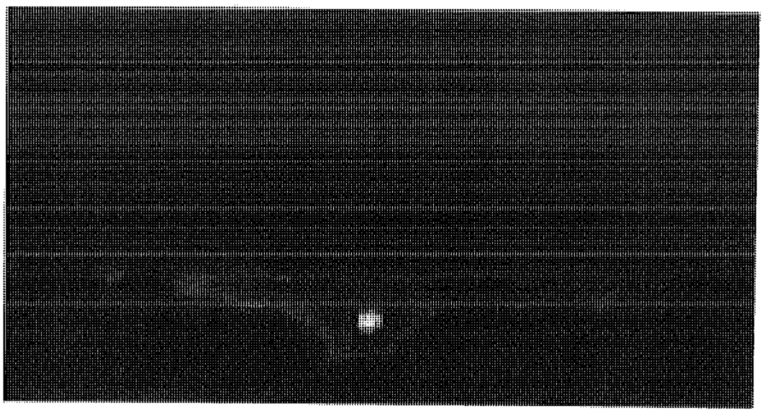

Figure 22. Pseudo-color matched filter image of SBT: 3m depth, Boston Bay

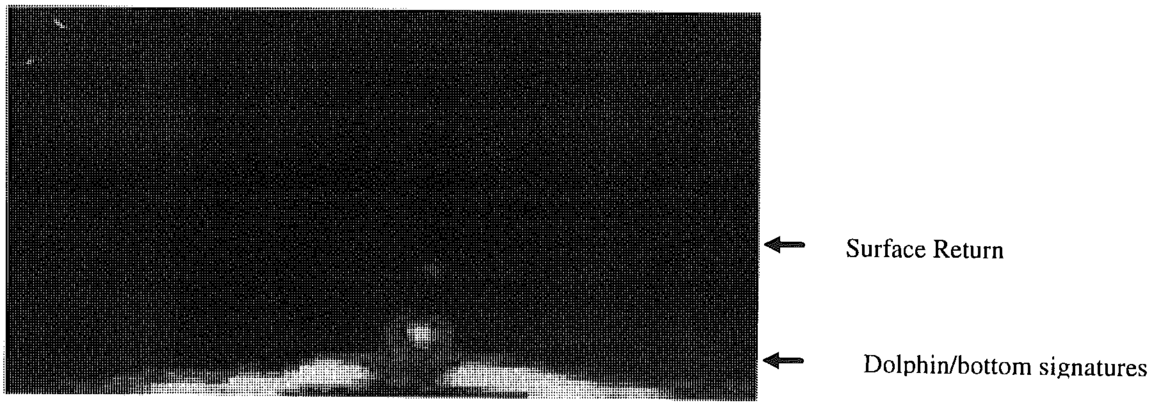

Figure 23. Pseudo-color matched filter image of Dolphin near bottom: 7m depth, Boston Bay

The following examples illustrate the raw data content and the associated signal processing for several instances over Boston Bay and one over the Great Australian Bight (a reef). These do not contain quantitative information beyond the depth of the objects of interest (SBT, dolphin or bottom), though that sort of information will be the subject of the analysis that is currently under way for ONR and NOAA.

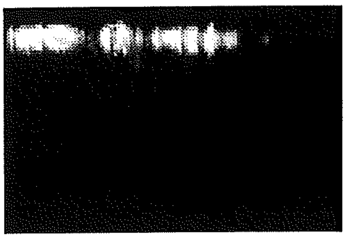

Figure 24. Raw bf91/49

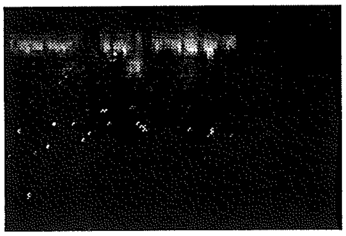

Figure 25. R^2 and exp() corrected bf91/49

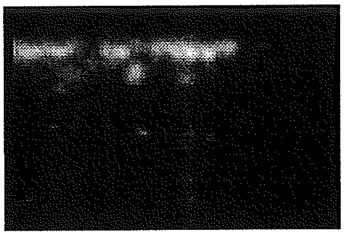

Figure 26. 2D Match-filtered bf91/49

Data from fileset bf91.bin were collected over the Lucky S farms in Boston Bay. These imagery show SBT signatures a few meters below the surface of the farm area.

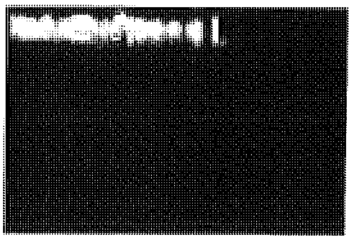

Figure 27. Raw bf91/55

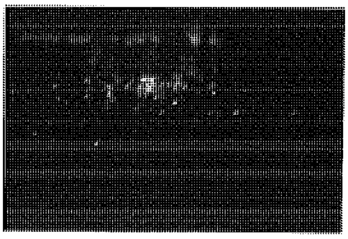

Figure 28. R^2 and exp() corrected bf91/55

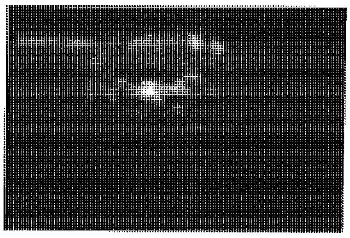

Figure 29. 2D Match-filtered bf91/55

Data from fileset bf91.bin were collected over the Lucky S farms in Boston Bay. These imagery show SBT signatures at approximately 8 meters below the surface of the farm area. In the exp() corrected image, the surface-shadow signatures of several tuna are also evident, indicating that at least a few fish were at the surface feeding or such.

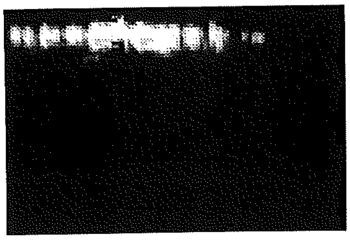

Figure 30. Raw bf91/59

Figure 31. R^2 and exp() corrected bf91/59

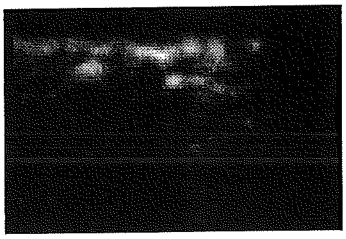

Figure 32. 2D Match-filtered bf91/59

Data from fileset bf91.bin were collected over the Lucky S farms in Boston Bay. These imagery show SBT signatures a few meters below the surface of the farm area. Several signatures are apparent, perhaps up to 4.

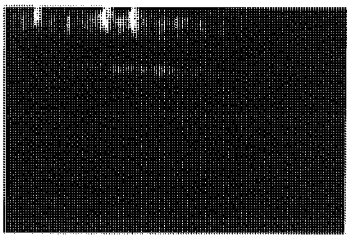

Figure 33. Raw bot14/104

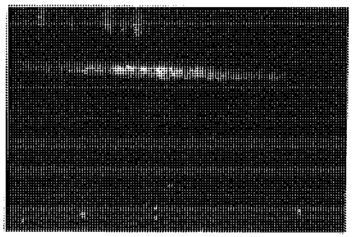

Figure 34. R^2 and exp() corrected bot14/104

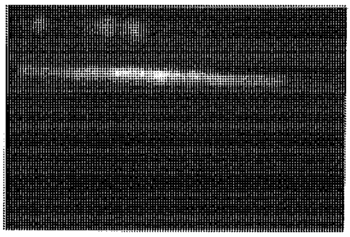

Figure 35. 2D Match-filtered bot14/104

Data from fileset bot14.bin, where the STIL sensor was flown from land into the Boston Bay area. These images show data for 10m bottom depth; the dataset has data from the beach out to 20m or so. The bottom features are clearly evident in this image.

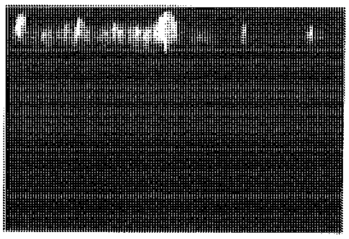

Figure 36. Raw bot14/240

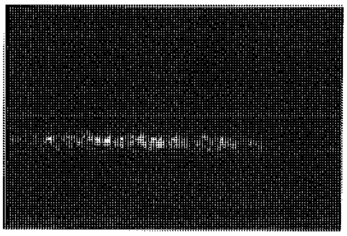

Figure 37. R^2 and exp() corrected bot14/240

Data from fileset bot14.bin, where the STIL sensor was flown from land into the Boston Bay area. These images show data for 20m bottom depth. Here the bottom is still obvious, but it is clear that the noise is beginning to dominate the image statistics.

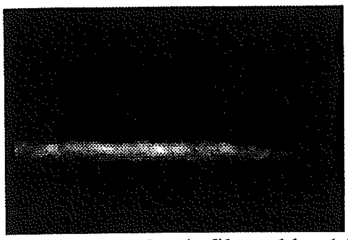

Figure 38. Match-filtered bot14/240

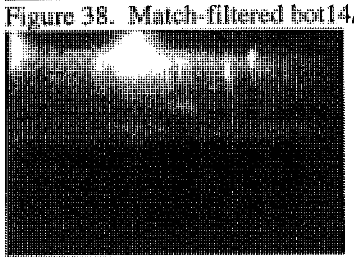

Figure 39. Raw dolphin3/174

Data from fileset dolphin3.bin, which was collected in Boston Bay. Several dolphin can be seen: one is above the surface (caused a CCD bloom), two are near the bottom, and one is near the surface (perhaps another as well).

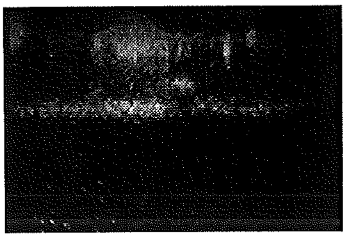

Figure 40. R^2 and exp() corrected dolphin3/174

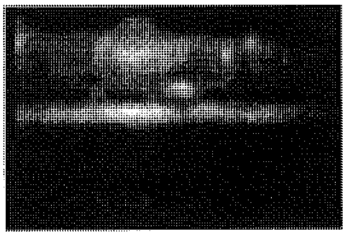

Figure 41. Match-filtered dolphin3/174

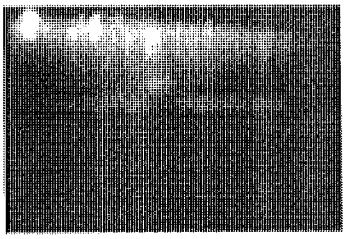

Figure 42. Raw dolphin3/175

Data from fileset dolphin3.bin, which was collected in Boston Bay. This frame shows a clear reflection and associated shadow signature for the dolphin. The depth of the dolphin is 8-9m, with a bottom depth of 11m.

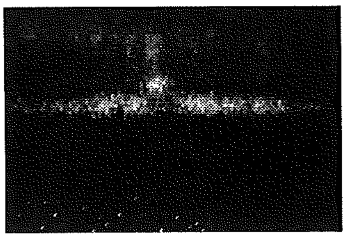

Figure 43. R^2 and exp() corrected dolphin3/175

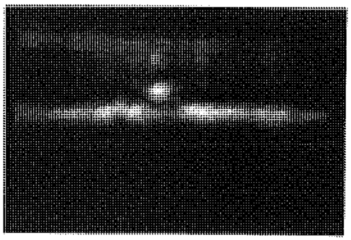

Figure 44. Match-filtered dolphin3/175

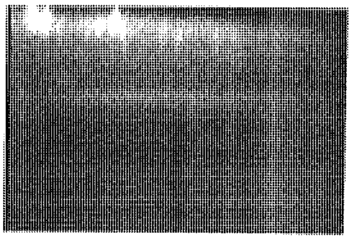

Figure 45. Raw dolphin3/176

Data from fileset dolphin3.bin, which was collected in Boston Bay. This is a faint dolphin signature (far left) near the bottom. Without the beam homogenizer in place, the laser beam profile is gaussian, leading to decreased light levels at the edge of the field of view.

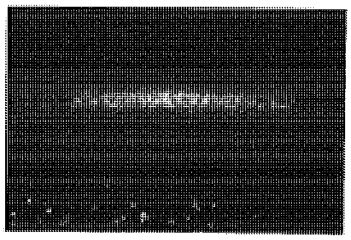

Figure 46. R^2 and exp() corrected dolphin3/176

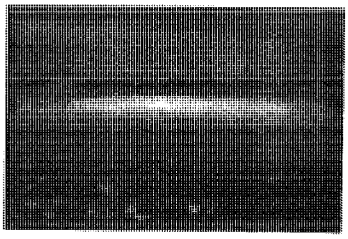

Figure 47. Match-filtered dolphin3/176

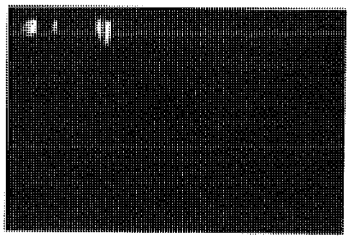

Figure 48. Raw reef21/67

Data from fileset reef21.bin, which was collected during spotting flights based out of Ceduna. The noisy nature of the data is quite evident here, as well as the larger depth extent of the imagery. The bottom is near 25m here, and performance is inhibited by the presence of reef foam. This foam is likely to be part of the inhomogeneity visible at the right side of the images (both 67 and 72).

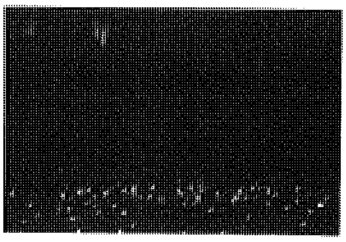

Figure 49. R^2 and exp() corrected reef21/67

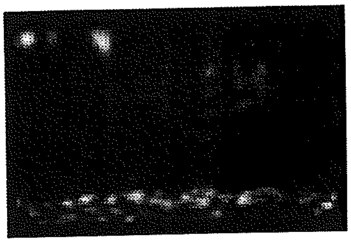

Figure 50. Match-filtered reef21/67

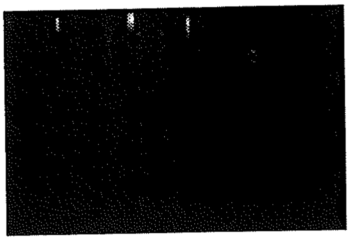

Figure 51. Raw reef21/72

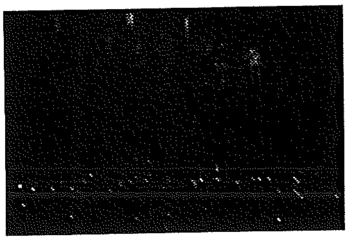

Figure 52. R^2 and exp() corrected reef21/72

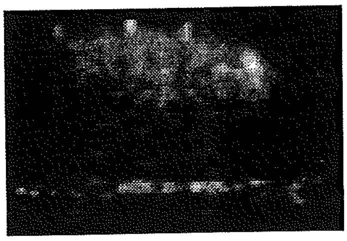

Figure 53. Match-filtered reef21/72

Data from fileset reef21.bin. Again note the noisy nature of the data (see below comments on camera noise issues found in later experiments). It is also clear that the data normalization and filtering are essential for making practical use of the data.

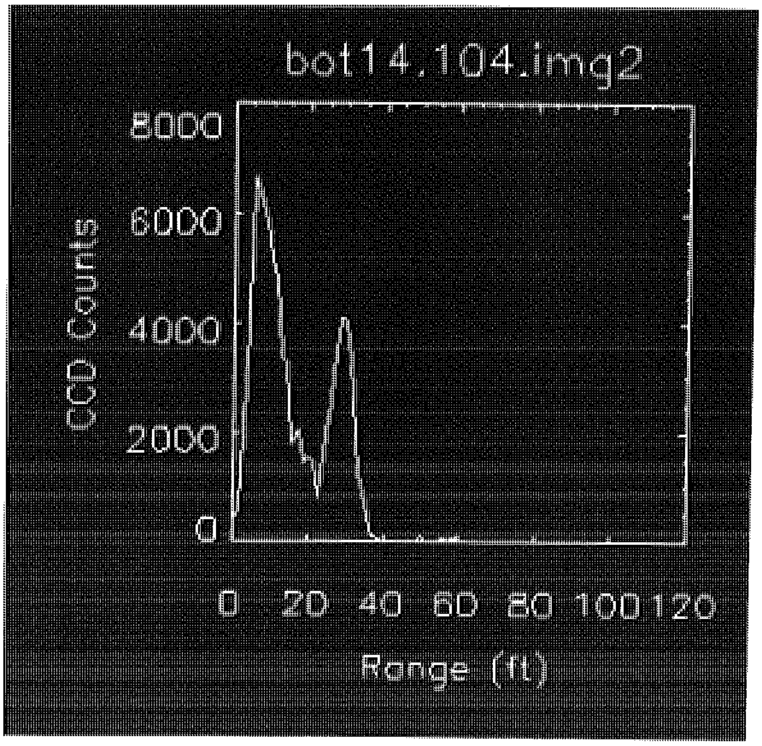

Figure 54. Bottom profile from Boston Bay at 30' depth.

Depth slice (one column) from the greyscale raw data showed above in Figure 33. The surface and bottom returns are the obvious features in this plot.

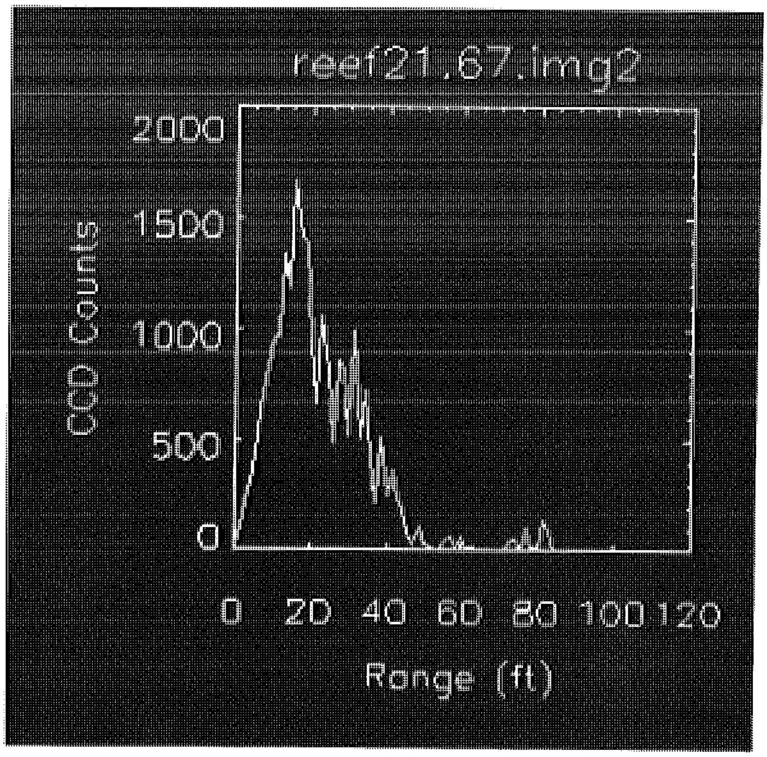

Figure 55. Bottom profile from GAB for 75' depth.

Depth slice (one column) from the greyscale raw data showed above in Figure 48. The surface return is quite obvious, but the bottom return , while discernable, is not obvious except in the filtered image. The excess noise is quite evident here.

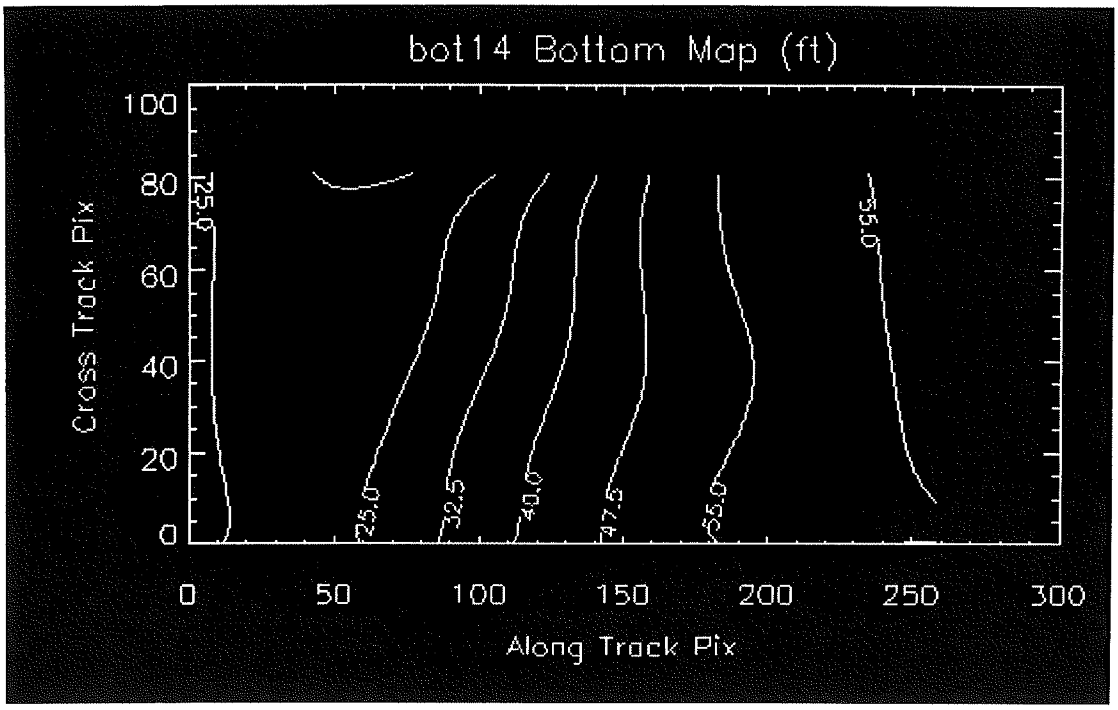

Figure 56. Contour plot of bottom depth in Boston Bay for a 15 x 150m area. Depths 25-65 ft.

Both of these contour plots illustrate the 3D use of STIL data, albeit in a simple fashion. For each of these plots, a series of 2D data (azimuth/range) were match-filtered for bottom depth and the depths were stored in a 2D array. This array was then fitted and used to generate the contour maps shown here. As such, the contour maps show the use of STIL for generating depth profiles for bottom features and/or distributed objects in the water (fish schools), provided adequate signature is available for detection. Given the weak nature of the reef21 bottom data, this provides some encouraging feedback on the utility of STIL for SBT school detection, apart from assessments of individual fish statistics.

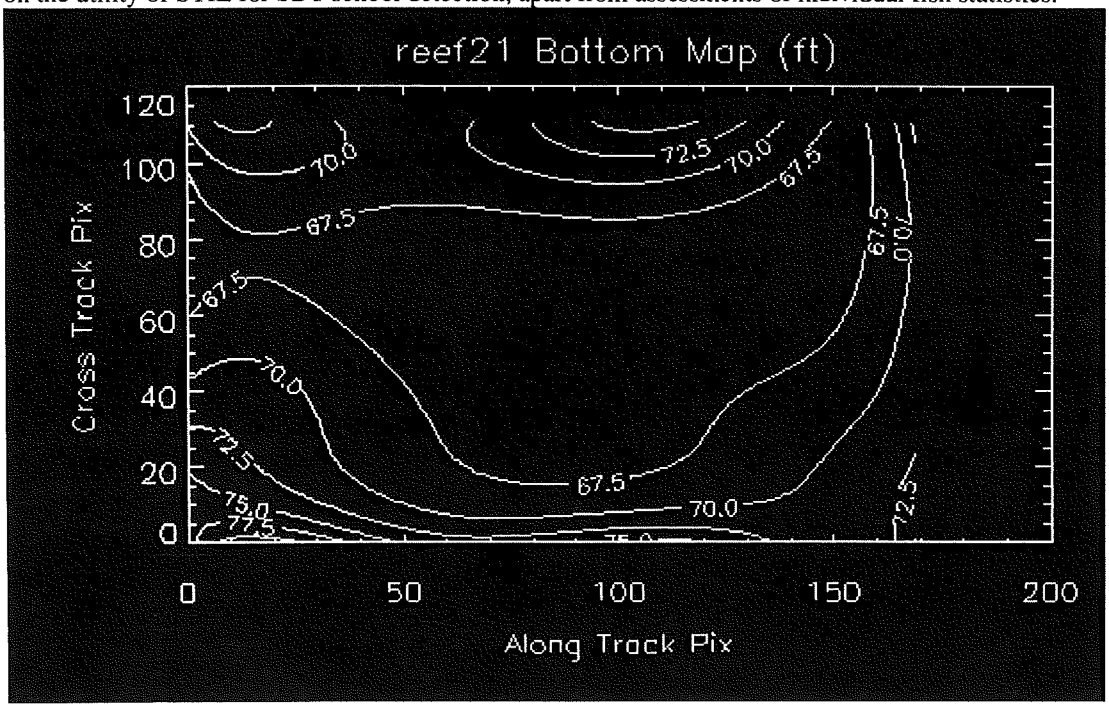

Figure 57. Contour plot of bottom depth in the GAB for a 15 x 100m area. Depths 67-77 ft.

A few summary comments are in order regarding the previous pages of image and reduced data. First, the STIL sensor is performing well as a LIDAR, in the most general sense. This is illustrated by the signal returns received from SBT, dolphin and bottom features. The SBT have been imaged to nearly 10m, and the dolphin have likewise been imaged clearly, even in the more turbid bay waters. The bottom features have been observed to 25m in the open ocean and to nearly 20m in the bay area (this is still under review). The open ocean data are in keeping with expectation, especially in lieu of the increased scattering near reefs due to additional dissolved air and foam. So the sensor is performing well in the general sense and we have demonstrated unambiguous detections of SBT and dolphin to reasonable depths, including the surface (though this data was not shown here – we are presently working on this issue and the associated data reduction).

However, the sensor is not performing as designed. As part of the analysis of data from recent boat tests, a noise analysis was conducted in order to compare various STIL experiments in a statistical sense (fractional fluctuations of volume backscatter). The airborne and shipborne STIL data show a dramatic increase in noise over previous sets, and a noise level that appears gain-dependent. This indicates that there is a significant problem in the receiver electronics (the noise was 10X worse than previous). This problem was not discerned in the airborne data analysis, because it was not clear that the air-water interface could not introduce significant light fluctuations due to solar contributions. However, the boat data showed the same noisy behavior as the airborne data, confirming that an electronics issue was at hand. The problem is currently being addressed, and has to do with either electrical isolation of the CCD camera or control/interfacing of the MCP (micro-channel plate) gain section in the streak tube. So the bad news is that the data contained significant electronic noise; the good news is that it can and will be corrected. This will aid quite a bit in detecting faint signatures of SBT or yellowfin, as they can easily be masked by noise levels when the depths are significant.

In spite of the noise levels, the ongoing analysis will seek to estimate SBT abundance in the volumes imaged over the farms. These are likely to be very coarse estimates, but will still serve to bring out some additional technical issues for consideration. More importantly, the analysis will use the current data for experiment planning and sensor optimization for the upcoming yellowfin trials (most likely at the end of the Summer, owing to schedule conflicts with the ONR efforts), so that those will yield more realistic estimates of the true sensor performance for fish schools and individual fish statistics, as possible.

More will be communicated on the analysis efforts as these progress. For the present time, the above images and comments can serve as a data overview, albeit qualitative. Statistics for detectability will have to be discussed and elaborated in separate, subsequent memoranda.

Q&A Regarding STIL Technology and Aerial Surveys[1]

<u>Laser design</u>. The present laser design seems adequate in terms of its energy per pulse, but its 100 Hz PRF (pulse repetition frequency) is still lower than desired. Ideally, a 400 Hz system would be preferable from a along-track resolution point of view (60 m/s $\div$ 400 /s = 15 cm), but this has implications for the receiver design, using the existing technology as a baseline. From a receiver technology standpoint, a 200 Hz PRF would work better, since this would only require a modification to firmware on the SMD CCD camera and APAC509 digital I/O subassemblies. The 200 Hz PRF would have a 30 cm along-track resolution, again based on a 60 m/s (120 knots) ground speed. However, a juvenile tuna at 16 kg only has 20-25 cm of breadth at its mid-section, so that even a 200 Hz laser would want to confine the along-track projected beam to 20 cm. This would, strictly speaking, result in slight undersampling of the target in its volume; however, this undersampling would not produce significant errors in the resultant data, based on current understanding of schooling behavior and packing density.

[1] Technical Issues (as per A. Cowling, T. Polachek note)

Polarizers. Other sensors have benefitted from the use of a polarizer when near-surface phenomena are to be observed. It is anticipated that this would also be true for the present case, but it was not successfully evaluated during this experiment. The principal reason is that the polarizer could not be adjusted to its optimum point, which would be critical for rejecting surface specular reflection (the lack of a real-time display and an adjustable mount were the main factors preventing optimizing). Several data sets were collected with the polarizer in its presumed optimum position, and a reduced volume backscatter was observed near the surface, but the actual surface reflection performance has yet to be carefully evaluated.

Even if the polarizer is optimum for surface reflection mitigation, it is not yet clear that a polarizer would be the *best* way to attack the problem. Fish at the surface would also have a specular term that may well be the dominant return signal, especially given that the fish would have a layer of water on its body between it and the air. Also, the polarizer will reduce the near-surface volume backscatter, leading to a smaller shadow signature for surface and near-surface fish, which may be the only high-confidence verification of a legitimate surface fish return. So, while the advantages of a polarizer are apparent, its disadvantages may be more significant, depending on the importance of detecting fish at or very near the surface.

Real-time Display. One of the subassemblies of the sensor that were left unfinished prior to this experiment was the real-time display. It was known that this would be a liability to the experiment, but it was felt (at the time) that the digitally stored data were the critical item. It is still true that the digital data are vital, especially in terms of the value to understanding the engineering issues that are essential to sensor optimization. However, it is now clear that the real-time display would have enabled the experiment to progress much more rapidly and would have allowed for more accurate flying/searching operations to be conducted. It is anticipated that the real-time display will be integrated during late April of 1997, pending delivery of the display daughtercard from Alex Systems.

Data storage and management. The data for this experiment was recorded directly to JAZZ media, which are removable hard-disk cartridges capable of storing up to 1 GB (1e9 bytes) of data at rates comparable with permanent hard disks. The observed data rate was 0.5-1 MB/sec for in-flight recording. After several of the JAZZ media became full, they were archived to DAT tape cartridges, which can store 2-8 GB per cartridge, depending on length and compression. This method is very cost effective and allows for easy transfer of data to and from the flight system, and also facilitates on-site analysis of data using a laptop and removable JAZZ drive.

Incidence angle. The sensor was initially installed in the Aerocommander with its receiver/transmitter optics aligned perpendicular to the aircraft fore/aft axis (nadir-viewing, for zero pitch and roll). During data collection, the rear elevators were adjusted to provide approximately 4° of tilt, which yielded an observable reduction in surface reflection ("glint"). To further reduce the glint, the sensor was tilted aft by about 5 cm (using a 2x4 between the sensor forward mount and the floor, and then tightening the bolts to sandwich the parts together); this contributed another 4° tilt, for a total of 4-8° tilt, depending on aircraft attitude. This also helped, though it may be necessary to design in some more sensor tilt to subsequent efforts, if other approaches do not help reduce the glint adequately. For the most part, the tilt achieved its goal of reducing glint.

<u>Sensor design adaptation to tuna</u>. It is clear from the present experiment that the sensor is not yet optimum for detecting tuna, though it may not be far away from quite a useful point of operation, given the enhancements already scheduled that will address many of the shortcomings observed in this experiment. Given adequate transmitter power and receiver sensitivity (both are depth- and clarity-dependent issues), the principal issue with tuna is attaining adequate resolution in all three dimensions. The tuna cross section in the water is fairly small: the 16 kg tuna used for ground tests in the present experiment was 70 cm long and up to 25 cm in breadth, but it is clearly not rectangular and therefore does not easily map to a rectangular pixel. Furthermore, the first order analysis of the tuna signature data collected in air indicates the tuna reflectivity is low (2-3%, which is consistence with published research to date) and that the LIDAR cross section is likely to be as low at 25% its physical cross section. The physical cross section is around 50% the equivalent rectangular cross section (i.e., if the fish were perfectly rectangular).

The implications are as follows. If one were to design a system with tuna-sized pixels (e.g. 25 x 75cm), the effective reflectivity in that pixel would be 2% * 25% * 50% = 0.25% reflectivity. Now in order to detect something, image contrast is required. Contrast in monochromatic marine LIDAR systems is usually achieved with respect to the volume backscatter of water, which will contribute approximately 0.1% backscattered light per meter of water depth. So the inherent contrast for such a (perfectly centered) tuna in the hypothetical tuna-pixel (and assuming 1m depth resolution, which is about right for most current Nd:Yg lasers) would be 0.25/0.1 = 2.5, before accounting for any sensor or environmental noise sources. While a contrast of 2.5 is not untenable as a final performance figure, it's not the place to start (one would accept that as a compromise position in difficult regimes, but it's preferable to start higher and then allow the engineering tradeoffs to barter away performance in exchange for cost or feasibility). The achievable contrast is also reduced by the loss of shadow signature caused by the tuna under-filling the pixel, allowing light to propagate and backscatter from the water volume surrounding the body of the fish (and still within the pixel). This geometrical effect also makes it quite difficult to detect a tuna right at the surface, as the surface reflection is likely to match the tuna, and the lack of a shadow signature would further mask its presence.

The solution, as observed in this experiment, is to increase the cross-track and along-track resolution as much as possible, and set the depth resolution to a compromise position between light level and actual required resolution, a figure that is ultimately limited by the laser pulsewidth (so it is about 1m in water, at present). At 250 feet altitude, the sensor provided pixels with 6 cm resolution perpendicular to aircraft heading (and approximately 18 cm in the direction of heading, with the sweep speed nominally yielding depth bins of 45 cm). This yielded immediate improvements in performance over the 1000 and 500 foot altitudes, though a few tuna signatures were observed in 500 foot data. In fact, as soon as the altitude was reduced to 250 feet, the shadow signatures of surface tuna became obvious in the raw data, in keeping with the above discussion. The increase in light sensivity also helped improve the performance by providing more water volume backscatter throughout the imaged water column (sensivity increases as the inverse range squared, so a factor of 4 from 1000 to 500, and a factor of 16 from 1000 to 250), but the shadow signatures for surface objects required resolution more than illumination.

The most appropriate resolution for individual fish registration is probably around 10-15 cm in the along- and cross-track dimensions, and perhaps 50 cm in depth, as this would allow the fish to be as close as 50 cm under the surface and still have a clear reflection signature, regardless of any shadow signature. The resolution can most likely be less, if entire schools are imaged, as the aggregate signature will contribute enough backcattered light to provide good contrast with respect to the surrounding water volume. This question cannot be addressed as directly at present, as no open-ocean fish schools were imaged in this experiment. However, meeting the resolution requirements that are apparent at present seems within reach of current planned improvements (200 Hz PRF, 2X receiver aperture, firmware modifications for more pixels, as needed).

General design features for a tuna survey LIDAR. The comments in the previous paragraphs can be summarized and augmented as follows. For juvenile bluefin tuna, voxels of 10 x 15 x 50 cm would provide detectable signatures of tuna in the first 10 m of coastal water, and the first 20m of open ocean water. The laser required for this performance would need to deliver approximately 3 W at 532 nm (so 15 mJ per pulse at 200 Hz) and the receiver aperture would need a clear aperture of around 100 mm. A real-time display is also required, and it would be best served by coupling it with some modest real-time processing. The processing needed would most likely be background subtraction (so that the surface return does not dominate the display) and moving-window frame integration or stacking (amounting to an along-track lowpass filter that would have the effect of enhancing the presence of extended targets such as schools). When coupled with a push-button operator station (as opposed to a PC keyboard), the sensor configured this way would be quite useful in surveying an area for marine life.

STIL vs. Gated systems. The motivation behind the development of the STIL sensor was to provide a LIDAR sensor with high resolution in all three spatial dimensions, since both the gated (Fisheye) and flying spot (LADS) approaches give up resolution in one or two (respectively) dimensions to attain higher resolution in the remaining ones. Arete has performed technical evaluations on these types of technologies, and has figured prominently in their development and optimization (as a subcontactor, most often) during the past 10-12 years. These evaluations and the resultant conclusions, combined with opportune timing and technology, led to the development of the STIL sensor.

As the present problem seems to be driven by resolution requirements, the STIL is the best choice. However, even if resolution were not as critical, say in along- and cross-track dimensions, then the STIL approach is still probably the best choice, since it can provide full volume coverage with minimal receivers and modest laser energies per pulse (high PRF, high energy lasers are very costly to build, own and operate), and since it does not require a scanner or optimal gating control to completely remove the surface contribution (for the gated sensor, this is vital; for the flying spot, it's of comparable importance to the STIL sensor).

Gated systems *can* provide meaningful data when the school depth is known or reasonably bounded, or when the packing density is high. So for imaging Sardine, for instance, the gated system may still make sense. But for more dispersed schools such as tuna, the gated sensor will not have adequate range resolution to provide adequate contrast for detection when a depth range of more than a couple of meters is of interest. Gated systems *can* achieve 1m depth resolution, but a single-receiver system would then provide only 1m of depth information, plus any objects that are very near the surface (again, though, this assumes the pixels are sized appropriately for the target, as discussed above), since these would typically yield good shadow signatures in a gated system.

Tuna Detection

Summary of detections. The experimental effort just concluded yielded detections of single tuna at the surface (surface and shadow signature) and from 2-5 m water depth in the tuna farms near Port Lincoln, which had diffuse attenuation coefficients ranging from 0.2/m to 0.4/m. The shelf waters near Ceduna had corresponding attenuation coefficients in the neighborhood of 0.08/m, so comparable tuna signatures would be expected nominally at 6-15 m, and limiting detection is probably somewhere around 20m for single tuna.

The tuna signatures at 2-5m were fairly pronounced, which is consistent with current physical models for the STIL sensor. It is not clear why so few tuna were observed between the near-surface and bottom regions, unless the observation that "the tuna are mostly down deep" is correct, and the surface tuna are only a small portion of the total population.

Tuna as targets. As pointed out earlier, detecting single tuna is fairly challenging and requires good resolution in all three spatial dimensions. The STIL technology is well suited to high resolution imaging, but the current sensor configuration is not yet at resolutions that will likely yield optimum data for the tuna survey, again based on single tuna detection. Detection of schools is likely to be easier, but it's difficult to estimate performance issues without either data or careful simulation/modeling. Both the simulation/modeling and data collection will be pursued in the months ahead, after making enhancements to the sensor (laser, receiver and data acquisition).

Quantitative measurement of fish/school size.

Inter-farm comparisons. As we did not image any real school behavior in the farm data (we obtained mainly surface and shallow water data on single tuna), such a comparison is not likely to be fruitful. However, some analysis will be conducted in the weeks ahead (under Salton-Kennedy funding) to assess the consistency and basic nature of the LIDAR signature of tuna. To the extent that inter-farm differences can be ascertained from such analysis, these will be summarized and communicated to CSIRO at that time.

Open ocean results. As we were unable to obtain any data over schools in the open ocean, due mainly to seasonal conditions, there are no data to analyze for such schools. However, several useful datasets were collected that will provide some insights into environmental conditions (water clarity, for instance), including a dataset over a 20m reef. These data will be analyzed in the weeks ahead to assess the sensor water penetration in such waters. Consequently, though we cannot say anything about the *target* signature (SBT), we did gain some useful data on the *background*, which is an important aspect of the SBT detection problem.

Depth estimation for wild schools.

The depth-estimation capability of the sensor was clearly demonstrated in this trial for tuna, dolphin and bottom features. Based on our current understanding of the sensor sensitivity, tuna reflectivity and packing density, it still seems reasonable that depth estimates of the top of the school could be made to 20 or 30m in open ocean waters. Hopefully, subsequent experimentation and limited simulation (using the single-tuna signature data obtained with CSIRO) this Spring and Summer will help quantify this a bit better.

Sub-surface school detection of schools not visible to spotters.

Based on the few days that were spent spotting near Ceduna, SA, it is clear that the LIDAR would be able to detect schools not detectable to the spotter. It is not clear what the actual depth-penetration capability of a good spotter is, but it is known that a spotter cannot "see" during high seas and low visibility, whereas the LIDAR is not so limited by these environmental factors. So the LIDAR would at least be able to aid a spotter in overcoming weather deficiencies. Furthermore, if a spotter is only seeing 10m into the water under normal conditions, then the LIDAR would quite likely extend his reach an additional 10-20m, again depending on the precise nature of the school signature.

Short and medium term LIDAR potential for tuna survey.

<u>General</u>. The short-term potential for tuna surveys with ASTIL will be improved markedly in the next several weeks, as pre-planned improvements to the baseline sensor configuration will be implemented. These include the real-time display, swath extension (from 7° to 15°), increased collection efficiency (roughly 2X aperture) and higher laser PRF. This will improve the ability to find and detect tuna.

Also, if current assumptions about schooling are correct, the schools should be observable to 20 or 30m, as stated above. So, given that a real-time display is available and the penetration of the sensor will be improved in the next month, the short-term potential seems quite good, based on current understanding of the data collected to date. However, as we do not yet have any real data on *open ocean* schools, only the potential, or anticipated performance, can be realistically considered. So perhaps it is more appropriate to speak of anticipated performance, rather than survey potential.

The medium-term potential is quite difficult to comment on. The most that can be said is that it will certainly be better than the short-term, since data collection, analysis and sensor performance optimization will be pursued in the short-term under several on-going initiatives within Arete.

<u>Resources</u>. The recent trial in South Australia benefited significantly from the infusion of Arete capital and human resources to modify, integrate and test the ASTIL sensor. A very limited amount of contract revenue was also applied to this effort, as there was significant overlap with other contract objectives. Consequently, the cost of the effort was mostly hidden to CSIRO, beyond the cost a the single engineer/analyst (Arete paid for the other engineer) and the sensor shipment to and from the United States.

So while the cost sharing was completely acceptable and generally very effective for this demonstration (and, in truth, it represented the reality of the shared risk to the experiment), it would be unreasonable to assume that a similar infusion of capital will be possible in subsequent testing. However, it is not anticipated that such capital will be necessary, beyond periodic parts replacement due to normal wear and tear on the sensor, or in the event that the upcoming experiments and analyses suggest specific improvements that would require further engineering and parts procurement specifically for meeting the tuna survey requirements. So it is to these latter two items that discussions of resources should be directed.

The parts replacement cost for future endeavors will most likely be factored into the cost of conducting experiments (amortized appropriately), though it's difficult to predict any specific values at this time. However, as Arete is committed to making sensible business and scientific advances in the markets that it has access to, such amortized costs will be minimized, to the extent possible, so that solid progress in commercial and scientific areas can be made by both parties.

If further experimentation indicates the need for sensor modifications or optimizations that are specific to the tuna problem, then we would need to negotiate development costs, or possibly identify a cost-sharing plan that is amenable to both CSIRO and Arete. The cost-sharing option would be of interest mainly if there was clear commercial potential (so that costs could be recovered through subsequent profits, as Arete is a for-profit organization).

In general, the resources needed will scale with the number of experiments required. It is still advisable to have two engineers for intensive experiment periods, and the cost of transportation and lodging would also need to be included. The specific costs can be addressed better once a specific work plan is identified. For planning purposes, CSIRO should allow enough budget for aircraft, engineering support (flying/analysis), and some pre-test and post-test analysis. Pre-test analysis would be confined to making sure the experiment is scaled and planned properly (feasibility issues can be addressed as well, of course); post-test analysis is generally useful for assuring the data are used to maximum benefit.

<u>Timing and logistics</u>. We should have a much better idea of the utility of further work with LIDAR in the conduct of tuna surveys by October 1997, after which time we will have had more opportunities to image fish schools in the open ocean near Southern California and Hawaii, perhaps. Consequently, we should be ready to commit to further testing or postpone/cancel such testing at that time. Hopefully, we will also be able to estimate appropriate costs for Arete to support CSIRO sometime prior to the start of the next budget cycle for CSIRO, so that funds will be available to support further testing should the sensor performance prove adequate for the survey requirements.

Future collaboration.

<u>General</u>. The recent experiment was greatly facilitated by the joint efforts of Arete and CSIRO to image SBT with the ASTIL sensor. Given the successful conduct of the recent experiment and the professional cordiality that has characterized the interaction with CSIRO, Arete has every reason to look forward to continued collaboration on such issues (and others that may arise) in the months and years ahead. Arete has ongoing initiatives in many aspects of marine remote sensing, including both passive and active sensors on ship-borne, underwater, and airborne platforms. Many of these may prove to be of interest to CSIRO in the course of time.

Specific to 1998 survey year. Arete will continue to analyze the data collected with CSIRO to address issues pertaining to the Salton-Kennedy Grant (yellowfin tuna dolphin bycatch and LIDAR technology demonstration for surveys) and other ongoing efforts at Arete. To the extent possible under our current contracts, Arete will be pleased to make full use of the data collected to date for advancing the technical interests of CSIRO. Consequently, CSIRO will be kept informed of ongoing sensor improvements, results from the Salton-Kennedy effort, and if it desires to, will be welcome to provide review of technical objectives of the Salton-Kennedy effort and be an observer in that effort.

Arete will also be pleased to continue to conduct survey experiments jointly with CSIRO, provided the technical objectives can be met and adequate funds can be identified to support the effort. Joint efforts in which CSIRO provides the marine biological and fisheries expertise and Arete addresses the sensor technology and data analysis issues are very sensible and are beneficial to both organizations.